Nonlinear Optics - introduction

Lecture Notes

Chapters 1 to 5

Introduction to nonlinear optics
Nonlinear susceptibilities
Nonlinear wave equations
2nd order nonlinearities
3rd order nonlinearities

Nicolas Dubreuil

Date : January 11, 2026

Contents

Chapter 1

Introduction to nonlinear optics

This first chapter provides an introduction to the optical nonlinear effects. The origin of the nonlinearities is described through a standard model based on the classical anharmonic oscillator, which allows to derive approximated relations for the linear and nonlinear susceptibilities in the vicinity of an energy transition of the medium. Finally various nonlinear effects, to be studied in more details in the next chapters, will be introduced.

Contents

1.1 Learning outcomes

The learning outcomes of this chapter are the following:

By the end of this chapter, students will be able to:

- provide a classical description for the origin of the nonlinear susceptibilities,
- cite the principal nonlinear effects that arise in a 2nd and 3rd order nonlinear materials,
- derive the relation between the macroscopic polarization and the electric field (the so-called constitutive relations of nonlinear optics).

By the end of this chapter, students will be start to understand:

- the capability of light matter interactions in modifying light properties : frequency generation, optical rectification...,
- how perturbative models can be used to describe and derive a nonlinear problem in physics,
- the link between the microscopic and macroscopic terms in Maxwell's equations (induced dipole, macroscopic polarization and fields).

1.2 Basics of nonlinear optics

In the following, a dielectric material is considered, which is composed of microscopic entities (atoms, molecules, ions...). The medium is then described as a collection of electric dipoles which, under the action of an external oscillating electric field $\boldsymbol{\mathcal{E}}$, oscillate and radiate collectively a source term called the *macroscopic polarization* $\boldsymbol{\mathcal{P}}$.

Nonlinear optical effects occur when the macroscopic polarization $\boldsymbol{\mathcal{P}}$ magnitude is no longer proportional to the applied electric field amplitude $\boldsymbol{\mathcal{E}}$. The polarization $\boldsymbol{\mathcal{P}}$ is the source term that is included into the Maxwell's equations to describe the propagation of electromagnetic fields in a medium.

The relationship between $\boldsymbol{\mathcal{P}}$ and $\boldsymbol{\mathcal{E}}$ takes generally a complicated form. A first attempt consists in considering that both the nonlinear polarization and the electric field keep the same polarization state, allowing a scalar description respectively denoted $\mathcal{P}$ and $\mathcal{E}$. A second assumption considers an instantaneous response of the material. Vectorial relations that take into account the finite time response of the material will be introduced in chapter 2. Under these assumptions, the induced polarization can be expanded in terms of a power series in the field strength:

$$\mathcal{P}(t) = R^{(1)}\mathcal{E}(t) + R^{(2)}\mathcal{E}(t)\mathcal{E}(t) + R^{(3)}\mathcal{E}(t)\mathcal{E}(t)\mathcal{E}(t) + \cdots, \tag{1.1}$$

where the coefficients $R^{(i)}$ are taken constant as a first approximation. Note that the power series expansion is valid as long as the amplitude of the incident field is much weaker than the atomic electric field strength.

Let's consider an applied monochromatic field at ω propagating along the direction z, $\mathcal{E}(t) = A\cos(\omega t - kz)$. The first order term of (1.1) depicts the linear response of the material, with the generation of a macroscopic polarization term at ω:

$$\mathcal{P}^{(1)}(t) = R^{(1)}A\cos(\omega t - kz).$$

By increasing the magnitude of the applied field, the strength of the second order term may appear no longer negligible. In addition to the linear response, the material will generate a macroscopic polarization with a second order term $\mathcal{P}(t) = \mathcal{P}^{(1)}(t) + \mathcal{P}^{(2)}(t)$, with:

$$\mathcal{P}^{(2)}(t) = R^{(2)} A^2 \cos^2(\omega t - kz) = \frac{R^{(2)}}{2} A^2 \left(1 + \cos(2\omega t - 2kz)\right).$$

The quadratic response of the material induces a polarization term at frequencies equal to 0 and 2ω. One can anticipate the possibility to generate inside the material a static field and a novel beam at twice the frequency of the applied field. These nonlinear interactions refer respectively to the **optical rectification** effect and the **second harmonic generation** effect that will be studied in details in chapter 4.

A more general situation consider the interaction of two waves at ω_1 and ω_2 that leads, in addition to terms at 0, $2\omega_1$ and $2\omega_2$, to polarization terms at $\omega_3 = \omega_1 \pm \omega_2$. These terms originate from the experimental observation of a beam at either the **sum- or the difference-frequency** of the two incident beam frequencies !

The consequence of the 3rd order nonlinear response in (1.1), assuming a single applied fied at ω, yields:

$$\mathcal{P}^{(3)}(t) = R^{(3)} A^3 \cos^3(\omega t - kz) = R^{(3)} \frac{3A^3}{4} \cos(\omega t - kz) + R^{(3)} \frac{A^3}{4} \cos(3\omega t - 3kz),$$

as a third order polarization term. It shows the possibility of a **third-harmonic generation** following the propagation of a beam at ω inside a material. Interestingly, an additional polarization term at ω is expected. This term clearly differs from the linear contribution as it is proportional to the cube of the applied field amplitudes and denotes its nonlinear behavior. Actually, the polarisation term at ω is the sum of the linear and third order terms:

$$\mathcal{P}(t) = \left(R^{(1)} + R^{(3)} \frac{3A^2}{4}\right) A \cos(\omega t - kz),$$

showing that the propagation of an optical beam through a material may induce a modification of its linear properties, namely the refractive index and the absorption. The modification of the refractive index leads to the so called **optical Kerr effects** that will be studied in section 5.4.

The relationship between the incident electric field and the macroscopic polarization will be described in more details, especially the determination of the nonlinear susceptibilities and their relations to the coefficients $R^{(i)}$. However, the expansion of the material response subject to an optical field excitation in a power series of the field strength provide physical insights in the variety of nonlinear effects and applications of nonlinear optics.

Comment:
Nonlinear interactions are governed by nonlinear coefficients, which are related to the material properties as it will be clarified in the next section, and by the magnitude of the optical field amplitudes. The latter means that **nonlinear effects are governed by the optical beam intensities**, so the power density per unit of surface, as the intensity is proportional to field amplitude square.

1.3 Physical origins of the optical nonlinearities

Basic concepts of nonlinear optics can be introduced using simple models that lead to a relationship between the applied field strength and the induced polarization in metals or plasma-gas, and in dielectric media. In the case of metals or plasma-gas, the model presented in appendix A describes the motion of a free charge gas subject to the Lorentz force induced by an electromagnetic wave. For dielectric media, a classical model that describes the motion of bound charges

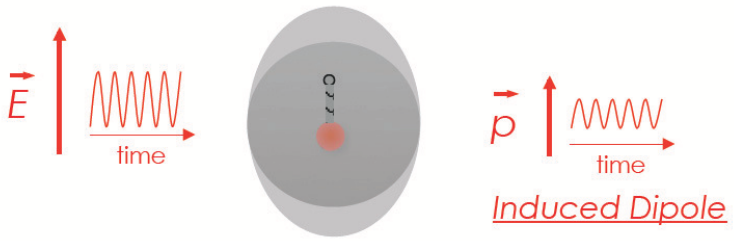

Fig. 1.1. Classical description of the dipolar interaction between an applied electromagnetic field and polarized entity.

(electrons) under the action of an external field gives rise to the determination of relationships for the induced dipole and for the macroscopic polarization. This model is presented in details below.

In the linear regime, both models allow to retrieve expressions of the conductivity for metals and the susceptibility for dielectric medium. Beside the simplicity of those models, they allow the prediction of most of the nonlinear effects to be studied in more details in the following part of the course.

1.3.1 Classical anharmonic oscillator model

A linearly polarized plane wave at ω is propagating through a dielectric material. It interacts with the atoms or the molecules that constitute the material and induces a polarization $\boldsymbol{\mathcal{P}}(z,t)$:

$$\boldsymbol{\mathcal{P}}(z,t) = N\boldsymbol{p}(z,t), \tag{1.2}$$

where $\boldsymbol{p}(z,t)$ is the induced microscopic dipole and N the density of atoms or molecules. According to a classical description of this interaction, depicted in Fig. 1.1, the dipole originates from the modification of the trajectories of the valence electrons induced by the time varying external field through the Coulomb force. The motion of the ion cores is neglected.

Subsequently, the field amplitude of the linearly polarized monochromatic plane wave, which propagates along the direction (Oz) with a wavevector k, is given by :

$$\begin{aligned} \boldsymbol{\mathcal{E}}(z,t) &= \left[A(\omega)e^{-\imath(\omega t-kz)} + A(-\omega)e^{+\imath(\omega t-kz)}\right]\boldsymbol{x}, \\ &= \boldsymbol{E}(\omega)e^{-\imath\omega t} + \boldsymbol{E}(-\omega)e^{+\imath\omega t}, \end{aligned}$$

where vector $\boldsymbol{x}$ indicates the direction of polarization of the wave. The electric field $\boldsymbol{\mathcal{E}}(z,t)$ is assumed to be a purely real quantity. In the following, the conjugate of the complex field amplitude $\boldsymbol{E}(\omega)$ will be denoted by :

$$\boldsymbol{E}(\omega)^\star = \boldsymbol{E}(-\omega) \tag{1.3}$$

Notation :

- $\boldsymbol{\mathcal{E}}(z,t)$ is a purely real quantity,
- $\boldsymbol{E}(\omega)^\star = \boldsymbol{E}(-\omega)$ is the complex conjugate of the complex field amplitude $\boldsymbol{E}(\omega)$

For the sake of simplicity, we are considering an entity (atoms or molecules) with a single valence electron, with a uniaxial $\boldsymbol{x}$ motion induced by an external electric field linearly polarized along the $\boldsymbol{x}$ direction. The expression of the induced dipole is :

$$\boldsymbol{p}(z,t) = -e\,x(z,t)\boldsymbol{x}, \tag{1.4}$$

where the quantity $-e$ is the charge of one electron and the function $x(z,t)$ represents the instantaneous position of the electron. Its position is given with respect to its equilibrium

position (no applied field). In order to get an expression for the polarization $\boldsymbol{\mathcal{P}}(z,t)$ induced by a given external field $\boldsymbol{\mathcal{E}}(z,t)$, one can solve the following equation of motion for the electron:

$$\frac{d^2x}{dt^2} + \alpha\frac{dx}{dt} + \omega_0^2 x + \beta x^2 + \gamma x^3 + \cdots = \frac{-e}{m}\boldsymbol{x}\cdot\boldsymbol{\mathcal{E}}(z,t). \tag{1.5}$$

Conversely to the case of classical harmonic oscillator, we have voluntarily introduced restoring force terms that nonlinearly depend on the coordinate $x(z,t)$. Actually, the expression $\omega_0^2 x + \beta x^2 + \gamma x^3 + \cdots$ corresponds to the Taylor expansion of the restoring force. The right hand side term of (1.5) describes the driven Coulomb force. Considering the case of a dilute material, the local field is assumed to be equal to the macroscopic external field $\boldsymbol{\mathcal{E}}(z,t)$.

In general, this equation does not have an analytical solution with a simple expression. However, taking into account that the harmonic term $\omega_0^2 x$ dominates the anharmonic ones, the equation can be solved by means of a perturbation method for which the general solution takes the form:

$$x = \lambda x^{(1)} + \lambda^2 x^{(2)} + \lambda^3 x^{(3)} + ..., \tag{1.6}$$

where λ is a parameter set between 0 and 1. Using such a perturbative approach, one can derive the expressions for the linear and nonlinear polarizations.

Linear polarization

Firstly, the anharmonicity terms are neglected (not included) and the equation of motion becomes:

$$\frac{d^2x}{dt^2} + \alpha\frac{dx}{dt} + \omega_0^2 x = \frac{-e}{m}\left[A(\omega)e^{-\imath(\omega t-kz)} + A(-\omega)e^{+\imath(\omega t-kz)}\right]\boldsymbol{x}\cdot\boldsymbol{x}. \tag{1.7}$$

One solution of the driven regime (steady-state solution) takes the following form:

$$x^{(1)}(z,t) = a(\omega)e^{-\imath(\omega t-kz)} + a(-\omega)e^{+\imath(\omega t-kz)}. \tag{1.8}$$

Substituting (1.8) in (1.7) gives:

$$a(\omega) = \frac{-eA(\omega)}{m\mathcal{D}(\omega)},$$

with $\mathcal{D}(\omega) = \omega_0^2 - \omega^2 - \imath\alpha\omega$. Following the form of the driven solution (1.8), the induced dipole is directly proportional to the applied electric field :

$$\boldsymbol{p}^{(1)}(z,t) = \alpha^{(1)}(\omega)A(\omega)e^{-\imath(\omega t-kz)}\boldsymbol{x} + CC,$$

with $\alpha^{(1)} = \frac{e^2}{m\mathcal{D}(\omega)}$ the first order polarizability (or linear polarizability) of the entity. If we assume that all the dipoles are identical and aligned along the single direction $\boldsymbol{x}$, and since the linear susceptibility is defined by the relation

$$\boldsymbol{\mathcal{P}}^{(1)}(z,t) = \epsilon_0\chi^{(1)}(\omega)\boldsymbol{E}(\omega)e^{-\imath\omega t} + CC,$$

one can find an expression of the linear susceptibility of the material :

$$\boxed{\chi^{(1)}(\omega) = \frac{Ne^2}{\epsilon_0 m(\omega_0^2 - \omega^2 - \imath\alpha\omega)}.} \tag{1.9}$$

The susceptibility is a complex quantity. The real part of the susceptibility is related to the dispersion of the material (the refractive index), while its imaginary part is related to the absorption (or gain) coefficient. The figure 1.2 show the typical behavior of these two parts around the resonance frequency ω_0.

As a first conclusion, we can say that the harmonic oscillator model well described the behavior of the linear susceptibility : we were able to recover the well known shape of the dispersive and absorption behavior of a material near to a resonance.

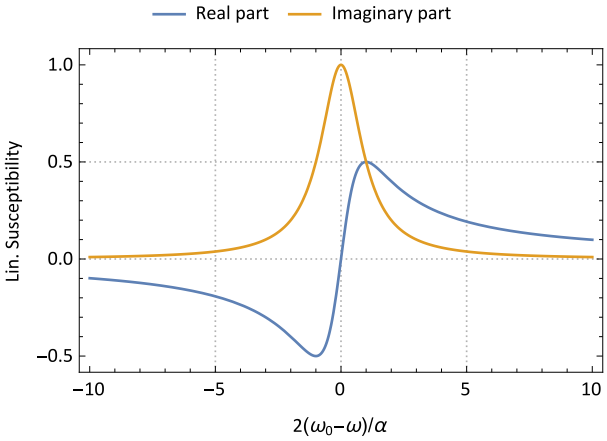

Fig. 1.2. Real and imaginary parts of the linear susceptibility around the frequency ω_0.

2nd order nonlinear polarization

The quadratic anharmonic term of the restoring force is now introduced in the equation of motion of the oscillator :

$$\frac{d^2x}{dt^2} + \alpha\frac{dx}{dt} + \omega_0^2 x + \beta x^2 = \frac{-e}{m}\boldsymbol{x}\cdot\boldsymbol{\mathcal{E}}(z,t). \tag{1.10}$$

Considering a weak applied electric field, the quadratic term of the restoring force will be kept much smaller than the linear term. Assuming that $\beta x^2 \ll \omega_0^2 x$, one seeks a solution of the form:

$$x(z,t) = \lambda x^{(1)}(z,t) + \lambda^2 x^{(2)}(z,t) + \cdots, \tag{1.11}$$

where λ represents the strength of the perturbation and can be arbitrarily set between 0 and 1. This solution is substituted in (1.10), and considering that $x^{(1)}$ is the solution of (1.7), we find that $x^{(2)}$ is solution of the equation :

$$\frac{d^2x^{(2)}}{dt^2} + \alpha\frac{dx^{(2)}}{dt} + \omega_0^2 x^{(2)} = -\beta\left(x^{(1)}\right)^2. \tag{1.12}$$

This equation describes the motion of a harmonic oscillator with a driven force proportional to $\left(x^{(1)}\right)^2$, which contains oscillating terms at the frequencies $\pm 2\omega$ and 0. One can seek a steady-state solution of the form :

$$x^{(2)}(z,t) = b(0) + b(2\omega)e^{-2\imath(\omega t - kz)} + b(-2\omega)e^{+2\imath(\omega t - kz)}. \tag{1.13}$$

After substitution in (1.12) and identification between the terms oscillating at the same frequency, we find the expressions :

$$\begin{cases} b(0) = \dfrac{-2\beta e^2 |A|^2(\omega)}{m^2\mathcal{D}(0)\mathcal{D}(\omega)\mathcal{D}(-\omega)} \\ b(\pm 2\omega) = \dfrac{-\beta e^2 A^2(\pm\omega)}{m^2\mathcal{D}(\pm 2\omega)\mathcal{D}(\pm\omega)\mathcal{D}(\pm\omega)}, \end{cases}$$

where $\mathcal{D}(\omega) = \omega_0^2 - \omega^2 - \imath\alpha\omega$.

The expression for the second order induced dipole, which is proportional to $x^{(2)}(z,t)$, is then:

$$\boldsymbol{p}^{(2)}(z,t) = 2\alpha^{(2)}(\omega,-\omega)A(\omega)A(-\omega)\boldsymbol{x} + \alpha^{(2)}(\omega,\omega)A(\omega)A(\omega)e^{-2\imath(\omega t - kz)}\boldsymbol{x} + CC,$$

with

$$\alpha^{(2)}(\omega_1,\omega_2) = \frac{\beta e^3}{m^2\mathcal{D}(\omega_1+\omega_2)\mathcal{D}(\omega_1)\mathcal{D}(\omega_2)},$$

the second order polarizability of the material. Finally, a second order polarization and a second order nonlinear susceptibility can be defined by:

$$\boldsymbol{\mathcal{P}}^{(2)}(z,t) = 2\epsilon_0\chi^{(2)}(\omega,-\omega)A(\omega)A(-\omega)\boldsymbol{x} + \epsilon_0\chi^{(2)}(\omega,\omega)A(\omega)A(\omega)e^{-2\imath(\omega t-kz)}\boldsymbol{x} + CC,$$

with

$$\chi^{(2)}(\omega_1,\omega_2) = \frac{N\alpha^{(2)}(\omega_1,\omega_2)}{\epsilon_0}.$$

The total macroscopic polarization induced inside the material is then given by the sum :

$$\begin{aligned}\boldsymbol{\mathcal{P}}(z,t) &= \boldsymbol{\mathcal{P}}^{(1)}(z,t) + \boldsymbol{\mathcal{P}}^{(2)}(z,t)\\ &= \boldsymbol{P}^{(2)}(0) + \boldsymbol{P}^{(1)}(\omega)e^{-\imath\omega t} + \boldsymbol{P}^{(2)}(2\omega)e^{-2\imath\omega t} + CC.\end{aligned} \tag{1.14}$$

with :

$$\begin{aligned}\boldsymbol{P}^{(2)}(0) &= 2\epsilon_0\chi^{(2)}(\omega,-\omega)E(\omega)E(-\omega)\boldsymbol{x}\\ \boldsymbol{P}^{(2)}(2\omega) &= \epsilon_0\chi^{(2)}(\omega,\omega)E(\omega)E(\omega)\boldsymbol{x}\end{aligned}$$

The macroscopic polarization being generated inside the material contains terms oscillating at the frequencies ω (linear response), $\omega = 0$ and $\pm 2\omega$.

The expression (1.14) shows that the polarization that is radiated inside the materials contains new frequency components. The term with a frequency component at $\omega = 0$ corresponds to the creation of a static field inside the material. This process is referred to as *optical rectification*. A second component radiated at the frequency 2ω describes the *second harmonic generation* (SHG) nonlinear effect. As in the case of the optical rectification, the amplitude of the polarization is proportionnal to the square of the applied electric field amplitude, which is the signature of a nonlinear response.

This simple model enables a description of the nonlinear response of dipoles excited by a an external oscillating electric field. The nonlinear response originates from the anharmonicity in the restoring force that is no longer proportional to the deformation of the electronic cloud surrounding the nucleus. As the linear susceptibility, the nonlinear interaction can be strengthened once the frequency of the interacted electric fields is close to a material resonance.

An other comment concerns the wavevector related to the polarization component at 2ω, which is equal to $2k(\omega)$. In general, it will differ from the wavevector $k(2\omega)$ of the electric field at 2ω and freely propagating along the direction z. The value of the wavevector $k(2\omega)$ is set through the dispersion relation of the material. However, the *phase matching condition*, in this case $k(2\omega) = 2k(\omega)$, must be fulfilled in order to efficiently generate a beam at the second harmonic. If not, the nonlinear polarization at 2ω is not radiated in phase with the electric field at 2ω and the second-harmonic beam can not generated.

3rd order nonlinear polarization

Following the second order perturbation, the next step is the case of a dipole governed by a restoring force that contains a cubic term $\omega_0^2 x + \gamma x^3$. For simplification, we have omitted the quadratic term in this expression. The equation of motion for such a dipole is then given by :

$$\frac{d^2x}{dt^2} + \alpha\frac{dx}{dt} + \omega_0^2 x + \gamma x^3 = \frac{-e}{m}\boldsymbol{x}\cdot\boldsymbol{\mathcal{E}}(z,t). \tag{1.15}$$

Actually, a material with a collection of dipoles governed by such an equation of motion exhibits a center of symmetry. Indeed, equation (1.15) remains the same after the following substitution : $x \to -x$ and $E \to -E$. The medium supports a *centro-symmetry.*

As in the previous cases, we seek a solution of (1.15) with the form given by (1.6). After substitution, one can show that the second order steady state solution vanishes and the equation of motion is reduced to:

$$\frac{d^2x^{(3)}}{dt^2} + \alpha\frac{dx^{(3)}}{dt} + \omega_0^2 x^{(3)} = -\gamma\left(x^{(1)}\right)^3. \tag{1.16}$$

The motion is then equivalent to that of a harmonic oscillator driven by an external force containing terms oscillating at $\pm\omega$ and $\pm 3\omega$. The derivation of the previous equation exhibits the following expression for the third-order induced dipole:

$$\boldsymbol{p}^{(3)}(z,t) = 3\alpha^{(3)}(\omega,-\omega,\omega)A(\omega)A(-\omega)A(\omega)e^{-\imath(\omega t-kz)}\boldsymbol{x} + \alpha^{(3)}(\omega,\omega,\omega)A(\omega)A(\omega)A(\omega)e^{-3\imath(\omega t-kz)}\boldsymbol{x} + CC,$$

with

$$\alpha^{(3)}(\omega_1,\omega_2,\omega_3) = \frac{-\gamma e^4}{m^3\mathcal{D}(\omega_1+\omega_2+\omega_3)\mathcal{D}(\omega_1)\mathcal{D}(\omega_2)\mathcal{D}(\omega_3)},$$

the third order polarizability of the material. Assuming that the dipoles are all oriented along the direction $\boldsymbol{x}$, the expressions for the third order polarization and third order nonlinear susceptibility are:

$$\boldsymbol{\mathcal{P}}^{(3)}(z,t) = 3\epsilon_0\chi^{(3)}(\omega,-\omega,\omega)A(\omega)A(-\omega)A(\omega)e^{-\imath(\omega t-kz)}\boldsymbol{x} + \epsilon_0\chi^{(3)}(\omega,\omega,\omega)A(\omega)A(\omega)A(\omega)e^{-3\imath(\omega t-kz)}\boldsymbol{x} + CC,$$

with

$$\chi^{(3)}(\omega_1,\omega_2,\omega_3) = \frac{N\alpha^{(3)}(\omega_1,\omega_2,\omega_3)}{\epsilon_0}.$$

The total macroscopic polarization generated inside the material is then given by the sum :

$$\begin{aligned}\boldsymbol{\mathcal{P}}(z,t) &= \boldsymbol{\mathcal{P}}^{(1)}(z,t) + \boldsymbol{\mathcal{P}}^{(3)}(z,t)\\ &= \boldsymbol{P}(\omega)e^{-\imath\omega t} + \boldsymbol{P}(3\omega)e^{-3\imath\omega t} + CC.\end{aligned}$$

and contains terms oscillating at the frequencies ω (with both a linear and nonlinear contribution) and $\pm 3\omega$.

The polarization term vibrating at the frequency $\pm 3\omega$ is responsible for the *3rd harmonic generation* (THG) :

$$\boldsymbol{P}^{(3)}(3\omega) = \epsilon_0\chi^{(3)}(\omega,\omega,\omega)E(\omega)E(\omega)E(\omega)\boldsymbol{x}$$

Like the second harmonic generation, this nonlinear effect requires to fulfill a phase matching condition, which is given by the relation : $3k(\omega) = k(3\omega)$.

For the term vibrating at ω, it is interesting to notice that it will affect the linear properties of the material. Indeed, the complex amplitude of the macroscopic polarization at ω is :

$$\boldsymbol{P}^{(3)}(\omega) = 3\epsilon_0\chi^{(3)}(\omega,-\omega,\omega)E(\omega)E(-\omega)E(\omega)\boldsymbol{x}$$

$$\begin{aligned}\boldsymbol{P}(\omega) &= \boldsymbol{P}^{(1)}(\omega) + \boldsymbol{P}^{(3)}(\omega)\\ &= \epsilon_0\left[\chi^{(1)}(\omega) + 3\chi^{(3)}(\omega,-\omega,\omega)E(\omega)E(-\omega)\right]E(\omega)\boldsymbol{x}\\ &= \epsilon_0\chi^{(1)}_{eff}(\omega)E(\omega)\boldsymbol{x}.\end{aligned}$$

This relation shows that the nonlinear response of the dipole at ω will modify the linear susceptibility $\chi^{(1)}(\omega)$ of the material through the quantity $3\chi^{(3)}(\omega,-\omega,\omega)E(\omega)E(-\omega)$. This modification is directly proportional to the field intensity and affects both the real part, which is related to the refractive index, and the imaginary part, related to the absorption (or gain). The modification of the refractive index refers to the *optical Kerr effect*, while the modification of the absorption refers to the *two-photon absorption* effect.

Chapter 2

Nonlinear susceptibilities

In the previous chapter, we have introduced a simple model that provides physical insight in the origin of the nonlinear interactions. In the case of dielectric media, approximated expressions for the nonlinear susceptibilities can be derived from the anharmonic classical oscillator model that describes the motion of bounded electrons subject. Assuming a collection of identical dipoles, we have been able to give the relations between the macroscopic polarization terms and the applied optical fields. Hereafter, and considering the finite response time of a material, the tensorial relation between the interacted electrical fields (vectors) and the nonlinear susceptibility (tensors) are introduced. The relation between the nonlinear susceptibilities and the impulse response of the material is demonstrated. The properties of the nonlinear susceptibility tensors are presented in details, with a focus on their symmetry properties.

Contents

2.1 Learning outcomes

The learning outcomes of this chapter are the following:

By the end of this chapter, students will know:

- the relation between the macroscopic polarization and the electric field (the so-called constitutive relations of nonlinear optics)
- the basic properties of nonlinear susceptibility tensors.

By the end of this chapter, students will be skilled at:

- Manipulating the nonlinear susceptibility tensor components and, with given incident fields, calculate the components of nonlinear polarisation vector.

2.2 Linear susceptibility

The constitutive relation between the linear polarization $\boldsymbol{P}(t)$ and the incident electric field $\boldsymbol{E}(t)$ in the frequency domain is given by:

$$\boxed{\boldsymbol{P}(\omega) = \epsilon_0 \underline{\underline{\chi}}^{(1)}(\omega)\boldsymbol{E}(\omega),}$$

where we have introduced the linear susceptibility $\underline{\underline{\chi}}^{(1)}(\omega)$. One can show that the linear susceptibility is directly proportional to the Fourier transform of system's impulse response :

$$\underline{\underline{\chi}}^{(1)}(\omega) = 2\pi \,\mathrm{TF}\left[\underline{\underline{R}}^{(1)}(t)\right].$$

A time invariant system implies that the impulse response does not depend on the time of excitation, but it directly depends on the time delay between the response and the excitation. This assumption yields:

$$\begin{aligned} \boldsymbol{\mathcal{P}}(t) &= \epsilon_0 \int \underline{\underline{R}}^{(1)}(t-\tau)\boldsymbol{\mathcal{E}}(\tau)d\tau, \\ &= \epsilon_0 \int \underline{\underline{R}}^{(1)}(\tau)\boldsymbol{\mathcal{E}}(t-\tau)d\tau \end{aligned} \tag{2.1}$$

A causal system implies that $\underline{\underline{R}}^{(1)}(\tau) = 0$ for $\tau < 0$.
The conventions for the Fourier transform that will be used in the course are :

Convention for the Fourier transform :

$$\boldsymbol{E}(t) = \int \boldsymbol{E}(\omega)e^{-\imath\omega t}d\omega$$

$$\boldsymbol{E}(\omega) = \frac{1}{2\pi}\int \boldsymbol{E}(t)e^{+\imath\omega t}dt$$

The reality of the function $\underline{\underline{R}}^{(1)}(t)$ implies that $\underline{\underline{\chi}}^{(1)}(\omega)^\star = \underline{\underline{\chi}}^{(1)}(-\omega)$. Finally, the causality property enables to derive the Kramers-Kronig relations that relates the real and imaginary parts of the linear susceptibility.

2.3 Nonlinear susceptibility tensors

Following this reminder on the linear propagation regime of electromagnetic waves, we next study the case of the nonlinear propagation. As in the linear case, it requires to set a general form for the relation between the macroscopic polarization $\boldsymbol{\mathcal{P}}$ and the electric field $\boldsymbol{\mathcal{E}}$. We consider first an incident electromagnetic field upon a causal and time invariant system with a nonlinear impulse response. Subsequently, the electric dipole approximation is assumed, which consists in neglecting the quadripole term in the constitutive relation and the polarization term is developed in power series expansion of the electric field:

$$\boldsymbol{\mathcal{P}}(t) = \boldsymbol{\mathcal{P}}^{(1)}(t) + \boldsymbol{\mathcal{P}}^{(2)}(t) + \boldsymbol{\mathcal{P}}^{(3)}(t) + \cdots, \tag{2.2}$$

where $\boldsymbol{\mathcal{P}}^{(1)}(t)$ is a linear function of $\boldsymbol{\mathcal{E}}$ (linear response), $\boldsymbol{\mathcal{P}}^{(2)}(t)$ is a quadratic function of $\boldsymbol{\mathcal{E}}$ (2nd order nonlinear response), etc. Having defined the nonlinear response of the material in the time domain, we can write this relation in the frequency domain and define a nonlinear susceptibility, similarly to the case of a linear susceptibility. The properties of the nonlinear susceptibility tensors will be presented in details, especially their symmetry properties.

2.3.1 Nonlinear impulse response

A generalization of the linear time response (2.1) applied to the 2nd order yields:

$$\boldsymbol{\mathcal{P}}^{(2)}(t) = \epsilon_0 \int\int \underline{\underline{\underline{T}}}^{(2)}(t;\tau_1,\tau_2)\boldsymbol{\mathcal{E}}(\tau_1)\boldsymbol{\mathcal{E}}(\tau_2)d\tau_1 d\tau_2, \tag{2.3}$$

with $\underline{\underline{\underline{T}}}^{(2)}(t;\tau_1,\tau_2)$ the 2nd order nonlinear impulse response, which is a 3rd order tensor in order to fully describe the quadratic dependance of the 2nd order nonlinear polarization. For a given applied field $\boldsymbol{E}(t)$, and assuming a given function $\underline{\underline{\underline{T}}}^{(2)}(t;\tau_1,\tau_2)$, the relation (2.3) determines the time evolution of the 3 vectorial components for the second order polarization $\boldsymbol{\mathcal{P}}^{(2)}(t)$, which is induced by the nonlinear interaction between the incident field and the medium. The ith component is given by:

$$\mathcal{P}_i^{(2)}(t) = \epsilon_0 \sum_{(j,k)} \int\int T_{ijk}^{(2)}(t;\tau_1,\tau_2)\mathcal{E}_j(\tau_1)\mathcal{E}_k(\tau_2)d\tau_1 d\tau_2, \tag{2.4}$$

where $T_{ijk}^{(2)}$ is the component ijk of the tensor $\underline{\underline{\underline{T}}}^{(2)}$, $\mathcal{E}_{i,j,k}$ and $\mathcal{P}_{i,j,k}$ are the three vectorial components of $\boldsymbol{\mathcal{E}}$ and $\boldsymbol{\mathcal{P}}$.

Properties of the nonlinear pulse response

- Symmetry condition: The tensor $\underline{\underline{\underline{T}}}^{(2)}$ can be expressed as the summation of a symmetric and an antisymmetric tensor:

$$T_{ijk}^{(2)}(t;\tau_1,\tau_2) = S_{ijk}^{(2)}(t;\tau_1,\tau_2) + A_{ijk}^{(2)}(t;\tau_1,\tau_2), \tag{2.5}$$

where

$$S_{ijk}^{(2)} = \frac{1}{2}\left[T_{ijk}^{(2)}(t;\tau_1,\tau_2) + T_{ikj}^{(2)}(t;\tau_2,\tau_1)\right]$$

is a symmetric tensor[1], and

$$A_{ijk}^{(2)} = \frac{1}{2}\left[T_{ijk}^{(2)}(t;\tau_1,\tau_2) - T_{ikj}^{(2)}(t;\tau_2,\tau_1)\right]$$

[1] $S_{ijk}^{(2)}(t;\tau_1,\tau_2) = S_{ikj}^{(2)}(t;\tau_2,\tau_1)$

is an antisymmetric tensor[2]. Substituting (2.5) in (2.4) shows that the antisymmetric tensor does not contribute to the expression of P_i and vanishes. In conclusion, the tensor $\underline{\underline{\underline{T}}}^{(2)}$ is symmetric and :

$$T^{(2)}_{ijk}(t;\tau_1,\tau_2) = T^{(2)}_{ikj}(t;\tau_2,\tau_1) \tag{2.6}$$

- **Time invariant response property:** As we have assumed a time invariance in the system response, the impulse response shall not depend on the time of excitation and the equality

$$\underline{\underline{\underline{T}}}^{(2)}(t+t_0;\tau_1,\tau_2) = \underline{\underline{\underline{T}}}^{(2)}(t;\tau_1-t_0,\tau_2-t_0)$$

is valid for any given time t. In particular, it is verified for $t=0$ and we can write an impulse response with a dependence on the time delay between the excitation and the response times:

$$\underline{\underline{\underline{T}}}^{(2)}(t;\tau_1,\tau_2) = \underline{\underline{\underline{R}}}^{(2)}(t-\tau_1,t-\tau_2). \tag{2.7}$$

The second order nonlinear time response is then rewritten into the form:

$$\begin{aligned}\boldsymbol{\mathcal{P}}^{(2)}(t) &= \epsilon_0 \int\int \underline{\underline{\underline{R}}}^{(2)}(t-\tau_1,t-\tau_2)\boldsymbol{\mathcal{E}}(\tau_1)\boldsymbol{\mathcal{E}}(\tau_2)d\tau_1 d\tau_2,\\ &= \epsilon_0 \int\int \underline{\underline{\underline{R}}}^{(2)}(\tau_1,\tau_2)\boldsymbol{\mathcal{E}}(t-\tau_1)\boldsymbol{\mathcal{E}}(t-\tau_2)d\tau_1 d\tau_2.\end{aligned} \tag{2.8}$$

- **Causal system:** The causality property implies that $\underline{\underline{\underline{R}}}^{(2)}(\tau_1,\tau_2)=0$ for $\tau_1<0$ and $\tau_2<0$.

- **Real function:** The field vectors are real quantities which imply the reality of the nonlinear impulse response.

- **Intrinsic permutation property:** We have shown that the tensor $\underline{\underline{\underline{R}}}^{(2)}$ is symmetric. It means that the component $R^{(2)}_{ijk}(\tau_1,\tau_2)$ is invariant through the simultaneous permutation of the couple of indices (j,τ_1) and (k,τ_2).

nth order nonlinear pulse response

The nth nonlinear contribution to the response function is given by :

$$\boldsymbol{\mathcal{P}}^{(n)}(t) = \epsilon_0 \int\int\cdots\int \underbrace{\underline{\underline{\underline{R}}}}_{n}^{(n)}(t;\tau_1,\tau_2,\cdots,\tau_n)\boldsymbol{\mathcal{E}}(t-\tau_1)\boldsymbol{\mathcal{E}}(t-\tau_2)\cdots\boldsymbol{\mathcal{E}}(t-\tau_n)d\tau_1 d\tau_2\cdots d\tau_n. \tag{2.9}$$

The properties listed for the 2nd order nonlinear time response are generalized to any nth order nonlinear time response.

2.3.2 2nd order nonlinear susceptibility

In order to derive a relation between the polarization and the electric field in the frequency domain, the polarization $\boldsymbol{\mathcal{P}}^{(2)}(t)$ is written in terms of Fourier components:

$$\begin{aligned}\boldsymbol{\mathcal{P}}^{(2)}(t) &= \int \boldsymbol{P}^{(2)}(\omega)e^{-\imath\omega t}d\omega\\ &= \epsilon_0 \int\int \underline{\underline{\underline{R}}}^{(2)}(\tau_1,\tau_2)\boldsymbol{\mathcal{E}}(t-\tau_1)\boldsymbol{\mathcal{E}}(t-\tau_2)d\tau_1 d\tau_2.\end{aligned}$$

[2] $A^{(2)}_{ijk}(t;\tau_1,\tau_2) = -A^{(2)}_{ikj}(t;\tau_2,\tau_1)$

Substituting the relation $\boldsymbol{\mathcal{E}}(t-\tau) = \int \boldsymbol{E}(\omega) e^{-\imath\omega(t-\tau)} d\omega$, we obtain:

$$\boldsymbol{\mathcal{P}}^{(2)}(t) = \epsilon_0 \int\int \underline{\underline{\chi}}^{(2)}(\omega;\omega_1,\omega_2)\boldsymbol{E}(\omega_1)\boldsymbol{E}(\omega_2) e^{-\imath(\omega_1+\omega_2)t} d\omega_1 d\omega_2, \tag{2.10}$$

where we have introduced a 2nd order nonlinear susceptibilities $\underline{\underline{\chi}}^{(2)}(\omega;\omega_1,\omega_2)$ that turns to be proportional to the Fourier transform of the nonlinear pulse response,

$$\begin{aligned} \underline{\underline{\chi}}^{(2)}(\omega;\omega_1,\omega_2) &= \int\int \underline{\underline{R}}^{(2)}(\tau_1,\tau_2) e^{\imath(\omega_1\tau_1+\omega_2\tau_2)} d\tau_1 d\tau_2. \\ &= (2\pi)^2 \mathrm{TF}\left[\underline{\underline{R}}^{(2)}(\tau_1,\tau_2)\right]. \end{aligned}$$

As the complexe amplitude for the 2nd order nonlinear polarization is $\boldsymbol{P}^{(2)}(\omega) = \frac{1}{2\pi}\int \boldsymbol{\mathcal{P}}^{(2)}(t) e^{\imath\omega t} dt$, it yields:

$$\boldsymbol{P}^{(2)}(\omega) = \frac{\epsilon_0}{2\pi}\int\int \underline{\underline{\chi}}^{(2)}(\omega;\omega_1,\omega_2)\boldsymbol{E}(\omega_1)\boldsymbol{E}(\omega_2) d\omega_1 d\omega_2 \int e^{-\imath(\omega_1+\omega_2)t} e^{\imath\omega t} dt.$$

The latter integral is equal to the Dirac function $\delta(\omega-\omega_1-\omega_2)$ that is equal to 0 except for $\omega = \omega_1+\omega_2$. Finally, we find the constitutive relation for the 2nd order nonlinear optical interactions :

$$\boxed{\boldsymbol{P}^{(2)}(\omega) = \epsilon_0 \int\int \underline{\underline{\chi}}^{(2)}(\omega;\omega_1,\omega_2)\boldsymbol{E}(\omega_1)\boldsymbol{E}(\omega_2)\delta(\omega-\omega_1-\omega_2) d\omega_1 d\omega_2,} \tag{2.11}$$

which is equal to 0 except for $\omega = \omega_1+\omega_2$.

This constitutive relation demonstrates that the interaction between waves at ω_1 and ω_2 through a 2nd order nonlinear leads to the generation of a polarization term at the frequency $\omega = \omega_1+\omega_2$. In case of two single frequencies at ω_1 and ω_2, the relation is simply equal to

$$\boxed{\boldsymbol{P}^{(2)}(\omega=\omega_1+\omega_2) = \epsilon_0 \underline{\underline{\chi}}^{(2)}(\omega=\omega_1+\omega_2;\omega_1,\omega_2)\boldsymbol{E}(\omega_1)\boldsymbol{E}(\omega_2)} \tag{2.12}$$

Notice that the frequency arguments can take either positive or negative values, which comes from the assumption for the electric field $\boldsymbol{\mathcal{E}}(t)$ to be a purely real quantity (see (1.3)).

As an illustration and depending on the interacting frequency components, we can list a variety of 2nd order nonlinear interactions :

- A situation where $\omega_1 = \omega_2$ generates a polarization $\boldsymbol{P}^{(2)}(2\omega)$: second harmonic generation,
- A situation where $\omega_1 = -\omega_2$ generates a static polarization $\boldsymbol{P}^{(2)}(0)$: optical rectification,
- A situation where $\omega_1 = \omega$ and $\omega_2 = 0$ describes the electro-optic effect,
- A situation where $\omega_1 \neq \omega_2$ generates a polarization $\boldsymbol{P}^{(2)}(\omega_1+\omega_2)$ and $\boldsymbol{P}^{(2)}(\omega_1-\omega_2)$: respectively the sum and difference frequency generation.

Each vectorial component of the polarization can be expressed in terms the tensorial components $\chi^{(2)}_{ijk}(\omega=\omega_1+\omega_2;\omega_1,\omega_2)$ and the electric field components $E_{i,j,k}(\omega)$:

$$P^{(2)}_i(\omega_1+\omega_2) = \epsilon_0 \sum_{jk} \chi^{(2)}_{ijk}(\omega_1+\omega_2;\omega_1,\omega_2) E_j(\omega_1) E_k(\omega_2).$$

In accordance with the constitutive relation (2.11), each component might also require to sum over the frequency arguments:

$$P_i(\omega = \omega_p + \omega_q) = \epsilon_0 \sum_{jk} \sum_{(pq)} \chi^{(2)}_{ijk}(\omega = \omega_p + \omega_q; \omega_p, \omega_q) E_j(\omega_p), E_k(\omega_q).$$

$$\boldsymbol{P}(\omega = \omega_p + \omega_q) = \epsilon_0 \sum_{(pq)} \underset{\equiv}{\chi}^{(2)}(\omega = \omega_p + \omega_q; \omega_p, \omega_q) \boldsymbol{E}(\omega_p) \boldsymbol{E}(\omega_q),$$

where we have considered here a discrete number of frequency components.

2.3.3 3rd order nonlinear susceptibility

In the same way, the constitutive relation for the 3rd order nonlinear optical interactions is defined:

$$\boxed{\boldsymbol{P}^{(3)}(\omega = \omega_p + \omega_q + \omega_r) = \epsilon_0 \textstyle\sum_{(pqr)} \underset{\equiv\equiv}{\chi}^{(3)}(\omega = \omega_p + \omega_q + \omega_r; \omega_p, \omega_q, \omega_r) \boldsymbol{E}(\omega_p) \boldsymbol{E}(\omega_q) \boldsymbol{E}(\omega_r)} \tag{2.13}$$

Summing over the frequency arguments gives the relations:

$$P^{(3)}_i(\omega = \omega_p + \omega_q + \omega_r) = \epsilon_0 \sum_{jkl} \sum_{(pqr)} \chi^{(3)}_{ijkl}(\omega = \omega_p + \omega_q + \omega_r; \omega_p, \omega_q, \omega_r) E_j(\omega_p) E_k(\omega_q) E_l(\omega_r)$$

$$\boldsymbol{P}^{(3)}(\omega = \omega_p + \omega_q + \omega_r) = \epsilon_0 \sum_{(pqr)} \underset{\equiv\equiv}{\chi}^{(3)}(\omega = \omega_p + \omega_q + \omega_r; \omega_p, \omega_q, \omega_r) \boldsymbol{E}(\omega_p) \boldsymbol{E}(\omega_q) \boldsymbol{E}(\omega_r)$$

2.3.4 nth order nonlinear susceptibility

The generalization to the nth order nonlinear interactions is straightforward. The related constitutive relation for the nth order nonlinear polarization vector implies the interaction of n electric field vectors through an $n+1$ rank tensor.

2.3.5 Properties of the nonlinear susceptibility tensors

- Real functions: The reality of the quantities $\boldsymbol{P}(t)$ and $\boldsymbol{E}(t)$ implies

$$\chi^{(2)}_{ijk}(\omega_3; \omega_1, \omega_2)^\star = \chi^{(2)}_{ijk}(-\omega_3; -\omega_1, -\omega_2).$$

- Intrinsic permutation symmetry: The two quantities :

$$\chi^{(2)}_{ijk}(\omega_3; \omega_1, \omega_2) E_j(\omega_1) E_k(\omega_2)$$

and

$$\chi^{(2)}_{ikj}(\omega_3; \omega_2, \omega_1) E_k(\omega_2) E_j(\omega_1)$$

are identical.

$$\chi^{(2)}_{ijk}(\omega_3 = \omega_1 + \omega_2; \omega_1, \omega_2) = \chi^{(2)}_{ikj}(\omega_3 = \omega_1 + \omega_2; \omega_2, \omega_1).$$

- **Purely real quantity:** In situations where the frequencies of the interacted waves are far from any material resonances, the expressions established within the classical anharmonic oscillator model (see section (1.3.1) show that the nonlinear susceptibilities are purely real quantities[3]. More generally, the quantum mechanical derivation of susceptibilities shows that *in a lossless medium*, the components $\chi^{(2)}_{ijk}(\omega_3 = \omega_1 + \omega_2, \omega_1, \omega_2)$ are real.

- **Degeneracy Factor:** We consider the case of a three-wave mixing between waves at ω_1, ω_2 and $\omega_3 = \omega_1 + \omega_2$. The nonlinear polarization components at ω_3 is:

$$P_i(\omega_3) = \epsilon_0 \sum_{jk} \left[\chi^{(2)}_{ijk}(\omega_3; \omega_1, \omega_2) E_j(\omega_1) E_k(\omega_2) + \chi^{(2)}_{ijk}(\omega_3; \omega_2, \omega_1) E_j(\omega_2) E_k(\omega_1) \right]. \quad (2.14)$$

The intrinsic permutation symmetry for the nonlinear susceptibilities implies that the two right hand side terms are equal (they differ by a permutation between the frequency arguments ω_1 and ω_2), and yields:

$$P_i(\omega_3) = 2\epsilon_0 \sum_{jk} \chi^{(2)}_{ijk}(\omega_3; \omega_1, \omega_2) E_j(\omega_1) E_k(\omega_2).$$

The factor 2 in the latter equation is called the *degeneracy factor* and relies on the fact that the interacted wave are discernible. Waves are discernible if they differ either in frequency, in polarization, in wave vector (in the direction of propagation), in spatial mode. In the case of the second-harmonic generation, the degeneracy factor is equal to 2 as $j \neq k$. If not, it takes the value 1, meaning that the interacted waves at ω can not be distinguished.

To summarize, the second-order nonlinear polarization components can be expressed as:

$$P_i(\omega_3) = D^{(2)} \epsilon_0 \sum_{jk} \chi^{(2)}_{ijk}(\omega_3; \omega_1, \omega_2) E_j(\omega_1) E_k(\omega_2), \quad (2.15)$$

with $D^{(2)}$ the degeneracy factor that accounts for the number of distinct permutation between the applied fields. It can take the values :

- $D^{(2)} = 1$ in the case of one distinct field,
- $D^{(2)} = 2$ in the case of 2 distinct fields.

The degeneracy factor for the third order nonlinear polarization components take the values:

- $D^{(2)} = 1$ in the case of one distinct field,
- $D^{(2)} = 3$ in the case of 2 distinct fields,
- $D^{(2)} = 3! = 6$ in the case of 3 distinct fields.

- **Kleinman's symmetry:** For a lossless medium, it can be shown that a sufficient condition is

$$\chi^{(2)}_{ijk}(\omega_3 = \omega_1 + \omega_2; \omega_1, \omega_2) = \chi^{(2)}_{jki}(-\omega_1 = \omega_2 - \omega_3; \omega_2, -\omega_3) = \chi^{(2)}_{kji}(-\omega_2 = \omega_1 - \omega_3; \omega_1, -\omega_3). \quad (2.16)$$

This condition can be derived (see tutorial) in a simple way from the expression of the average power transferred by the electromagnetic field to the medium per volume unit[4]:

$$-\frac{\partial W}{\partial t} = \langle \boldsymbol{\mathcal{E}} \cdot \frac{\partial \boldsymbol{\mathcal{P}}}{\partial t} \rangle,$$

[3] The damping terms can be neglected in this case.
[4] Cf. A. Yariv, *Quantum Electronics*, Third edition, Chapter 5.

where $\langle ... \rangle$ stands for a time average. The simultaneous permutations of the indices with the frequency arguments in (2.16) can be further extended by neglecting the dispersion of the nonlinear susceptibilities for any strong non-resonant interaction. The relation (2.16) becomes:

$$\begin{aligned} \chi^{(2)}_{ijk}(\omega_3 = \omega_1 + \omega_2; \omega_1, \omega_2) &= \chi^{(2)}_{jki}(\omega_3 = \omega_1 + \omega_2; \omega_1, \omega_2) = \chi^{(2)}_{kji}(\omega_3 = \omega_1 + \omega_2; \omega_1, \omega_2) \\ &= +\text{Intrinsic permutations} \end{aligned} \tag{2.17}$$

In conclusion, the nonlinear susceptibilities in lossless media, which implies no exchange of energy between the nonlinear medium and the interacted waves, support a full permutation of the indices, without permuting the frequencies.

- **Contracted notations:** Let us introduce the tensor $d_{ijk} = \frac{1}{2}\chi^{(2)}_{ijk}$. We assume that the component d_{ijk} is symmetric in its last two indices. This assumption is valid whenever Kleinman's symmetry condition is valid or and in addition is valid in general for two wave mixing (as $\omega_1 = \omega_2 = \omega$).

  The notation d_{ijk} is then replaced by a contracted notation d_{il} according to the correspondence between indices l and (j, k) given in Tab. 2.1.

Tab. 2.1. Relations between d_{ijk} and the contracted notation d_{il}.

jk	11	22	33	23 ou 32	13 ou 31	12 ou 21
l	1	2	3	4	5	6

  Notice that the contracted notation may differ by a factor 1/2 in different textbooks or in nonlinear crystal datasheets.

- **Spatial symmetries:** The symmetry properties of materials allow a significant reduction in the number of tensor components to be determined. Among those symmetries, let consider a nonlinear medium with a centrosymmetry. It means that nonlinear susceptibility tensor is invariant through the transformation $i \to -i$, with $i = x, y, z$, the three spatial coordinates. Because of the transformations $\boldsymbol{E} \to -\boldsymbol{E}$ and $\boldsymbol{P} \to -\boldsymbol{P}$ under the centro-symmetry, we conclude that all the components of the tensor $\underline{\underline{\underline{\chi^{(2)}}}}(\omega_3, \omega_1, \omega_2)$ must vanish identically. More generally, centro-symmetric materials do not support any *even* order optical nonlinearities.

Chapter 3

Nonlinear wave equations

In the previous chapters, we have introduced the constitutive relations for nonlinear optics that explicite in particular the relation between the electric field and the macroscopic polarization vector by means of nonlinear susceptibility tensors. In the present chapter we examine the modification of the electromagnetic field during its propagation through a material subject to optical nonlinear interactions by deriving nonlinear wave equations in various situations.

At first, we demonstrate a generic equation in the case of the propagation of a stationary and uniform monochromatic wave through a nonlinear material. Assuming the slowly varying approximation for the envelop of the fields, the nonlinear wave equation takes the form of a first order differential equation. The importance of the phase matching condition will be underlined and discussed in details. As the most common method to fulfill the phase matching condition utilizes the birefringence properties of materials, a short reminder on optics in anisotropic materials is presented. We next show that the nonlinear propagation of waves in an anisotropic material can be treated as the propagation in an isotropic material by priorly decompose the incoming field other the eigen polarization states, namely the ordinary and the extraordinary fields.

To complete, we derive nonlinear wave equations for temporal and spatial wave-packets, which can be applied to describe the nonlinear propagation of laser pulses and laser beams through a nonlinear material. Finally, we consider the case of nonlinear interactions that take place in a waveguide and derive a specific nonlinear wave equation under the weak guidance approximation.

Contents

3.1 Learning outcomes

The learning outcomes of this chapter are the following:

By the end of this chapter, students will be skilled at:

- deriving and solving the nonlinear wave equation in a parametric situation under the undepleted pump approximation,
- Determining the phase matching conditions for a given nonlinear interaction and achieving/fulfilling this condition by exploiting birefringence properties of materials.

By the end of this chapter, students will understand:

- Nonlinear optics is an essential tool to create novel optical frequencies generated through the interaction of incident beams within nonlinear materials,
- Nonlinear effects are subject to phase matching conditions.

3.2 Linear wave equation

In this section, we briefly recall the properties of the wave propagation through a linear dielectric medium.

3.2.1 Linear wave equation in an anisotropic medium

The linear propagation of the electromagnetic fields in a dielectric medium, free of charges and current is governed by the following Maxwell's equations :

$$\begin{cases} \nabla \times \boldsymbol{\mathcal{E}} = -\dfrac{\partial \boldsymbol{B}}{\partial t} & \nabla \cdot \boldsymbol{\mathcal{D}} = 0 \\ \nabla \times \boldsymbol{H} = \dfrac{\partial \boldsymbol{\mathcal{D}}}{\partial t} & \nabla \cdot \boldsymbol{B} = 0, \end{cases} \tag{3.1}$$

with the constitutive relations $\boldsymbol{\mathcal{D}} = \epsilon_0 \boldsymbol{\mathcal{E}} + \boldsymbol{\mathcal{P}}$ and $\boldsymbol{B} = \mu_0 \boldsymbol{H}$. In order to derive a wave equation for the electric field $\boldsymbol{\mathcal{E}}$, the magnetic field dependence is suppressed by taking the curl of the first equation, using the relation between $\boldsymbol{H}$ and $\boldsymbol{\mathcal{D}}$ and the constitutive relations:

$$\nabla \times \nabla \times \boldsymbol{\mathcal{E}}(t) + \frac{1}{c^2} \frac{\partial^2 \boldsymbol{\mathcal{E}}}{\partial t^2} = -\mu_0 \frac{\partial^2 \boldsymbol{\mathcal{P}}}{\partial t^2}. \tag{3.2}$$

In the Fourier domain, this wave equation becomes :

$$\nabla \times \nabla \times \boldsymbol{E}(\omega) - \frac{\omega^2}{c^2} \boldsymbol{E}(\omega) = \omega^2 \mu_0 \boldsymbol{P}(\omega). \tag{3.3}$$

An anisotropic medium is characterized by the tensorial relation between vectors $\boldsymbol{\mathcal{D}}$ and $\boldsymbol{\mathcal{E}}$. Conversely to an isotropic medium, the direction of the two vectors may differ:

$$\boldsymbol{D}(\omega) = \epsilon_0 \underline{\underline{\epsilon}}(\omega)\, \boldsymbol{E}(\omega), \tag{3.4}$$

with $\underline{\underline{\epsilon}}(\omega) = 1 + \underline{\underline{\chi}}^{(1)}(\omega)$. The principle axes define a basis for which the matrix $\underline{\underline{\epsilon}}$ is diagonal. For an electric field polarized along one of the principal axes, the medium is equivalent to an isotropic medium.

In the following, we recall the main propagation properties of a plane wave in a linear anisotropic medium. The complex field amplitude of the plane wave is defined as :

$$\boldsymbol{E}(\omega) = A(\omega)e^{\imath \boldsymbol{k}\cdot\boldsymbol{r}}\boldsymbol{e}. \tag{3.5}$$

Substituting this form into the wave equation (3.3) yields:

$$\boldsymbol{k} \times (\boldsymbol{k} \times \boldsymbol{e}) + \frac{\omega^2}{c^2}\underline{\underline{\epsilon}}(\omega)\boldsymbol{e} = 0. \tag{3.6}$$

This equation explicits the dependence between the wavevector and the direction of polarization of the electric field in an anisotropic medium. For a given propagation direction we need to determine both the refractive index n and the polarization of the field, which requires to solve (3.6). One can show that the values of n for a given propagation direction defined by a unitary vector $\boldsymbol{s}$, with $\boldsymbol{k} = |k|\boldsymbol{s} = n(\omega/c)\boldsymbol{s}$, are solution of the Fresnel's equation:

$$\frac{s_x^2}{n^2 - n_x^2} + \frac{s_y^2}{n^2 - n_y^2} + \frac{s_z^2}{n^2 - n_z^2} = \frac{1}{n^2}, \tag{3.7}$$

where (s_x, s_y, s_z) are the direction of propagation coordinates defined along the principal directions, denoted (x, y, z), and n_x, n_y, n_z are the principal refractive indices[1]. Actually, the Fresnel's equation is a quartic polynomial equation[2]. For a direction of propagation $\boldsymbol{s} = (s_x, s_y, s_z)$, one can show that this equation admits 2 positive roots for n. Each solution for the refractive index n is associated a polarization direction for the electric field given by the equation (3.6).

Finally, one can conclude that for any direction of propagation, two waves can propagate (independently) with phase velocity $v_1 = c/n_1$ and $v_2 = c/n_2$ where n_1 and n_2 are solutions of the Fresnel's equation (3.7).

The index of ellipsoid

An equivalent method to determine the refractive indices and the related directions of the electric fields is based on the index of ellipsoid. The latter is determined by calculating the electric energy density stored in a medium :

$$w_e = \frac{1}{2}\boldsymbol{E}\cdot\boldsymbol{D} = \frac{1}{2}\sum_{j,k} E_k \epsilon_{kj} E_j,$$

or equivalently,

$$2w_e = \epsilon_{XX}E_X^2 + \epsilon_{YY}E_Y^2 + \epsilon_{ZZ}E_Z^2 + 2\epsilon_{YZ}E_Y E_Z + 2\epsilon_{XZ}E_X E_Z + 2\epsilon_{XY}E_X E_Y. \tag{3.8}$$

The surface of constant energy forms an ellipsoid as the coefficients ϵ_{XX}, ϵ_{YY} and ϵ_{ZZ} are positive in case of a lossless material[3]. Equation (3.8) can be reduced to :

$$2w_e = \epsilon_{xx}E_x^2 + \epsilon_{yy}E_y^2 + \epsilon_{zz}E_z^2, \tag{3.9}$$

where x, y, z refers to the principal dielectric axes for which $\underline{\underline{\epsilon}}$ is diagonal. The constant energy surfaces in the space (D_x, D_y, D_z) form ellipsoids defined by:

$$2w_e = \frac{D_x^2}{\epsilon_{xx}} + \frac{D_y^2}{\epsilon_{yy}} + \frac{D_z^2}{\epsilon_{zz}}. \tag{3.10}$$

[1] For a wave polarized along one of the principal axes, for instance x, the relation $D_x = \epsilon_x E_x$ is satisfied, where $\epsilon_x = \epsilon_0(1 + \chi_{xx}^{(1)})$ is the permitivity. The refractive index is defined as : $n_x^2 = c^2\epsilon_x\mu_0$.

[2] A quartic polynomial equation is an equation of the form : $n^4 + an^3 + bn^2 + cn + d = 0$.

[3] Assuming a field polarized along the direction X, the electric energy density is equal to $2w_e = \epsilon_{xX}E_X^2$, meaning that $w_e > 0$ implies that $\epsilon_{XX} > 0$

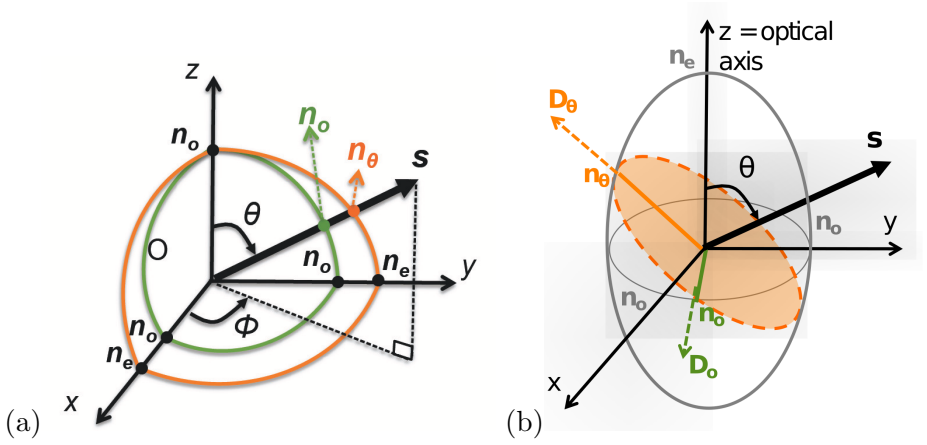

Fig. 3.1. (a) Intersection between the wavevector direction $\boldsymbol{s}$ and the surface of indices for a uniaxial crystal. The two intersections give the two refractive indices n_o and n_θ, which can be seen on the index of ellipsoid (b) showing the directions for the related ordinary $\boldsymbol{e}_o$ and extraordinary $\boldsymbol{e}_\theta$ waves.

One can rewrite the latter equation using the new variable $\boldsymbol{r} = \frac{\boldsymbol{D}}{\sqrt{2w_e\epsilon_0}}$ and $\epsilon_i = n_i^2$:

$$\frac{x^2}{n_x^2} + \frac{y^2}{n_y^2} + \frac{z^2}{n_z^2} = 1, \tag{3.11}$$

It defines the index of ellipsoid equation that is used to determine, for any direction of propagation, the two refractive indices and the associated direction for $\boldsymbol{D}$. The two axes of the ellipse formed by the intersection between the plane perpendicular to $\boldsymbol{s}$, the direction of propagation, and the ellipsoid, are equal to $2n_a$ and $2n_b$. Their related field $\boldsymbol{D}_a$ and $\boldsymbol{D}_b$ are parallel to these two axes (see figure 3.1(b)).

Uniaxial birefringent media

An uniaxial birefringent medium exhibits two identical principal refractive indices : $n_x = n_y = n_o$ and $n_z = n_e \neq n_o$. We consider the propagation of a wave along the direction $\boldsymbol{s}$, which is defined in the crystallographic principle axes of the crystal in terms of the Euler's Angles:

$$\boldsymbol{s} = \begin{vmatrix} \cos\phi\sin\theta \\ \sin\phi\sin\theta \\ \cos\theta \end{vmatrix}.$$

Solutions of Eq. (3.7) are graphically represented in Fig. 3.1(a). Along the given propagation direction $\boldsymbol{s}$, the medium exhibits two refractive indices n_o and n_θ:

$$\left(\frac{1}{n_\theta}\right)^2 = \left(\frac{\cos\theta}{n_o}\right)^2 + \left(\frac{\sin\theta}{n_e}\right)^2,$$

which are respectively related to the polarization states $\boldsymbol{e}_o$ and $\boldsymbol{e}_\theta$ (see Fig. 3.1(b)):

$$\boldsymbol{e}_o = \begin{vmatrix} \sin\phi \\ -\cos\phi \\ 0 \end{vmatrix}, \quad \boldsymbol{e}_\theta = \begin{vmatrix} -\cos\theta\cos\phi \\ -\cos\theta\sin\phi \\ \sin\theta \end{vmatrix}.$$

These two polarizations are called *ordinary* and *extraordinary* polarization states. They are orthogonal and define the eigen modes of the medium along the direction of propagation $\boldsymbol{s}$.

3.2.2 Field intensity

The intensity of a wave ω is given by the magnitude of the time averaged Poynting vector:

$$\langle \boldsymbol{\mathcal{S}} \rangle = \langle \boldsymbol{\mathcal{E}} \times \boldsymbol{H} \rangle. \tag{3.12}$$

The intensity associated with a field

$$\boldsymbol{\mathcal{E}}(t) = E_0 e^{-\imath(\omega t - kz)}\boldsymbol{e} + CC$$
$$\boldsymbol{H}(t) = H_0 e^{-\imath(\omega t - kz)}\boldsymbol{e} + CC$$

is

$$I = 2nc\epsilon_0 |E_0|^2, \tag{3.13}$$

with n the refractive index of the medium at ω. We have used the relation $|H_0| = \epsilon_0 nc|E_0|$ (see Maxwell's equations).

3.2.3 Transfer of energy between an electromagnetic field and a medium

The power per unit volume that is transferred from the field to the medium (specifically to the electric dipoles) is given by the relation:

$$-\frac{\partial W}{\partial t} = \langle \boldsymbol{\mathcal{E}} \cdot \frac{\partial \boldsymbol{\mathcal{P}}}{\partial t} \rangle. \tag{3.14}$$

We consider the simple case of the propagation of a monochromatic wave in the linear regime. The electric field and the macroscopic polarization take the following form:

$$\boldsymbol{\mathcal{E}}(t) = \boldsymbol{E}(\omega)e^{-\imath\omega t} + \boldsymbol{E}(-\omega)e^{+\imath\omega t}$$
$$\boldsymbol{\mathcal{P}}(t) = \boldsymbol{P}(\omega)e^{-\imath\omega t} + \boldsymbol{P}(-\omega)e^{+\imath\omega t},$$

with $\boldsymbol{P}(\omega) = \epsilon_0 \underline{\underline{\chi}}^{(1)}(\omega)\boldsymbol{E}(\omega)$. Substituting these relations into (3.14) leads to the equality:

$$-\frac{\partial W}{\partial t} = 2\omega\epsilon_0 \left(\boldsymbol{e} \cdot \underline{\underline{\chi}}^{(1)''}(\omega)\boldsymbol{e}\right) |E(\omega)|^2, \tag{3.15}$$

with $\underline{\underline{\chi}}^{(1)}(\omega) = \underline{\underline{\chi}}^{(1)'} + \imath\, \underline{\underline{\chi}}^{(1)''}$.

In conclusion, the absorption phenomenon is related to the imaginary part of susceptibility.

3.3 Nonlinear wave equations

Following the propagation of the electromagnetic field in the linear regime, we next study the propagation under the nonlinear regime. Besides the linear macroscopic polarization, we need to add in the constitutive relation $\boldsymbol{\mathcal{D}} = \epsilon_0\boldsymbol{\mathcal{E}} + \boldsymbol{\mathcal{P}}$ a nonlinear source term $\boldsymbol{\mathcal{P}}^{(NL)}$. The wave equation (3.2), which is valid is the linear regime, contains now a nonlinear polarization vector:

$$\nabla \times \nabla \times \boldsymbol{\mathcal{E}}(\boldsymbol{r},t) + \frac{1}{c^2}\frac{\partial^2 \boldsymbol{\mathcal{E}}(\boldsymbol{r},t)}{\partial t^2} = -\mu_0 \frac{\partial^2 \boldsymbol{\mathcal{P}}^{(1)}(\boldsymbol{r},t)}{\partial t^2} - \mu_0 \frac{\partial^2 \boldsymbol{\mathcal{P}}^{(NL)}(\boldsymbol{r},t)}{\partial t^2}, \tag{3.16}$$

In the time Fourier domain, the wave equation becomes:

$$\nabla \times \nabla \times \boldsymbol{E}(\boldsymbol{r},\omega) - \frac{\omega^2}{c^2}\boldsymbol{E}(\boldsymbol{r},\omega) = \omega^2\mu_0 \boldsymbol{P}^{(1)}(\boldsymbol{r},\omega) + \omega^2\mu_0 \boldsymbol{P}^{(NL)}(\boldsymbol{r},\omega). \tag{3.17}$$

In the case of a material with a local response of the the linear contribution:

$$\boldsymbol{P}^{(1)}(\boldsymbol{r},\omega) = \epsilon_0 \underline{\underline{\chi}}^{(1)}(\boldsymbol{r},\omega)\boldsymbol{E}(\boldsymbol{r},\omega),$$

which leads to nonlinear wave equation:

$$\boxed{\nabla \times \nabla \times \boldsymbol{E}(\boldsymbol{r},\omega) = \frac{\omega^2}{c^2}\underline{\underline{\epsilon}}(\boldsymbol{r},\omega)\boldsymbol{E}(\boldsymbol{r},\omega) + \omega^2\mu_0 \boldsymbol{P}^{(NL)}(\boldsymbol{r},\omega)} \tag{3.18}$$

with the relative permitivity defined as,

$$\underline{\underline{\epsilon}}(\boldsymbol{r},\omega) = 1 + \underline{\underline{\chi}}^{(1)}(\boldsymbol{r},\omega).$$

We next specify the derivation of Eq. (3.18) for different cases, illustrating the related approximations that can be conducted.

3.3.1 Nonlinear propagation of a plane wave in a isotropic medium

Whereas, the propagation of a plane wave in a nonlinear regime does not fit with any realistic experimental situation (or very rarely), the corresponding nonlinear wave equation takes a simple form and underlines the main conditions under which an efficient nonlinear interaction will occur.

Actually, the following development corresponds to the propagation of a wave through a nonlinear material for which the transverse or temporal behaviors are not taken into account. For instance and for the case of a beam propagation, it would mean that the diffraction effect is neglected in the derivation of the nonlinear propagation.

An other simplification consists in assuming first an isotropic and homogeneous medium implying that the left hand side term of (3.18) is reduced to:

$$\nabla \times \nabla \times \boldsymbol{E}(\boldsymbol{r},\omega) = \nabla(\nabla \cdot \boldsymbol{E}) - \Delta \boldsymbol{E} = -\Delta \boldsymbol{E}.$$

The equation $\nabla \cdot (\boldsymbol{D}) = \nabla \cdot (\underline{\underline{\epsilon}}\boldsymbol{E}) = 0$ implies $\nabla \cdot \boldsymbol{E} = 0$, the permitivity being described by a scalar quantity, which does not depend on the spatial coordinate. The nonlinear wave equation becomes:

$$\Delta \boldsymbol{E}(\omega) + \frac{\omega^2}{c^2}\epsilon \boldsymbol{E}(\omega) = -\omega^2 \mu_0 \boldsymbol{P}_{NL}(\omega) \tag{3.19}$$

We next consider a plane wave propagating along the direction z, $\boldsymbol{E}(z,\omega) = A(z)e^{\imath kz}\boldsymbol{e}$. After substitution in (3.19), one gets:

$$\frac{\partial^2 A(z)}{\partial z^2} + 2\imath k \frac{\partial A(z)}{\partial z} = -\frac{\omega^2}{\epsilon_0 c^2}\boldsymbol{e} \cdot \boldsymbol{P}_{NL}(z,\omega)e^{-\imath kz},$$

taking into account the dispersion relation $k^2(\omega) = \frac{\omega^2}{c^2}\epsilon(\omega)$ for the material. A very frequent approximation consists in neglecting the variation of the field envelope $A(z)$ on a typical length of the order of the wavelength λ. Such an assumption stands for the *slowly varying envelope approximation*

$$\left|\frac{\partial^2 A(z)}{\partial z^2}\right| \ll \left|2k\frac{\partial A(z)}{\partial z}\right|,$$

and relies on the generally weak efficiency of the nonlinear interactions. Based on that, the nonlinear wave equation takes the very simple form:

$$\boxed{\frac{\partial A(z)}{\partial z} = \frac{\imath\omega}{2\epsilon_0 nc}\boldsymbol{e} \cdot \boldsymbol{P}_{NL}(z,\omega)e^{-\imath kz}} \tag{3.20}$$

We conclude that a wave at ω can be modified by a nonlinear term source $\boldsymbol{P}_{NL}(z,\omega)$ at ω if $\boldsymbol{e} \cdot \boldsymbol{P}_{NL}(z,\omega) \neq 0$. The second condition is related to the phase-matching condition related to the fact that the nonlinear polarisation amplitude $\boldsymbol{P}_{NL}(z,\omega)$ contains a phase term.

As an illustration, we next consider the case of the second-harmonic generation induced by the propagation of a wave ω in a $\chi^{(2)}$ material. The complex amplitude of the nonlinear polarization generated at 2ω is given by:

$$\begin{aligned}\boldsymbol{P}_{NL}(z,2\omega) &= \epsilon \underline{\underline{\chi}}^{(2)}(2\omega;\omega,\omega)\boldsymbol{e}_1\boldsymbol{e}_1 A^2(z,\omega)e^{2\imath \boldsymbol{k}(\omega)\cdot\boldsymbol{r}} \\ &= \boldsymbol{\Pi}_{NL}(z,\omega)\, e^{2\imath \boldsymbol{k}(\omega)\cdot\boldsymbol{r}},\end{aligned}$$

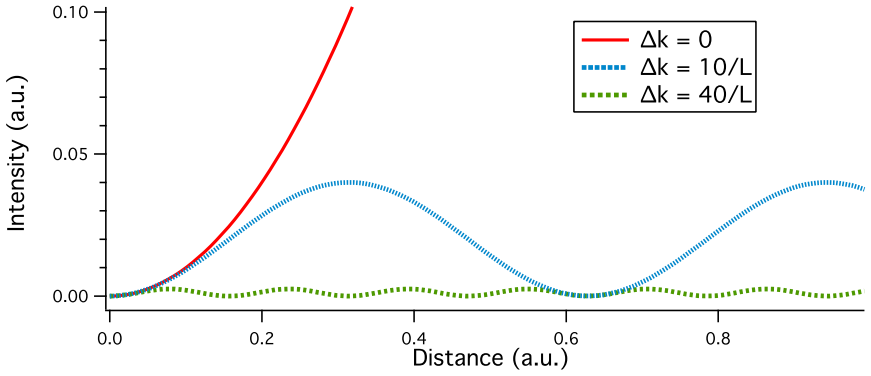

Fig. 3.2. Beam intensity evolution with the distance for three phase-matching conditions : $\Delta k = 0$, $\Delta k = 10/L$, $\Delta k = 40/L$, with L the thickness of the nonlinear material.

with $\mathbf{\Pi}_{NL}(z, 2\omega)$ the envelope amplitude of the nonlinear polarization. Even if the condition $\boldsymbol{e}_2 \cdot \boldsymbol{P}_{NL}(z, 2\omega) \neq 0$ would be respected, the second condition to be fulfilled in order to maximize the second-harmonic wave will be : $2\boldsymbol{k}(\omega) \cdot \boldsymbol{r} = \boldsymbol{k}(2\omega) \cdot \boldsymbol{r}$. This condition refers to the **phase-matching condition** that is discussed in the next paragraph.

3.3.2 Phase-matching condition

Following the previous illustration, the complex amplitude on the nonlinear polarisation is written in terms of an envelope $\mathbf{\Pi}_{NL}$ and a phase terme :

$$\boldsymbol{P}_{NL}(z, \omega) = \mathbf{\Pi}_{NL}(z, \omega)\, e^{\imath \boldsymbol{k}_p(\omega) \cdot \boldsymbol{r}}, \tag{3.21}$$

with $\boldsymbol{k}_p$ the wavevector related to the nonlinear polarization, which depends on the wavevectors of the interacted waves. The nonlinear wave equation (3.20) then takes the form :

$$\frac{\partial A(z)}{\partial z} = \frac{\imath\omega}{2\epsilon_0 nc} \boldsymbol{e} \cdot \mathbf{\Pi}_{NL}(z, \omega) e^{-\imath \Delta k z}, \tag{3.22}$$

with $\Delta k z = (\boldsymbol{k}_p - \boldsymbol{k}) \cdot \boldsymbol{z}$ the phase miss-match between the nonlinear polarization and the free-wave at ω. Assuming a very weak nonlinear interaction (also called, *parametric interaction*), we can suppose that the strength of the nonlinear polarisation is constant along z, i.e. $\mathbf{\Pi}_{NL}(z, \omega) \simeq Const.$. In such condition, the wave equation (3.22) can be easily integrated and the intensity evolution of the wave is given by:

$$\boxed{I(z) = \frac{\omega^2}{2nc\epsilon_0} |\boldsymbol{e} \cdot \mathbf{\Pi}_{NL}(\omega)|^2 \,\mathrm{sinc}^2\left(\frac{\Delta k L}{2}\right) L^2.} \tag{3.23}$$

The figure (3.2) shows the intensity evolution (3.23) for three phase-matching conditions: $\Delta k = 0$, $\Delta k = 10/L$, $\Delta k = 40/L$, with L the thickness of the nonlinear material. While the intensity grows with the square of the distance (under the assumption of a parametric interaction) in a case of a perfect phase-matching situation, it follows an oscillating behavior since $\Delta k \neq 0$. As the periodicity increases with Δk, the maximum intensity of the wave inversely decreases with Δk.

In the case of a non-phase matched interaction, it can be useful to define the **coherence length** $L_c = \pi/\Delta k$, which is equal to half of a period of the oscillating feature of the intensity.

3.3.3 Stationary nonlinear wave equation in a anisotropic medium

Most of the nonlinear materials exhibits birefringent properties, which will be of strong interest to fulfill the phase matching condition. In this paragraph, the stationary nonlinear propagation

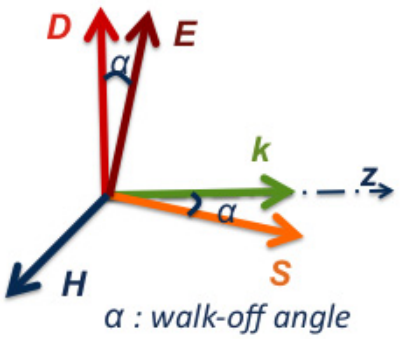

Fig. 3.3. Directions of $(\boldsymbol{D}, \boldsymbol{H}, \boldsymbol{k})$ for an electromagnetic wave propagating along the direction z in an anisotropic medium.

of a wave in an anisotropic material is described. A wave at ω, with a wavevector $\boldsymbol{k}$ is considered:

$$\boldsymbol{E}(\boldsymbol{r}, \omega) = A(\boldsymbol{r}) e^{\imath \boldsymbol{k}\cdot\boldsymbol{r}} \boldsymbol{e}$$

After substitution in the general form of the wave equation (3.18), and few developments, we get:

$$\begin{aligned} -\left[\boldsymbol{k}\times(\boldsymbol{k}\times\boldsymbol{e}) + \frac{\omega^2}{c^2}\underline{\underline{\epsilon}}(\omega)\boldsymbol{e}\right] A(\boldsymbol{r}) & \\ +\imath\left[\nabla A\times(\boldsymbol{k}\times\boldsymbol{e}) + \boldsymbol{k}\times(\nabla A\times\boldsymbol{e})\right] + \nabla\times(\nabla A\times\boldsymbol{e}) &= -\omega^2\mu_0 \boldsymbol{P}_{NL}(z,\omega) e^{-\imath\boldsymbol{k}\cdot\boldsymbol{r}} \end{aligned} \quad (3.24)$$

The decomposition of the wave along the eigen polarization states $\boldsymbol{e}_o$ and $\boldsymbol{e}_\theta$, i.e. $\boldsymbol{E} = \boldsymbol{E}_o + \boldsymbol{E}_\theta$, solutions of the Fresnel's equation (3.6), yields the simplification:

$$+\imath\left[\nabla A\times(\boldsymbol{k}\times\boldsymbol{e}) + \boldsymbol{k}\times(\nabla A\times\boldsymbol{e})\right] + \nabla\times(\nabla A\times\boldsymbol{e}) = -\omega^2\mu_0 \boldsymbol{P}_{NL}(z,\omega) e^{-\imath\boldsymbol{k}\cdot\boldsymbol{r}},$$

We assume that the slowly-varying approximation is valid, which is consists in assuming that

$$\left| k\frac{\partial A}{\partial x_i} \right| \gg \left| \frac{\partial^2 A}{\partial x_i \partial y_i} \right|.$$

Actually, this assumption imply to neglect the diffraction effects and to consider the propagation of plane waves in a nonlinear anisotropic material. Following this assumption, we get :

$$2\imath\nabla A\cdot[(\boldsymbol{k}\times\boldsymbol{e})\times\boldsymbol{e}] = \omega^2\mu_0 \boldsymbol{e}\cdot\boldsymbol{\Pi}_{NL}(z,\omega) e^{\imath\Delta\boldsymbol{k}\cdot\boldsymbol{r}}$$

In the coordinate system $(\boldsymbol{D}, \boldsymbol{H}, \boldsymbol{k})$ (see the figure 3.3), the wave equation is:

$$\boxed{-\tan\alpha\frac{\partial A}{\partial x} + \frac{\partial A}{\partial z} = \frac{\imath\omega^2\mu_0}{2k\cos^2\alpha}\boldsymbol{e}\cdot\boldsymbol{\Pi}_{NL}(z,\omega) e^{\imath\Delta\boldsymbol{k}\cdot\boldsymbol{r}},} \quad (3.25)$$

with α the walk-off angle defined between the directions of propagation of the Poynting vector $\boldsymbol{\mathcal{S}}$ and the wave-vector $\boldsymbol{k}$. Neglecting the walk-off angle, the equation (3.25) takes exactly the form of the wave equation (3.20) that has been established in the case of the nonlinear propagation in a isotropic material.

In conclusion, the nonlinear propagation of waves in a anisotropic material can be treated as the propagation in a isotropic material by priorly decompose the incoming field other the eigen polarization modes, the ordinary and the extraordinary fields. We remind that the eigen modes are the solutions of the Fresnel's equation (3.6) for a given direction of propagation, corresponding to polarization states that keep unchanged along the propagation. Neglecting the walk-off angle, the nonlinear propagation of an electric field polarized either along the ordinary or the extraordinary direction, can be simply treated as the nonlinear propagation of a wave in a isotropic material.

3.4 Nonlinear wave equation for temporal and spatial wave-packets

As mentioned before, the description of nonlinear interactions with plane waves signifies that transverse and temporal effects have been neglected. In many situations, these assumptions will not be verified. The objective of this section is to provide a more accurate description of nonlinear effects that occur with focused beams, in a regime where diffraction effect can be no longer neglected, and optical pulses, accounting for dispersive effects. In both cases, the nonlinear wave equations are sustained by a linear term, describing the diffraction and/or the dispersion effects, corrected by a perturbative nonlinear terms driven by the nonlinear polarization vector that modifies the linear behavior of the interacted waves.

As nonlinear effects are driven by the field amplitudes, equivalently by the field intensities, one easily understands that numerous of nonlinear interactions evolve with focused beams and pulsed laser beams in order to reach high peak intensities. For the sake of clarity, we will derive hereafter separately two nonlinear wave equations for spatial and temporal wave-packets. The derivation of a spatio-temporal nonlinear wave equation, which accounts simultaneously for the spatial and temporal effects, would be straightforward. It would contain linear terms for diffraction and dispersion effects. The spatio-temporal dependence of the nonlinear polarisation term should also be taken into account.

3.4.1 Nonlinear propagation of optical beams

As it has been underlined during the course, the strength of the nonlinear interaction is governed by the magnitude of the electromagnetic fields in interaction. As a consequence, nonlinear optics experiments implies to focus laser beams in order to increase the beam intensity. In addition, diffraction effects are no longer negligible since the interaction length L is longer than the Rayleigh lengths L_R related to the interacted beams, as it is illustrated in the Figure 3.4. One can easily understand, the necessary tradeoff between beam focusing and interaction length : increasing the beam focusing inside the material to achieve higher intensity, implies a reduction of the interaction length through the reduction of the Rayleigh length.

The very common configuration depicted in Figure 3.4, an interaction with focused beams, illustrates the interest in deriving a nonlinear equation that includes transverse effects : the linear diffraction effect, and the spatial dependence in the amplitude of the nonlinear polarization term. The latter is directly related to the variation in the field envelop with the spatial coordinate $\boldsymbol{r}$.

We start with the general wave equation (3.16) and consider the propagation in a homogenous and isotropic medium, implying the equality that $\nabla\times\nabla\times\boldsymbol{E}(\boldsymbol{r},\omega) = -\Delta\boldsymbol{E}$. We can seek solutions of the form:

$$\boldsymbol{\mathcal{E}}(\boldsymbol{r},t) = A(\boldsymbol{r},z)e^{\imath kz}e^{-\imath\omega t}\boldsymbol{e} + CC,$$

and we consider that the spatial dependence of the nonlinear polarization is given by an envelope $\boldsymbol{\Pi}_{NL}(\boldsymbol{r},z)$ through the expression :

$$\boldsymbol{\mathcal{P}}(\boldsymbol{r},t) = \boldsymbol{\Pi}_{NL}(\boldsymbol{r},z)e^{\imath k_p z}e^{-\imath\omega t} + CC.$$

After substitution in (3.16), the nonlinear wave equation takes the form:

$$\frac{\partial^2 A(\boldsymbol{r},z)}{\partial z^2} + 2\imath k\frac{\partial A(\boldsymbol{r},z)}{\partial z} + \Delta_T A(\boldsymbol{r},z) = -\omega^2\mu_0\boldsymbol{e}\cdot\boldsymbol{\Pi}_{NL}(\boldsymbol{r},z)e^{\imath\Delta kz},$$

where Δ_T stands for the transverse Laplacian (over the radial coordinate $\boldsymbol{r} = (x,y)$), and $\Delta k = k_p - k$ is the phase missmatch between the nonlinear polarization and the free wave at ω. Assuming a weak nonlinear interaction, the slowing varying approximation leads to

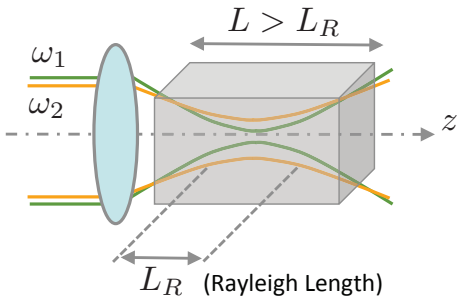

Fig. 3.4. Case of the nonlinear interaction between two focused beams at ω_1 and ω_2 in a nonlinear medium with a thickness L longer than the Rayleigh lengths L_R related to the beams.

$$\boxed{\frac{\partial A(\boldsymbol{r},z)}{\partial z}+\frac{1}{2\imath k}\Delta_T A(\boldsymbol{r},z)=\frac{\imath\omega}{2\epsilon_0 nc}\boldsymbol{e}\cdot\boldsymbol{\Pi}_{NL}(\boldsymbol{r},z)e^{\imath\Delta kz}} \tag{3.26}$$

Under the linear regime, $\boldsymbol{e}\cdot\boldsymbol{\Pi}_{NL}(\boldsymbol{r},z)=0$, the equation describes the deformation of the envelope $A(\boldsymbol{r},z)$ driven by the diffraction effect, which is described by the term $\frac{1}{2\imath k}\Delta_T A(\boldsymbol{r},z)$. In the nonlinear case, the efficiency of the nonlinear interaction will be directly related to the spatial overlapping, at a distance z, between the field envelope distribution $A(\boldsymbol{r},z)$ and the spatial distribution of the nonlinear polarization envelope $\boldsymbol{e}\cdot\boldsymbol{\Pi}_{NL}(\boldsymbol{r},z)$. The latter is governed by the spatial distribution of the interacted waves evolving under diffraction! Finally, if we neglect the diffraction effect, equation (3.26) retrieves the form of the nonlinear wave equation (3.20) in case of a plane wave.

3.4.2 Nonlinear propagation of optical pulses

A very efficient way to observe nonlinear effects consists in using the very high peak-power delivered by pulsed lasers. Similarly to the previous situation, with focused beam, shorter pulses (considering a fixed pulse energy) will increase the strength of the nonlinear response of a material. As the spectral linewidth increase for shorter pulse, one needs to account for the temporal distorsions effects driven by the frequency dependent refractive index of the material.

As an illustration, Figure 3.5 shows the evolution of two distinct optical pulses, nearby ω_1 and ω_2, along their propagation in a material. The group velocity mismatch, $v_{g1}\neq v_{g2}$, leads to a temporal walk-off between the two pulses, reducing their temporal overlapping ant their nonlinear interaction. A second order dispersive effect is related to the group velocity dependence with the frequency content of the pulse $v_g(\omega)$. This so-called chromatic dispersion effect induces a pulse spreading in time, which is accompanied by a reduction of the peak power.

Similarly to the case of the spatial beam propagation, we now need to proceed with the derivation of the nonlinear wave equation for a temporal wavepacket subject to the modification through both the linear dispersive effects and a time varying nonlinear polarization. As in the spatial case, one can seek the following forms for the electric field and for the time dependent nonlinear polarization:

$$\begin{aligned}\boldsymbol{\mathcal{E}}(z,t) &= A(z,t)e^{\imath\beta_0 z}e^{-\imath\omega_0 t}\boldsymbol{e}+CC,\\ \boldsymbol{\mathcal{P}}_{NL}(z,t) &= \boldsymbol{\Pi}_{NL}(z,t)e^{\imath\beta_p z}e^{-\imath\omega_0 t}+CC.\end{aligned}$$

Because we need to take into account for the dispersive properties of the material, i.e. the frequency dependent permittivity $\epsilon(\omega)$, we start with the equation (3.18) writing:

$$\begin{aligned}\boldsymbol{E}(z,\omega) &= \boldsymbol{e}\tilde{A}(z,\omega-\omega_0)e^{\imath\beta_0 z}\\ \boldsymbol{P}_{NL}(z,\omega) &= \tilde{\Pi}_{NL}(z,\omega-\omega_0)e^{\imath\beta_p z},\end{aligned}$$

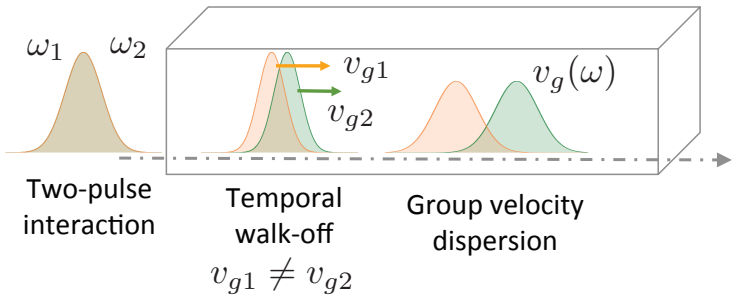

Fig. 3.5. Propagation of two pulses at ω_1 and ω_2 in a nonlinear medium. The temporal walk-off originates from the group velocity difference $v_{g1} \neq v_{g2}$ experienced by the two pulses. In addition, the variation of the group velocities with frequency induces a dispersion effect.

which gives

$$\frac{\partial^2 \tilde{A}(z,\omega-\omega_0)}{\partial z^2} + 2\imath\beta_0 \frac{\partial \tilde{A}(z,\omega-\omega_0)}{\partial z} + \left[\beta^2(\omega) - \beta_0^2\right] \tilde{A}(z,\omega-\omega_0) = -\omega^2 \mu_0 \boldsymbol{e} \cdot \tilde{\boldsymbol{\Pi}}_{NL}(z,\omega-\omega_0) e^{\imath\Delta\beta z}. \tag{3.27}$$

In the following, the pulse duration is supposed to be very small compare to the time period $1/\omega_0$ of the optical carrier. Its spectral linewidth being very narrow ($\Delta\omega \ll \omega_0$), one can use a Taylor's expansion of $\beta^2(\omega)$ around ω_0 :

$$\begin{aligned} \beta(\omega) &= \beta_0 + \beta_1 \Delta\omega + \frac{\beta_2}{2}\Delta\omega^2 + \cdots, \\ \beta^2(\omega) &\simeq \beta_0^2 + 2\beta_0\beta_1\Delta\omega + \left(\beta_1^2 + \beta_0\beta_2\right)\Delta\omega^2 + \cdots, \end{aligned}$$

with $\beta_i = \frac{\partial^i \beta}{\partial \omega^i}$ calculated for $\omega = \omega_0$. The wave equation is then expressed into the time domain:

$$\frac{\partial^2 A(z,t)}{\partial z^2} + 2\imath\beta_0 \frac{\partial A(z,t)}{\partial z} + 2\imath\beta_0\beta_1 \frac{\partial A(z,t)}{\partial t} - \left[\beta_1^2 + \beta_0\beta_2\right] \frac{\partial^2 A(z,t)}{\partial t^2} = \mu_0 \boldsymbol{e} \cdot \left[-\omega_0^2 \boldsymbol{\Pi}_{NL}(z,t) - 2\imath\omega_0 \frac{\partial \boldsymbol{\Pi}_{NL}(z,t)}{\partial t} + \frac{\partial^2 \boldsymbol{\Pi}_{NL}(z,t)}{\partial t^2}\right] e^{\imath\Delta\beta z}.$$

Considering that the envelope $A(t)$ travels at the group velocity $v_g = 1/\beta_1$, the wave equation can be simplified by introducing the retarded time variable $\tau = t - z/v_g$. The wave equation in the time base τ is then:

$$\frac{\partial^2 A(z,\tau)}{\partial z^2} - 2\beta_1 \frac{\partial^2 A(z,\tau)}{\partial z \partial \tau} + 2\imath\beta_0 \frac{\partial A(z,\tau)}{\partial z} - \beta_0\beta_2 \frac{\partial^2 A(z,\tau)}{\partial \tau^2} = \mu_0 \boldsymbol{e} \cdot \left[-\omega_0^2 \boldsymbol{\Pi}_{NL}(z,\tau) - 2\imath\omega_0 \frac{\partial \boldsymbol{\Pi}_{NL}(z,\tau)}{\partial \tau} + \frac{\partial^2 \boldsymbol{\Pi}_{NL}(z,\tau)}{\partial \tau^2}\right] e^{\imath\Delta\beta z}.$$

We then proceed with few assumptions in order to derive a simplified nonlinear wave equation:

- slowly varying approximation for the envelope that implies: $\left|\frac{\partial^2 A(z,\tau)}{\partial z^2}\right| \ll \left|\beta_0 \frac{\partial A(z,\tau)}{\partial z}\right|$,
- narrow spectral linewidth of the pulse, which means that $\left|\frac{\partial A(z,t)}{\partial \tau}\right| \ll \omega_0 A(z,\tau)$. If we suppose that the group velocity $v_g = 1/\beta_1$ is close to the phase velocity $v_\phi \simeq c/n_0$, then: $\left|2\beta_1 \frac{\partial^2 A(z,\tau)}{\partial z \partial \tau}\right| \ll 2\left|\beta_0 \frac{\partial A(z,\tau)}{\partial z}\right|$,
- finally, the slowly varying approximation for the envelope implies a slow variation of the nonlinear polarization envelope, which means that :

$$\omega_0^2 \boldsymbol{\Pi}_{NL}(z,\tau) \gg 2\omega_0 \frac{\partial \boldsymbol{\Pi}_{NL}(z,\tau)}{\partial \tau} \gg \frac{\partial^2 \boldsymbol{\Pi}_{NL}(z,\tau)}{\partial \tau^2}.$$

Following those assumptions, the nonlinear wave equation for a temporal wavepacket is:

$$\boxed{\frac{\partial A(z,\tau)}{\partial z} + \frac{\imath\beta_2}{2}\frac{\partial^2 A(z,\tau)}{\partial \tau^2} = \frac{\imath\omega}{2\epsilon_0 nc}\boldsymbol{e}\cdot\boldsymbol{\Pi}_{NL}(z,\tau)e^{\imath\Delta kz}} \tag{3.28}$$

Under the linear regime, $\boldsymbol{e}\cdot\boldsymbol{\Pi}_{NL}(z,\tau)=0$, the equation describes the temporal dispersion of the pulse $A(z,\tau)$ governed by the term $\frac{\imath\beta_2}{2}\frac{\partial^2 A(z,\tau)}{\partial\tau^2}$. Because we have only considered the 2nd order dispersive effects β_2, one could easily introduce higher order dispersive effects by simply extending the Taylor's expansion for $\beta(\omega)$. As in the case of the transverse wave packet propagation, the efficiency of the nonlinear interaction is related to the temporal overlapping, at a distance z, between the field envelope distribution $A(z,\tau)$ and the temporal distribution of the nonlinear polarization envelope $\boldsymbol{e}\cdot\boldsymbol{\Pi}_{NL}(z,\tau)$. The latter is governed by the temporal distribution of the interacted dispersed pulses !

3.5 Nonlinear wave equation in optical waveguides

A very interesting situation consists in studying nonlinear interactions inside a waveguide. For instance, a single mode waveguide enables to maintain a transverse confinement of light other a very long distance (thousand of kilometers in case of trans-oceanic fiber cables). Conversely to the case of focused beam, Rayleigh length is no longer a limit as the diffraction is strictly compensated by the refractive guiding effect of the waveguide. In addition, one reminds that a waveguide operates under a single mode regime for specific operating wavelength range. It means that we may have to consider the case of nonlinear interactions taking place inside a multimode waveguide, as illustrated in the Figure 3.6.

In order to derive the nonlinear wave equation in an optical waveguide, we start from the general form (3.18) that takes into account the inhomogeneity of the material (which is the case for an optical waveguide).

As in the previous situations, we need to give an expression for the first term of the left hand side of the equation:

$$\nabla\times\nabla\times\boldsymbol{E}(\boldsymbol{r},\omega) = \nabla(\nabla\cdot\boldsymbol{E}(\boldsymbol{r},\omega)) - \Delta\boldsymbol{E}(\boldsymbol{r},\omega)$$

Although $\nabla\cdot\boldsymbol{D}(\boldsymbol{r},\omega)=0$, the propagation of the light in an inhomogeneous medium does not imply the same equality for the electric field. We have to consider that : $\nabla\cdot\boldsymbol{E}(\boldsymbol{r},\omega)\neq 0$. The wave equation becomes:

$$\Delta\boldsymbol{E}(\boldsymbol{r},\omega) + \frac{\omega^2}{c^2}\underline{\underline{\epsilon}}(\boldsymbol{r},\omega)\boldsymbol{E}(\boldsymbol{r},\omega) = \nabla(\nabla\cdot\boldsymbol{E}(\boldsymbol{r},\omega)) - \omega^2\mu_0\boldsymbol{P}_{NL}(\boldsymbol{r},\omega). \tag{3.29}$$

Under the weak guidance approximation, it can been shown that the term $\nabla(\nabla\cdot\boldsymbol{E}(\boldsymbol{r},\omega))$ can be neglected (see the texbook on Guided Optics of Jean-Michel Jonathan).

The electric field propagating inside the waveguide into the z direction, along which the waveguide is invariant, can be decomposed over the transverse eigen modes of the waveguide:

$$\boldsymbol{\mathcal{E}}(\boldsymbol{r},z,t) = \sum_{p,m}\boldsymbol{e}_p\phi_m^p(\boldsymbol{r})A_p(z)e^{-i(\omega_m t-\beta_p(\omega_m)z)} + CC,$$

where we have assumed that the set of transverse modes (labelled with the indices p) form a complete base of normalized and orthogonal modes:

$$\int\int \phi_m^p(\boldsymbol{r})\phi_m^{p'}(\boldsymbol{r})^\star d^2\boldsymbol{r} = \delta_{pp'}.$$

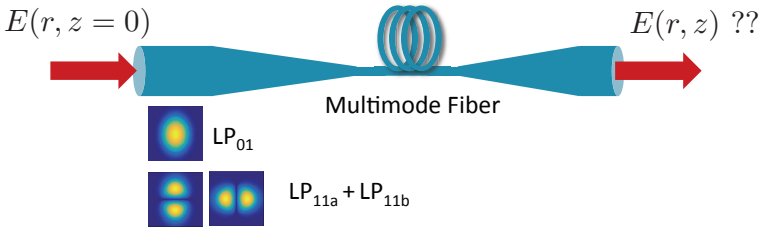

Fig. 3.6. Nonlinear interaction in a multimode wave-guide, like a few-mode fiber supporting the fundamental LP_{01} mode and the two-degenerated modes LP_{11a} and LP_{11b}.

Assuming first the case of a linear propagation under the weak guidance approximation (and neglecting the anisotropy of the waveguide), the wave equation is reduced to:

$$\Delta \boldsymbol{E}(\boldsymbol{r},\omega) + \frac{\omega^2}{c^2}\epsilon(\boldsymbol{r},\omega)\boldsymbol{E}(\boldsymbol{r},\omega) = 0 \tag{3.30}$$

Writing $\Delta \boldsymbol{E}(\boldsymbol{r},z,\omega) = (\nabla_T^2 + \frac{\partial^2}{\partial z^2})\boldsymbol{E}(\boldsymbol{r},z,\omega)$, and using the fact that $A(z)$ is constant (linear regime and invariance of the waveguide along the z direction), we find at the frequency ω_m:

$$\nabla_T^2 \phi_m^p(\boldsymbol{r}) + \left(\frac{\omega^2}{c^2} n^2(\boldsymbol{r},\omega_m) - \beta_p^2(\omega_m)\right)\phi_m^p(\boldsymbol{r}) = 0$$

We consider next the case of a nonlinear propagation. The nonlinear wave equation is simply derived from (3.30) by adding the nonlinear term source:

$$\Delta \boldsymbol{E}(\boldsymbol{r},\omega) + \frac{\omega^2}{c^2}\epsilon(\boldsymbol{r},\omega)\boldsymbol{E}(\boldsymbol{r},\omega) = -\omega^2\mu_0 \boldsymbol{P}_{NL}(\boldsymbol{r},\omega). \tag{3.31}$$

Next, we consider the nonlinear propagation of a wave at the frequency $\omega = \omega_m$ and defined by the transverse mode $\phi_m^p(\boldsymbol{r})$. Under the slowly varying envelope approximation, the equation (3.31) can be written is a simpler manner:

$$\sum_p \boldsymbol{e}_p \phi_m^p(\boldsymbol{r}) 2i\beta_p(\omega_m)\frac{\partial A_p(z)}{\partial z} e^{i\beta_p(\omega_m)z} = -\omega_m^2\mu_0 \boldsymbol{P}_{NL}(\boldsymbol{r},\omega_m)$$

Following the projection on a specific transverse mode $\phi_m^p(\boldsymbol{r})$, the nonlinear wave equation takes the form

$$\boxed{\frac{\partial A_p(z)}{\partial z} = \frac{i\omega_m^2\mu_0}{2\beta_p}\frac{\int\int \boldsymbol{e}_p.\boldsymbol{P}_{NL}(\boldsymbol{r},\omega_m)\phi_m^{p\star}(\boldsymbol{r})d^2\boldsymbol{r}}{\int\int \phi_m^p(\boldsymbol{r})\phi_m^{p\star}(\boldsymbol{r})d^2\boldsymbol{r}} e^{-i\beta_p(\omega_m)z}.} \tag{3.32}$$

This equation signifies that the modification in the envelop amplitude $A_p(z)$ contained in the transverse mode p is driven by an overlapping function between the vectorial transverse distribution of the nonlinear polarization term and the vectorial transverse distribution $\phi_m^p(\boldsymbol{r})$ of the transverse mode p of interest. The magnitude of the right hand side term governs the strength of the nonlinear coupling impacting the variation of the field intensity contained in the transverse mode p. We retrieve the condition discussed before that the nonlinear polarization vector should not be orthogonal to the polarization state of the transverse mode ($\boldsymbol{e}_p.\boldsymbol{P}_{NL} \neq 0$). Additionally, the nonlinear interaction is governed by the overlapping between the transverse distribution of the nonlinear polarization term and that of the specific guided mode p, implying that $\int\int \boldsymbol{P}_{NL}(\boldsymbol{r})\phi_m^{p\star}(\boldsymbol{r})d^2\boldsymbol{r} \neq 0$. Finally, and the following the expansion $\boldsymbol{P}_{NL}(z,\omega) = \boldsymbol{\Pi}_{NL}(z,\omega_m)\, e^{i\boldsymbol{k}_p(\omega_m).\boldsymbol{r}}$,, the phase matching condition is easily determined.

Chapter 4

2nd order nonlinearities

Contents

4.1 Manley-Rowe relations

Prior to the specific study of 2nd order nonlinear interactions, we give in the following a general description of the propagation of 3 waves $\omega_1, \omega_2, \omega_3$, with $\omega_1 + \omega_2 = \omega_3$, interacting in a lossless 2nd order nonlinear material. The lossless medium assumption means that the 3 wave interaction will take place without any exchange of energy between the waves and the material. Therefore, the three coupled nonlinear wave equations at ω_1, ω_2 and ω_3 should satisfy the energy conservation condition.

To verify it, we consider the simple situation of co-propagating plane waves for which the nonlinear wave equations are directly derived from (3.20) :

$$\begin{aligned}
\frac{dA_3(z)}{dz} &= \frac{\imath\omega_3}{2\epsilon_0 n_3 c}\boldsymbol{e}_3 \cdot \boldsymbol{P}_{NL}(z, \omega_3 = \omega_1 + \omega_2)e^{-\imath k_3 z}, \\
\frac{dA_2(z)}{dz} &= \frac{\imath\omega_2}{2\epsilon_0 n_2 c}\boldsymbol{e}_2 \cdot \boldsymbol{P}_{NL}(z, \omega_2 = \omega_3 - \omega_1)e^{-\imath k_2 z}, \\
\frac{dA_1(z)}{dz} &= \frac{\imath\omega_1}{2\epsilon_0 n_1 c}\boldsymbol{e}_2 \cdot \boldsymbol{P}_{NL}(z, \omega_1 = \omega_3 - \omega_2)e^{-\imath k_1 z}.
\end{aligned} \tag{4.1}$$

The derivation of the spatial evolution for the field intensities I_1, I_2 and I_3 is straightforward, reminding that $I = 2nc\epsilon_0|A|^2$ (3.13) :

$$\begin{aligned}
\frac{dI_3(z)}{dz} &= +\imath\epsilon_0\omega_3\chi^{(2)}_{eff}A_1A_2A_3^\star e^{\imath\Delta kz} + C.C., \\
\frac{dI_2(z)}{dz} &= -\imath\epsilon_0\omega_2\chi^{(2)}_{eff}A_1A_2A_3^\star e^{\imath\Delta kz} + C.C., \\
\frac{dI_1(z)}{dz} &= -\imath\epsilon_0\omega_1\chi^{(2)}_{eff}A_1A_2A_3^\star e^{\imath\Delta kz} + C.C.,
\end{aligned} \tag{4.2}$$

with $\Delta k = k_1 + k_2 - k_3$ the wave vector mismatch and $\chi^{(2)}_{eff}$ the effective nonlinear susceptibility given by :

$$\begin{aligned}
\chi^{(2)}_{eff} &= 2\ \boldsymbol{e}_3 \cdot \underline{\underline{\chi}}^{(2)}(\omega_3; \omega_1, \omega_2)\boldsymbol{e}_1\boldsymbol{e}_2 \\
&= 2\ \boldsymbol{e}_2 \cdot \underline{\underline{\chi}}^{(2)}(\omega_2; \omega_3, -\omega_1)\boldsymbol{e}_3\boldsymbol{e}_1 \\
&= 2\ \boldsymbol{e}_1 \cdot \underline{\underline{\chi}}^{(2)}(\omega_1; \omega_3, -\omega_2)\boldsymbol{e}_3\boldsymbol{e}_2.
\end{aligned} \tag{4.3}$$

These equalities between the nonlinear effective susceptibilities are the key point of the demonstration. They are actually justified by the lossless medium assumption allowing the full permutation between the indices of the susceptibility tensor (without exchanging the frequency arguments). In addition, the lossless assumption allows to treat them as purely real quantitates (see § 2.3.5). Note that these relations are written in the case of frequency non-degenerated waves ($\omega_1 \neq \omega_2$). For the degenerated case, coinciding with a specific configuration of second harmonic generation, there are only two equations at 2ω and ω which differ by a factor of 2, the degeneracy factor[1].

Following the interaction of the 3 waves in a lossless 2nd order nonlinear material, their intensity evolutions (4.2) follow the relation :

$$\frac{dI_3(z)}{dz} + \frac{dI_2(z)}{dz} + \frac{dI_1(z)}{dz} = 0, \tag{4.4}$$

[1] In the case of second harmonic generation, the nonlinear polarization expressions at 2ω and ω differ by a factor of 2: $\boldsymbol{P}^{(2)}(2\omega) = \epsilon_0\underline{\underline{\chi}}^{(2)}(2\omega; \omega, \omega)\boldsymbol{E}(\omega)\boldsymbol{E}(\omega)$, while, $\boldsymbol{P}^{(2)}(\omega) = 2\epsilon_0\underline{\underline{\chi}}^{(2)}(\omega; 2\omega, -\omega)\boldsymbol{E}(2\omega)\boldsymbol{E}(-\omega)$

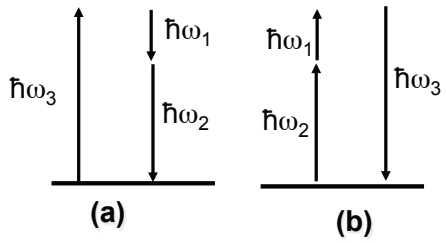

Fig. 4.1. Energy diagram based description of the interaction between 3 waves at ω_1, ω_2 and ω_3 in a lossless 2nd order nonlinear material: the annihilation (a) (resp. the creation (b)) of one photon at ω_3 must be accompanied by the simultaneous creation (resp. the annihilation) of one photon at ω_1 and one photon at o_2.

which means that the exchange of energy occurring between the 3 waves along their propagation into the nonlinear medium is done by conserving the total amount of intensity $I = I_1 + I_2 + I_3$ and $dI(z)/dz = 0$.

It is worth deriving a similar relation for the quantity $N_i = I_i/\hbar\omega_i$ related to the number of photons at ω_i propagating trough the material per unit of time and surface, which gives :

$$\frac{dN_1(z)}{dz} = \frac{dN_2(z)}{dz} = -\frac{dN_3(z)}{dz}. \tag{4.5}$$

These two relations refer to the so-called Manley-Rowe relations that depict the interaction between 3 waves in a lossless 2nd order nonlinear material. These two relations show that their interactions are governed by the conservation of the total energy carried by the 3 waves, in agreement with the lossless medium assumption. The second relation (4.5) is of particular relevance since it gives a description of the 3 wave interaction in terms of number of photons, in accordance with a quantum optics description. Actually, the "quantum" reading of the equality (4.5) would be the following : the annihilation (resp. the creation) of one photon at ω_3 must be accompanied by the simultaneous creation (resp. the annihilation) of one photon at ω_1 and one photon at o_2. The Manley-Rowe equations are consistent with a quantum-mechanical interpretation of the 3 wave interactions, which could be represented by the two energy diagrams depicted in Fig. 4.1.

4.2 Three-wave mixing interactions

Using the Manley-Rowe relations, we next give general comments about the different Three-wave mixing interactions that can be explored in 2nd order nonlinear medium. For all situations, we consider the interaction between 3 waves at ω_1, ω_2 and ω_3, where $\hbar\omega_1 + \hbar\omega_2 = \hbar\omega_3$, inside a lossless $\underline{\underline{\chi}}^{(2)}$ material.

The various three-wave mixing interactions studied in this course are depicted in Figure 4.2:

(a) Sum-Frequency Generation (SFG) is presented in chart (a) where the interaction of two incident intense beams at ω_1 and ω_2 generate a third beam at $\omega_3 = \omega_1 + \omega_2$. Two photons, respectively at ω_1 and ω_2, generate one photon at ω_3. The direction of propagation of the beam at ω_3 is given by the phase matching condition: $\boldsymbol{k}_3 = \boldsymbol{k}_1 + \boldsymbol{k}_2$. The most well-known situation is the Second-Harmonic Generation (SHG) where an intense pump beam at ω propagates through a $\underline{\underline{\chi}}^{(2)}$ material to generate a doubling in frequency beam at 2ω.

(b) Second-Harmonic Generation (SHG) can be seen as a frequency degenerate case of SFG with a single incident beam, $\omega_1 = \omega_2 = \omega$, which will be doubled in frequency: $\omega_3 = \omega + \omega = 2\omega$. As illustrated by chart (b), the generation of one photon at 2ω is governed by the simultaneous annihilation of 2 photons at ω. SHG is further studied in § 4.3. With a single incident beam along the wave vector $\boldsymbol{k}_\omega$, the SHG beam will be generated along te same direction since $\boldsymbol{k}_{2\omega} = 2\boldsymbol{k}_\omega$.

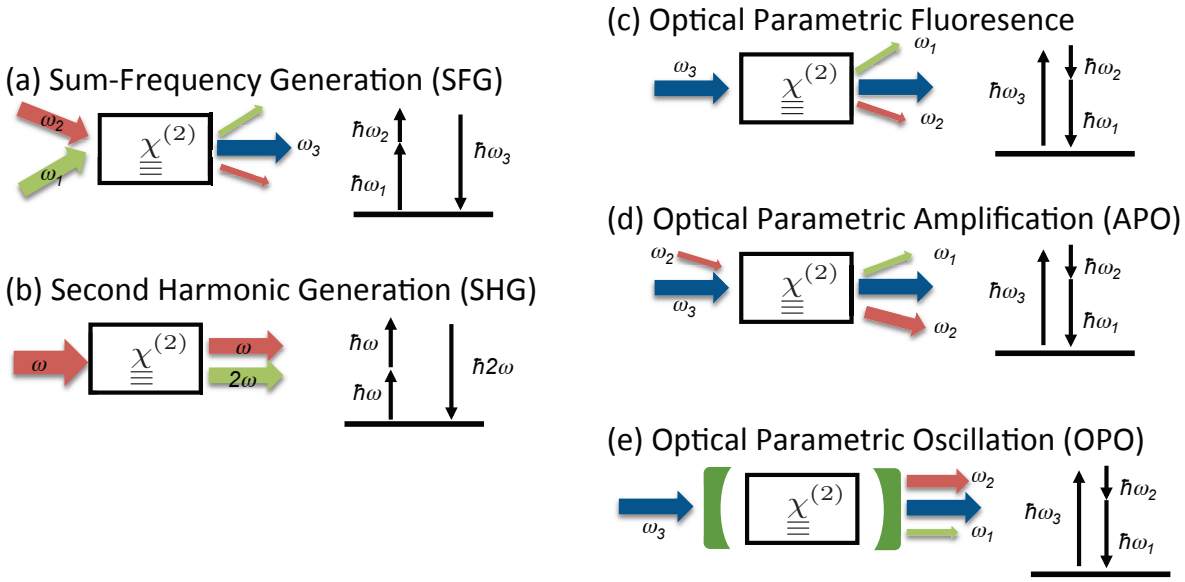

Fig. 4.2. Three wave mixing configurations, with the corresponding photon energies diagrams. (a) Sum-Frequency Generation. (b) Second-Harmonic Generation. Optical Parametric effects : (c) Fluorescence, (d) Amplification and (e) Oscillation.

(c) Optical Parametric Fluorescence (OPF) can be observed with a single intense beam at ω_3 incident onto the nonlinear crystal, which will generate photon pairs at ω_1 and ω_2 along the directions set by the phase matching relation $\boldsymbol{k}_1 + \boldsymbol{k}_2 = \boldsymbol{k}_3$. We will show below that such a nonlinear effect is not predicted through classical description conducted in this course. A complete description requires quantum physics approach, which is out of the scope of this introductive course.

(d) Optical Parametric Amplification (OPA) differs from the previous configuration by the adjonction of a weak beam at ω_2 (or ω_1) along the direction at which ω_2 (or ω_1) photons would be emitted through parametric fluorescence effect. As it will be shown in § 4.4 and conversely to the fluorescence effect, the parametric amplification can be perfectly described by solving coupled nonlinear wave equations. The solutions show that an amplification of the incident ω_2 (or ω_1) beam occurs at the expense of an intensity decrease of the pump beam ω_3. In agreement with the Manley-Rowe relations, a third beam at ω_1 (or ω_2) is simultaneously generated inside the crystal along the direction $\boldsymbol{k}_2 = \boldsymbol{k}_3 - \boldsymbol{k}_1$.

(d) Optical Parametric Oscillation (OPO) consists in inserting an OPA inside an optical cavity. The configuration described in chart (e) coincides with co-propagating OPA configuration, with the 3 waves propagating along the same direction, although non-collinear configuration such as in (d) could be set. In practices the mirrors get a reflection coating at either ω_1 or ω_2, in a singly resonant OPO, or at both ω_1 and ω_2 in a doubly resonant configuration. Once the pump intensity reaches a threshold value, the parametric amplification gain experienced by either ω_1 or ω_2 perfectly compensate for the cavity losses, and the cavity oscillation condition is satisfied. Two coherent beams at ω_1 and ω_2 exit from the cavity. The OPO behaviors will be studied in more details in § 4.4.

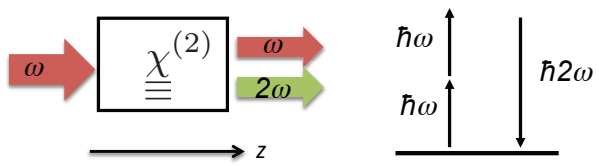

Fig. 4.3. Second Harmonic Generation scheme. An incident laser beam at ω generates, inside a 2nd order nonlinear crystal with a nonlinear susceptibility $\underline{\underline{\chi}}^{(2)}$, a nonlinear polarization at 2ω, which may generate an optical beam at the doubling frequency 2ω. The generation efficiency depends on the phase matching condition.

4.3 Second Harmonic Generation

As an introduction to nonlinear optics, we have first studied the behavior of an anharmonic oscillator subject to an excitation at the frequency ω. The oscillator in our case stands as a classical representation for an entity (an atom or a molecule) that is polarized through the application of an external electric field. By introducing a quadratic term in the expression of the restoring force, a second order contribution in the induced electric dipole has been derived. In particular, we have shown that a collection of such dipoles would generate a macroscopic polarization vibrating at the frequency 2ω (actually $\pm 2\omega$ as shown by the relation (1.14)).

In this section, we are going to study in more details this nonlinear effect, which refers to the Second Harmonic Generation (SHG) effect[2]. It was the first nonlinear effect to be experimentally demonstrated few months after the realization of the Ruby Laser in 1962. The SHG effect is schematically represented in Fig. 4.3. It takes place in a nonlinear crystal with a non vanishing 2nd order susceptibility $\underline{\underline{\chi}}^{(2)}$ and we consider a lossless material, which means that the Manley-Rowe relations are valide. As a consequence, one can anticipate that the generation of one photon at 2ω is supported by the annihilation of simultaneously 2 incident photons at ω, as it is illustrated by the energy diagram in Fig. 4.3. At first, the SHG effect in a weak interaction approximation is considered, which means that the depletion of the beam at ω is considered negligible. By doing so, we will introduce the necessity to fulfill a phase matching condition in order to perform SHG with high efficiency. Prior to the study of SHG under perfect phase matching condition, achievements of phase matching in nonlinear materials is considered. In particular, the phase matching in birefringent material is discussed in details.

In the following, the theoretical description is treated with monochromatic plane waves. As a first attempt, we intend to neglect any transverse (diffraction) or temporal (group velocity walk-off, dispersion...) effects that would necessarily impact the efficiency of the process.

4.3.1 Undepleted pump approximation regime

A weak interaction efficiency is first considered, such that the depletion of the incident wave at ω can be neglected. Subsequently, the wave ω will be referred to the *pump* wave or beam. The variation of the field envelope $A(\omega)$ along the direction of propagation z being negligible, one seeks to solve the wave equation at 2ω:

$$\begin{aligned} \frac{dA_\omega(z)}{dz} &= 0 \\ \frac{dA_{2\omega}(z)}{dz} &= \frac{\imath(2\omega)}{2\epsilon_0 n_{2\omega} c} \boldsymbol{e}_{2\omega} \cdot \boldsymbol{P}_{NL}(z,2\omega) e^{-\imath \boldsymbol{k}_{2\omega}\cdot\boldsymbol{z}}. \end{aligned} \tag{4.6}$$

By substituting in (4.6) the expression for the nonlinear polarization

$$\begin{aligned} \boldsymbol{P}_{NL}(z,2\omega) &= \epsilon_0 \underline{\underline{\chi}}^{(2)}(2\omega;\omega,\omega)\boldsymbol{E}(z,\omega)\boldsymbol{E}(z,\omega) \\ &= \epsilon_0 \underline{\underline{\chi}}^{(2)}(2\omega;\omega,\omega)\boldsymbol{e}_\omega \boldsymbol{e}_\omega A_\omega^2(z) e^{\imath 2\boldsymbol{k}_\omega\cdot\boldsymbol{z}}, \end{aligned}$$

[2]It may also be referred to Doubling Frequency Effect.

the wave equation at 2ω is given by :

$$\frac{dA_{2\omega}(z)}{dz} = \frac{\imath(2\omega)}{2n_{2\omega}c}\chi^{(2)}_{\text{eff}}\ A^2_\omega(z)e^{\imath\Delta\boldsymbol{k}\cdot\boldsymbol{z}}, \tag{4.7}$$

with $\chi^{(2)}_{\text{eff}} = \boldsymbol{e}_{2\omega}\cdot\underline{\underline{\chi}}^{(2)}(2\omega;\omega,\omega)\boldsymbol{e}_\omega\boldsymbol{e}_\omega$ the effective nonlinear susceptibility and $\Delta\boldsymbol{k} = 2\boldsymbol{k}_\omega - \boldsymbol{k}_{2\omega}$ the wave vector missmatch. Under the undepleted pump approximation the integration of the last equation is straightforward :

$$A_{2\omega}(z) = \frac{\imath(2\omega)}{2n_{2\omega}c}\frac{\chi^{(2)}_{\text{eff}}\ A^2_\omega}{\Delta k}\ 2\sin\left(\frac{\Delta k}{2}z\right)e^{\imath\frac{\Delta k}{2}z}. \tag{4.8}$$

Assuming a configuration where the two waves at ω and 2ω are co-propagating along the same direction z we have set $\Delta\boldsymbol{k}\cdot\boldsymbol{z} = \Delta k\ z$.

Using the relation $I_{2\omega} = 2\epsilon_0 n_{2\omega}c|A_{2\omega}|^2$, the spatial evolution for the intensity of the beam generated along the crystal length z is:

$$I_{2\omega}(z) = \frac{(2\omega)^2}{2\epsilon_0 n^2_\omega n_{2\omega}c^3}\left|\chi^{(2)}_{\text{eff}}\right|^2\sin^2\left(\frac{\Delta k}{2}z\right)\frac{I^2_\omega}{(\Delta k)^2} \tag{4.9}$$

$$= \frac{(2\omega)^2}{8\epsilon_0 n^2_\omega n_{2\omega}c^3}\ \left|\chi^{(2)}_{\text{eff}}\right|^2\ \text{sinc}^2(\Delta kz/2)\ I^2_\omega\ z^2. \tag{4.10}$$

Under the undepleted pump approximation, one can easily evaluate the maximum efficiency than can be reached in a specific crystal:

$$\boxed{\eta_{\text{SHG}} = \frac{I_{2\omega}}{I_\omega} = \frac{(2\omega)^2}{8\epsilon_0 n^2_\omega n_{2\omega}c^3}\ \left|\chi^{(2)}_{\text{eff}}\right|^2\ \text{sinc}^2(\Delta kz/2)\ I_\omega\ z^2.} \tag{4.11}$$

In the case of a non-phase matched situation, i.e. $\Delta kz \neq 0$, and following the preliminary discussion we gave in 3.3.2, the beam intensity at 2ω evolves along the crystal with an oscillatory behavior, which is the consequence of successive constructive and destructive interferences between the nonlinear polarization term $\boldsymbol{P}^{(2)}(2\omega)$ generated inside the crystal and the free wave $\boldsymbol{E}(2\omega)$ that propagates inside the crystal. To give an illustration, the evolution of SHG efficiencies η_{SHG} with distance for phase matching Δk equal to $10/L$, $5/L$, $2.5/L$ and 0, defined respect to the crystal length L, are plotted in Figure 4.4. In case of $\Delta k \neq 0$, the maximum SHG efficiency is reached at a distance $L_c = \pi/\Delta k$, which refers to the coherence length (see p. 23). As an order of magnitude, one can take the example of an SHG experiment in Quartz plate at $\lambda = 1\ \mu$m. Taking the refractive index difference at ω and 2ω equal to 10^{-2}, the coherence length is 25 μm.

Although the maximum efficiency is reached for a perfect phase matching situation $\Delta k = 0$, in practice, this condition might not be perfectly fulfilled in practice, which does not signify that SHG can not been performed. For some application, it might be sufficient to minimize Δk in order to maximize the coherence length and the SHG efficiency, which is inversely proportional to $(\Delta k)^2$. As illustrated in Fig. 4.4, the maximum SHG efficiency increases with $1/\Delta k$ in case of of non-phase matched situations.

An other important comment concerns the dependence of SHG efficiency with the pump intensity. Because of the proportionality between η_{SHG} and I_ω, the quantity of SHG is expected to increase by focusing the pump beam inside the crystal. As it will be frequently underlined, nonlinear optics is related to beam intensity, and not to beam power. Now, we must remember the limit of our present model that does not include diffraction effects, for instance. Intending to increase the quantity of SHG, the beam size of the pump beam should be decreased. At a

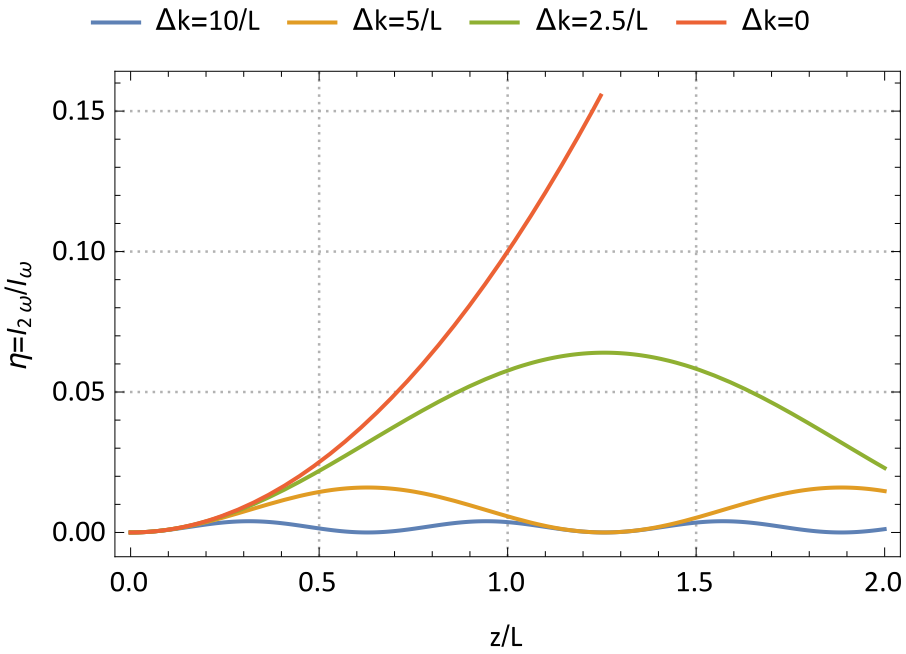

Fig. 4.4. Second Harmonic Generation efficiency under the undepleted pump approximation for phase matching conditions $\Delta k = 10/L,\ 5/L,\ 2.5/L$ and 0, with L the crystal length. The red curve $\Delta k = 0$ gives the maximum efficiency that can be achieved in the crystal for a given pump intensity I_ω.

certain point, the improvement will face the diffraction limit : by reducing the beam size, the Rayleigh length of the beam decreases, which tends to shorten the interaction length !

Despite these comments, the more important result concerns the necessity to fulfill the phase matching condition $\Delta k = 0$, which is required to benefit for the maximum SHG efficiency in a given configuration. In such a situation, η_{SHG} scales with I_ω and with L^2, the square of the crystal length. Of course, one would rapidly reach the limit of the undepleted pump approximation. Under such an efficient operating situation, the depletion of the pump intensity could not be neglected anymore.

Before, we study the general solution in that case, we give considerations towards the techniques to achieve the phase matching condition, which is one of the most critical point to achieve while dealing with 2 nd order nonlinear experiments.

4.3.2 Phase matching considerations

The achievement of the phase matching condition $\Delta k = 0$ implies, for SHG experiment, the equality $n(\omega) = n(2\omega)$ between the two refractive indices of the nonlinear material at ω and 2ω. In general, the frequency dependence of refractive index for lossless material shows a normal dispersion, meaning that refractive index increases with frequency. As illustrated in Fig. 4.6(a), the equality $n(\omega) = n(2\omega)$ might be impossible in practice, if we consider isotropic material.

One could argue that such a condition could be specifically fulfilled nearby an optical resonance by using the dispersive shape of the real part of the linear susceptibility, which locally undertakes an anomalous shape (with a negative slope of $dn/d\omega$). Such a situation remains exceptional, and can not be transposed over a broad operating frequency range and a large variety of materials !

Instead, we may prefer to exploit the birefrengent properties of materials. Following the reminder in 3.2, an anisotropic medium exhibits, at most, two refractive indices along a given

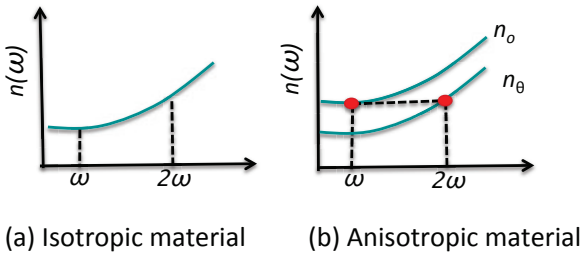

Fig. 4.5. Variation of the refractive index with frequency in material with normal dispersion. (a) Isotropic material for which $n(2\omega) \neq n(\omega)$. (b) Example of an anisotropic material for which one can achieve $n(2\omega) = n(\omega)$ for an extraordinary polarized 2ω wave and an ordinary polarized ω wave.

direction of propagation $\boldsymbol{z}$. Each refractive index, n_o or n_θ, referring to ordinary and extraordinary indices, is related to a specific eigen polarization state, either $\boldsymbol{e}_o$ or $\boldsymbol{e}_\theta$. Using the dispersion relation, phase matching can be achieved for instance by selectively propagating the pump beam at ω along the ordinary polarized state $\boldsymbol{e}_o$, and the 2ω wave along the extraordinary polarized state $\boldsymbol{e}_\theta$ as illustrated in Fig. 4.6(b).

In order to identify the different possibilities to achieve phase matching, we proceed by deriving the nonlinear wave equations at ω and 2ω in a anisotropic medium. Without loss of generality, we next consider the case of uniaxial crystals. We have shown in **??** that, in birefringent materials, the nonlinear wave equation can take the simple form derived in case of isotropic medium if the electric fields are decomposed along the eigen polarized states $\boldsymbol{e}_o$ and $\boldsymbol{e}_\theta$ (and if we neglect the walk-off angle). In the case of SHG experiment, the two waves at ω and 2ω will be decomposed into the sum of ordinary and extraordinary modes:

$$\boldsymbol{E}(\omega) = \boldsymbol{E}_o(\omega) + \boldsymbol{E}_\theta(\omega) \text{ and } \boldsymbol{E}(2\omega) = \boldsymbol{E}_o(2\omega) + \boldsymbol{E}_\theta(2\omega),$$

with

$$\begin{aligned}\boldsymbol{E}_o(\omega) &= A_o(\omega)\boldsymbol{e}_o \exp \imath(\boldsymbol{k}_o(\omega).\boldsymbol{z})\\ \boldsymbol{E}_\theta(\omega) &= A_\theta(\omega)\boldsymbol{e}_\theta \exp \imath(\boldsymbol{k}_\theta(\omega).\boldsymbol{z}),\end{aligned}$$

and

$$\begin{aligned}\boldsymbol{E}_o(2\omega) &= A_o(2\omega)\boldsymbol{e}_o \exp \imath(\boldsymbol{k}_o(2\omega).\boldsymbol{z})\\ \boldsymbol{E}_\theta(2\omega) &= A_\theta(2\omega)\boldsymbol{e}_\theta \exp \imath(\boldsymbol{k}_\theta(2\omega).\boldsymbol{z}).\end{aligned}$$

If we neglect the walk-off effect, the nonlinear wave equation (3.25) derived for anisotropic medium is similar to that of isotropic medium. Keeping in mind the electric field decomposition, the SHG problem requires the derivation of 4 coupled wave equations: 2 at ω and 2 at 2ω. To identify the different phase matching situations, it is sufficient to set the equation at 2ω (or ω):

$$\frac{dA_o(2\omega)}{dz} = \frac{\imath(2\omega)}{2\epsilon_0 n_o(2\omega)c}\boldsymbol{e}_o \cdot \boldsymbol{P}_{NL}(2\omega)e^{-\imath \boldsymbol{k}_o(2\omega)\cdot\boldsymbol{z}}, \tag{4.12}$$

$$\frac{dA_\theta(2\omega)}{dz} = \frac{\imath(2\omega)}{2\epsilon_0 n_\theta(2\omega)c}\boldsymbol{e}_\theta \cdot \boldsymbol{P}_{NL}(2\omega)e^{-\imath \boldsymbol{k}_\theta(2\omega)\cdot\boldsymbol{z}}. \tag{4.13}$$

with the nonlinear polarization at 2ω,

$$\begin{aligned}\boldsymbol{P}_{NL}(2\omega) &= \epsilon_0 \underline{\underline{\underline{\chi}}}^{(2)}(2\omega;\omega,\omega)\boldsymbol{E}(\omega)\boldsymbol{E}(\omega)\\ &= \epsilon_0 \underline{\underline{\underline{\chi}}}^{(2)}(2\omega;\omega,\omega)(\boldsymbol{E}_o(\omega)+\boldsymbol{E}_\theta(\omega))(\boldsymbol{E}_o(\omega)+\boldsymbol{E}_\theta(\omega))\\ &= \epsilon_0 \underline{\underline{\underline{\chi}}}^{(2)}(2\omega;\omega,\omega)[\boldsymbol{E}_o(\omega)\boldsymbol{E}_o(\omega)+\boldsymbol{E}_o(\omega)\boldsymbol{E}_\theta(\omega)+\boldsymbol{E}_\theta(\omega)\boldsymbol{E}_o(\omega)+\boldsymbol{E}_\theta(\omega)\boldsymbol{E}_\theta(\omega)].\end{aligned} \tag{4.14}$$

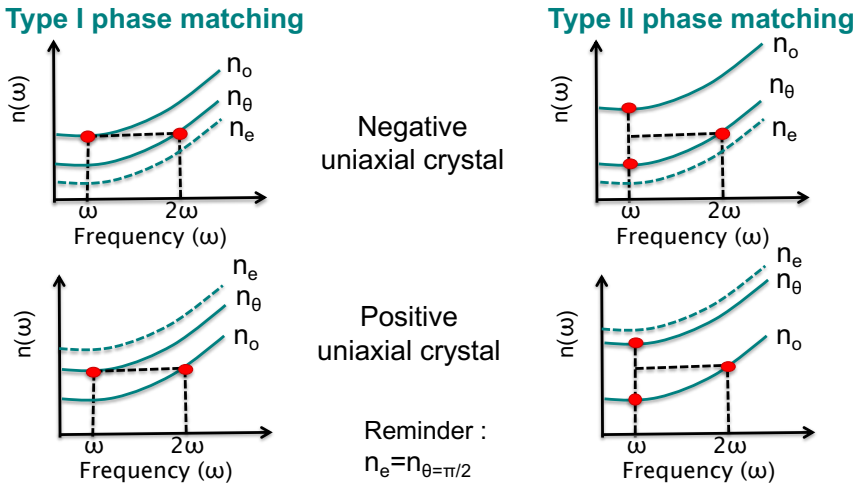

Fig. 4.6. Illustrations of types I and II phase matching realization for SHG in negative and positive uniaxial crystals, for a collinear configuration.

The substitution of (4.14) in wave equations (4.12) and (4.13) leads, for each polarization state, to 4 terms contributing to the generation of a wave at 2ω. Behind the apparent complexity of the wave equations, one needs to identify one of the terms that will efficiently contribute to the modification of the 2ω wave amplitude. The selection between the whole terms (actually, the 8 terms) is dictated by the possibility to achieve or not the phase matching condition, enabling to apply a selection between the different contribution terms. A quick analysis of the wave equations shows that 2 types of phase matching can be fulfilled:

- **Type I:** phase matching realized through either $\boldsymbol{k}_o(\omega)+\boldsymbol{k}_o(\omega) = \boldsymbol{k}_\theta(2\omega)$ or $\boldsymbol{k}_\theta(\omega)+\boldsymbol{k}_\theta(\omega) = \boldsymbol{k}_o(2\omega)$, leading to the necessary equality

$$n_o(\omega) = n_\theta(2\omega) \text{ or } n_\theta(\omega) = n_o(2\omega).$$

- **Type II:** phase matching realized through either $\boldsymbol{k}_o(\omega) + \boldsymbol{k}_\theta(\omega) = \boldsymbol{k}_\theta(2\omega)$ or $\boldsymbol{k}_o(\omega) + \boldsymbol{k}_\theta(\omega) = \boldsymbol{k}_o(2\omega)$, leading to the necessary equality

$$\frac{1}{2}\left(n_o(\omega) + n_\theta(\omega)\right) = n_\theta(2\omega) \text{ or } \frac{1}{2}\left(n_o(\omega) + n_\theta(\omega)\right) = n_o(2\omega)$$

Application: SHG in uniaxial crystals

With the help of a graph, such that of Fig. 4.6(b), one can easily show that the 2ω wave should be necessarily polarized along the ordinary direction in a positive uniaxial crystal ($n_e > n_o$) and along the extraordinary direction in a negative uniaxial crystal ($n_o > n_e$).

4.3.3 Phase-matched SHG regime

In the case of a perfect phase matching situation, the undepleted pump approximation given in 4.3.1 might become invalid as the pump intensity increases. To completely study such an SHG situation, the derivation of the two coupled wave equations at ω and 2ω is necessary.

We next consider the copropagating nonlinear interaction depicted in Fig. 4.3 where the ω and 2ω waves propagate along the direction $\boldsymbol{z}$, with the electric field amplitudes:

$$\boldsymbol{E}(\omega) = \boldsymbol{e}_1 A_1(z)\, e^{\imath k_1 z}$$
$$\boldsymbol{E}(2\omega) = \boldsymbol{e}_2 A_2(z)\, e^{\imath k_2 z}.$$

We suppose a type I phase matching, which means that the polarization states $\boldsymbol{e}_1$ and $\boldsymbol{e}_2$ coincide with the eigen polarization states $\boldsymbol{e}_o$ and $\boldsymbol{e}_\theta$. This assumption allows to treat the problem with

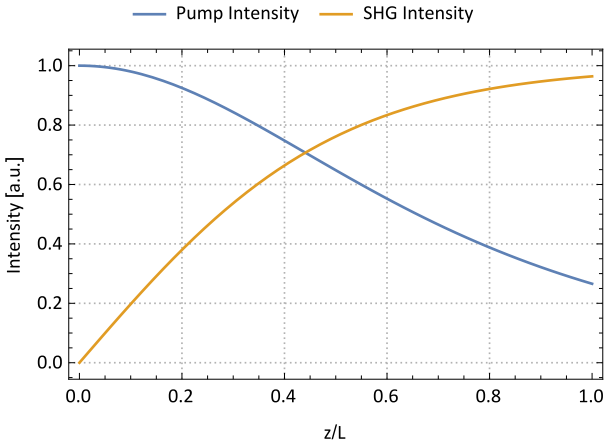

Fig. 4.7. Variation of pump intensity and the second harmonic intensity along the crystal length L in case of a perfect phase-matching SHG experiment.

only two wave equations. For a type II phase matching, one would have to set 3 coupled wave equations: two at ω (for $\boldsymbol{e}_o$ and $\boldsymbol{e}_\theta$) and one equation at 2ω (at $\boldsymbol{e}_o$ or $\boldsymbol{e}_\theta$). The wave equations for a type I phase matching $\Delta k = 2k_1 - k_2 = 0$, and neglecting the walk off, lead to

$$\frac{dA_1}{dz} = \frac{\imath(\omega)}{2n_1 c} 2\chi^{(2)}_{\text{eff}} A_2 A_1^\star, \tag{4.15}$$

$$\frac{dA_2}{dz} = \frac{\imath(2\omega)}{2n_2 c} \chi^{(2)}_{\text{eff}} A_1^2, \tag{4.16}$$

with the effective nonlinear susceptibility $\chi^{(2)}_{\text{eff}} = \boldsymbol{e}_1 \cdot \underline{\underline{\chi}}^{(2)}(\omega; 2\omega, -\omega)\boldsymbol{e}_2\boldsymbol{e}_1 = \boldsymbol{e}_2 \cdot \underline{\underline{\chi}}^{(2)}(2\omega; \omega, \omega)\boldsymbol{e}_1\boldsymbol{e}_1$. Note the difference into the degeneracy factor set to 2 in the first equation, while it is set to 1 into the second. The resolution of these two coupled equations is not difficult, although a little long[3]. Using the boundary conditions $A_1(z=0) = A_1(0)$ and $A_2(z=0) = 0$, one can show

$$A_1(z) = \frac{|A_1(0)|}{\cosh\left(q|A_1(0)|z\right)}, \tag{4.17}$$

$$A_2(z) = |A_1(0)| \tanh\left(q|A_1(0)|z\right), \tag{4.18}$$

with $q = \frac{\omega\chi^{(2)}_{\text{eff}}}{\sqrt{n_1 n_2 c}}$. The spatial evolutions for the pump and second harmonic beam intensities are plotted in Fig. 4.7. The graph illustrates the growth in SHG beam at the expense of the decrease in pump beam intensity inside the crystal. The maximum SHG efficiency under perfect phase matching interaction is

$$\eta_{\text{SHG}} = \tanh^2\left(qz\sqrt{\frac{I_1(0)}{2n_1 c\epsilon_0}}\right).$$

Although the theoretical efficiency may reach 100 %, it can neither be achieved in practice. Actually, the present model does not include major limiting effects like:

Walk-off effect: the wave equations used above are an approximation of (3.25) for which the walk-off effect is neglected. A reduction in SHG efficiency is expected because of the

[3]For those interested by the demonstration, please refer to the original article by Armstrong et al. Phys. Rev. **127**, p. 1918 (1962).

angular mismatch between the two Poynting vectors related to ω and 2ω waves. In a first approximation, one can compare the beam size Φ and the quantity $L\tan\alpha \simeq L\alpha$, which gives the beam deviation at the exit facet of a L thick crystal. The walk-off effect can be neglected if $\Phi \gg L\tan\alpha$.

Spatial effects: the present model treats the case of plane waves, and does not include inherent diffraction effect that accompagnes the propagation of finite size beam. For a beam with a diameter of $2w_0$, diffraction effect can be neglected since the Rayleigh length $Z_\mathrm{R} = \pi w_0^2/\lambda$ is much longer than the nonlinear crystal length: $Z_\mathrm{R} \gg L$.

Angular acceptance: as already mentioned, by focusing the beam inside the crystal we will increase the pump intensity and increase the SHG efficiency. Now, a reduction of the beam size is accompanied by an extension of the spatial frequency contents, namely the k vectors. Whereas, the phase-matching can be fulfilled around a specific $\boldsymbol{k}$ value, it might be imperfect for neighbouring values. As a consequence, the SHG beam profile would not match with that of the pump, because of the non uniformity of the SHG efficiency.

Temporal effects: in general these experiments are performed with pulsed laser in order to meet the required high peak powers. With typical crystal thickness of few centimeters, temporal effects could affect the SHG efficiency since the pulse duration are shorter than typically 100 ps, which corresponds to a pulse packet length of the order of 1 cm. For even shorter pulse, the group velocity difference between the ω and 2ω might also be an issue.

4.4 Optical parametric amplification, fluorescence and oscillation

We now describe a three-wave mixing that requires an intense beam at ω_3. The simultaneous propagation inside the crystal of the pump beam and a weaker signal beam at ω_1 (or ω_2) is expected to amplify the signal beam at the expanse of a decrease in the pump beam intensity. From Manley-Rowe relations, we know that such an interaction will also result in the generation of a third signal at $\omega_2 = \omega_3 - \omega_1$, which is usually referred to the *idler* beam. Such Optical Parametric Amplification effect is studied in 4.4.1. Following the understanding of this amplifier, one can easily envisioned to place it inside an optical cavity that would exhibit resonances either at the signal or idler frequencies, or at both. This problem is actually very similar to the study of a cavity laser, with few differences that will be underlined in 4.4.3.

4.4.1 Optical Parametric Amplification

Subsequently, we consider the propagation of 3 collinear waves at ω_1, ω_2 and $\omega_3 = \omega_1 + \omega_2$ inside a $\underline{\underline{\chi}}^{(2)}$ lossless crystal. The ω_3 beam is sent with a very high intensity, so that it is referred to the *pump* beam. Considering a weak efficiency for the nonlinear interaction, and that the signal and idler beam intensities are much weaker than that of the pump, the problem is solved assuming the undepleted pump approximation (or also called the parametric approximation): $I_3(z) \simeq$ Cste. Considering the collinear configuration depicted in Fig. 4.8, the simplified wave equations at ω_1 and ω_2 lead to

$$\frac{dA_1}{dz} = \frac{\imath\omega_1}{2n_1c}\chi^{(2)}_{\mathrm{eff}} A_3 A_2^\star e^{\imath\Delta kz}, \tag{4.19}$$

$$\frac{dA_2}{dz} = \frac{\imath\omega_2}{2n_2c}\chi^{(2)}_{\mathrm{eff}} A_3 A_1^\star e^{\imath\Delta kz}, \tag{4.20}$$

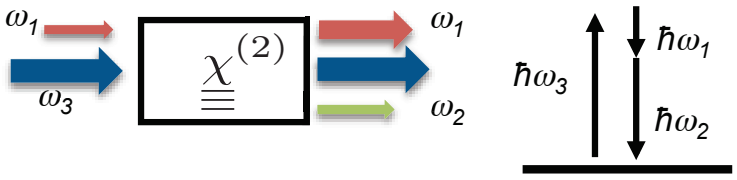

Fig. 4.8. Optical Parametric Amplification scheme. The interaction between an incident pump beam _3 with a weaker incident signal beam ω_1, results in amplification of the signal beam that is accompanied by the generation of a third beam $\omega_2 = \omega_3 - \omega_1$ (referred to *idler* beam).

with $\Delta k = k_3 - k_2 - k_1$ and $\chi^{(2)}_{\text{eff}} = 2 \times \boldsymbol{e}_1 \cdot \underline{\underline{\chi}}^{(2)}(\omega_1; \omega_3, -\omega_2)\boldsymbol{e}_3\boldsymbol{e}_2 = 2 \times \boldsymbol{e}_2 \cdot \underline{\underline{\chi}}^{(2)}(\omega_2; \omega_3, -\omega_1)\boldsymbol{e}_3\boldsymbol{e}_1$.

Before solving these two coupled equations, it is important to insist again on the assumptions that have been made. The beams are treated as monochromatic plane waves, which means for instance that their Rayleigh lengths are supposedly longer than the crystal length in order to neglect diffraction effects. The polarization states $\boldsymbol{e}_1$, $\boldsymbol{e}_2$ and $\boldsymbol{e}_3$ are supposed to coincide with eigen polarization states defined in the birefringent crystal for the direction of propagation z. Hereafter, walk-off effect will also be neglected.

To solve the problem, one needs to eliminate the $e^{\imath\Delta kz}$ phase term by introducing the new variables

$$
\begin{aligned}
a_1(z) &= \sqrt{\frac{n_1}{\omega_1}} A_1(z) e^{-\imath\Delta kz/2} \\
a_2^\star(z) &= \sqrt{\frac{n_2}{\omega_2}} A_2^\star(z) e^{+\imath\Delta kz/2} \\
a_3(z) &= \sqrt{\frac{n_3}{\omega_3}} A_3(z).
\end{aligned}
$$

Their substitution in (4.19) and (4.20) leads

$$
\begin{aligned}
\frac{da_1}{dz} + \imath\frac{\Delta k}{2} a_1 &= \imath\gamma_0 a_2^\star, \\
\frac{da_2^\star}{dz} - \imath\frac{\Delta k}{2} a_2^\star &= \imath\gamma_0^\star a_1,
\end{aligned}
$$

with

$$
\gamma_0 = \frac{\chi^{(2)}_{\text{eff}}}{c} \sqrt{\frac{\omega_1\omega_2}{n_1 n_2}} A_3.
$$

The derivatives of the previous equations enable to write

$$
\boxed{\frac{d^2 a_{1,2}}{dz^2} - \gamma^2 a_{1,2} = 0,} \tag{4.21}
$$

with the parametric gain defined as

$$
\boxed{\gamma^2 = |\gamma_0|^2 - \left(\frac{\Delta k}{2}\right)^2.} \tag{4.22}
$$

Before setting the solutions for signal and idler amplitudes, we need to emphasize the condition at which amplification can occur. Actually, it arises from (4.21) that the form of the solutions depends on the sign of the gain parameter γ^2. In case of a strong phase miss-matching condition, for which $\gamma^2 < 0$, the signal and idler amplitudes take oscillating solutions giving a very weak amplification directly related to $1/\Delta k$. In contrary, a situation with $\gamma^2 > 0$ insures non-oscillating solutions and optical amplification can take place even if $\Delta k \neq 0$. The condition to amplify the signal beam is then $|\gamma_0|^2 > \left(\frac{\Delta k}{2}\right)^2$.

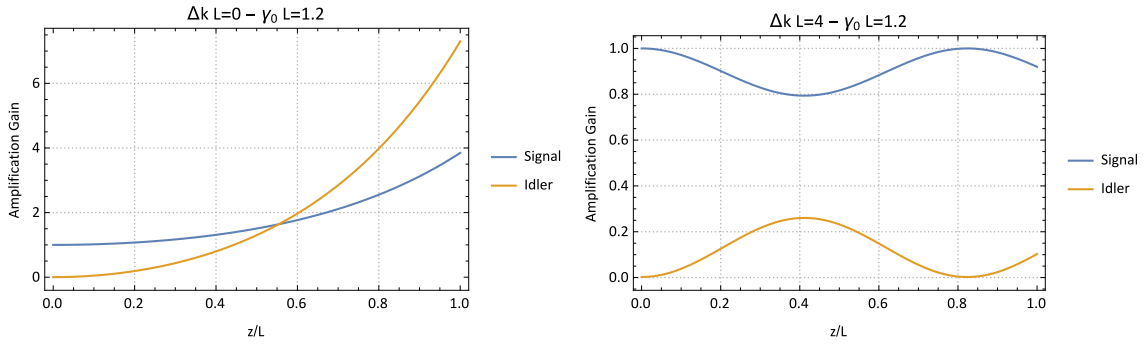

Fig. 4.9. Optical Parametric Amplification simulations : variations of the signal and idler beam intensities along the nonlinear crystal thickness L for $\gamma^2 > 0$ (left graph, with $\Delta k = 0$ and $\gamma_0 = 1.2/L$) and $\gamma^2 < 0$ (right graph, with $\Delta k = 4/L$ and $\gamma_0 = 1.2/L$).

Assuming next a positive parametric gain $\gamma^2 > 0$, one seeks solutions of the form $a_{1,2}(z) = C_{1,2}\exp(-\gamma z) + D_{1,2}\exp(+\gamma z)$ with the constants $C_{1,2}$ and $D_{1,2}$ to be determined with the boundary conditions

$$a_1(z=0) = \sqrt{\frac{n_1}{\omega_1}}A_1(0) \text{ and } a_2(z=0) = \sqrt{\frac{n_2}{\omega_2}}A_2(0).$$

The solutions are finally given by:

$$\boxed{A_{1,2}(z) = A_{1,2}(0)\left[\cosh(\gamma z) - \frac{\imath\Delta k}{2\gamma}\sinh(\gamma z)\right]e^{\imath\Delta k z/2} + \imath\frac{K_{1,2}}{\gamma}A^{\star}_{2,1}(0)\sinh(\gamma z)e^{\imath\Delta k z/2},} \quad (4.23)$$

with $K_{1,2} = \frac{\omega_{1,2}}{n_{1,2}c}\chi^{(2)}_{\text{eff}}A_3$ an amplification parameter that depends directly on the nonlinear susceptibility strength of the material and on the pump intensity.

Variations for signal and idler beam intensities are plotted in Figure 4.9 for $\gamma^2 > 0$ (with $\Delta k = 0$ and $\gamma_0 = 1.2/L$) and $\gamma^2 < 0$ (with $\Delta k = 4/L$ and $\gamma_0 = 1.2/L$). While in the first case (left graph) the two intensities increase gradually along the crystal thickness, they periodically oscillate in the second case (right graph). Note that the plotted solutions coincide with a situation where the idler beam intensity is set to 0 at $z = 0$ ($A_2(0) = 0$). In that case, and assuming a perfect phase-matching condition $\Delta k = 0$, the solutions are :

$$A_1(z) = A_1(0)\cosh(\gamma z) \text{ and } A_2(z) = \imath\frac{K_2}{\gamma}A^{\star}_1(0)\sinh(\gamma z). \quad (4.24)$$

In conclusion, the derivation of the nonlinear wave equations (4.19) and (4.20) shows that the interaction between a pump beam ω_3 and a weaker signal beam $\omega_1 < \omega_3$ can give rise to an optical amplification of the signal beam. Optical amplification occurs if $|\gamma_0|^2 > \left(\frac{\Delta k}{2}\right)^2$, with $\gamma_0 = \frac{\chi^{(2)}_{\text{eff}}}{c}\sqrt{\frac{\omega_1\omega_2}{n_1 n_2}}A_3$ the intrinsic parametric gain and $\Delta k = k_3 - k_2 - k_1$ the phase-matching term. For a given wavevector missmatch Δk, the pump intensity must reach the threshold value :

$$I_{3th} = \frac{(\Delta k)^2 n_1 n_2 n_3 c^3 \epsilon_0}{2(\chi^{(2)}_{\text{eff}})^2\omega_1\omega_2}, \quad (4.25)$$

which is calculated setting the equality $|\gamma_0|^2 = \left(\frac{\Delta k}{2}\right)^2$. The threshold intensity is null for $\Delta k = 0$, and its minimum value for $\Delta k \neq 0$ is achieved for $\omega_1 = \omega_2 = \omega_3/2$.

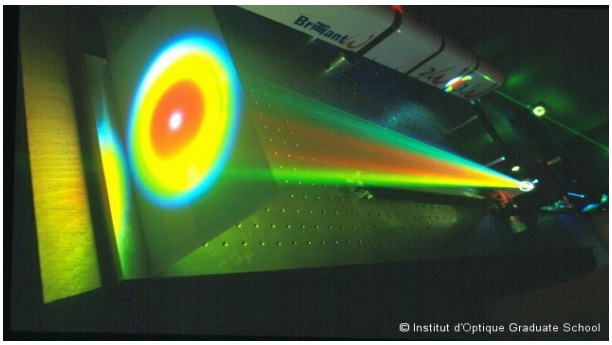

Fig. 4.10. Picture of an optical parametric fluorescence effect observed by pumping a 2nd order nonlinear crystal with a UV laser beam.

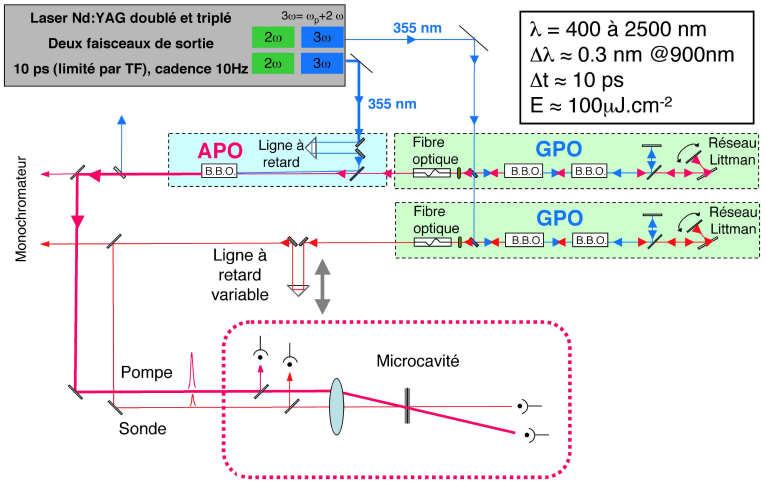

Fig. 4.11. Parametric amplification laser source that delivers two independent pulses, with a distinct control of their wavelength, and its application in a pump-probe experiment. UV pump pulses generate some parametric fluorescence effect in a first nonlinear crystal (BBO), which is amplified in a second. The beam is spectrally filtered and back reflected insight the two BBOs crystals for additional amplification. A short length of optical fiber is used to spatially filter the beam. The operating wavelength on the two lines can be selected independently.

4.4.2 Optical Parametric Fluorescence

The previous situation considers the interaction between a pump wave at ω_3 and a weaker signal beam at ω_1 (with $\omega_1 < \omega_3$) leading to the amplification of the signal beam at the expense of the pump for a perfect phase matching situation, and which is accompanied by the simultaneously generation of an idler beam at $\omega_2 = \omega_3 - \omega_1$. Now, it is interesting to note that, following the relation (4.23), the generation of the idler beam requires a non-zero incident signal beam. For boundary conditions $A_1(z = 0) = 0$ (and $A_2(z = 0) = 0$), no idler can be generated.

Yet, and as it is illustrated in the figure 4.10 picture, pumping a 2nd order nonlinear crystal with a UV laser beam results in the apparition at the crystal output of new frequencies arranged in rainbow circles. The description of such a fluorescence effect, which is not predicted by the previous classical model, requires the quantization of the electromagnetic fields. Such a quantum approach shows that the annihilation of a photon at ω_3 is expected and is accompanied by the creation simultaneously of one photon at ω_1 and one photon at ω_2. The directions toward which the photons are generated are given by the vectorial phase matching condition $\boldsymbol{k}_3 = \boldsymbol{k}_1 + \boldsymbol{k}_2$, and are distributed along circles in the case of uniaxial crystals (in accordance with the uncertainty principle of quantum mechanics).

Numerous of quantum optics experiments use this spectacular fluorescence effect as photons generated in a pair of signal and idler modes (defined by wavevectors that satisfy the phase matching condition) are correlated.

Parametric fluorescence effect is also used to generate seed light to be amplified through a succession of optical parametric amplifiers as illustrated in figure 4.11. Even more interestingly, fluorescence effect serves as a first step to initiate a parametric oscillation inside a cavity, giving rise to a new class of optical oscillators studied in the next paragraph.

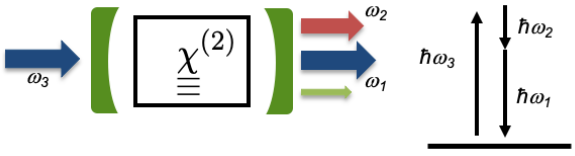

Fig. 4.12. Optical Parametric Oscillator (OPO) scheme. The interaction between an incident pump beam ω_3 and an intracavity nonlinear crystal gives rise to the generation of weak signal and idler beams through a parametric fluorescence effect. This beams serve as a seed that will be amplified after many reflections inside the cavity. The cavity oscillation occurs for a pump intensity at which the parametric gain strictly compensates for the cavity losses over one round-trip.

4.4.3 Optical Parametric Oscillation

In order to achieve a higher efficiency in the amplification of the seed signal generated by parametric fluorescence effect, the nonlinear material is inserted inside an optical cavity as illustrated in figure 4.12. Following the successive reflections on the two mirrors, the signal and idler beams are expected to experience amplification. Once the parametric gain exceeds the cavity losses over one round trip, an oscillation of the cavity is expected, similar to that observed in a laser. Such a source is called an Optical Parametric Oscillator (OPO).

At first, we consider the case of a singly resonant cavity for which the two mirrors of the cavity only reflect the signal beam. The mirrors are then coated with anti-reflection layers to prevent any reflection at the pump and idler wavelengths. Assuming a perfect phase matching and using the relation (4.24), the oscillation threshold for a singly resonant OPO is given by:

$$r_1 r_1' \cosh(\gamma_0 L) = 1, \tag{4.26}$$

where r_1 and r_1' stands for the reflectance of the two cavity mirrors and L the nonllinear crystal thickness. It is important to underline that the optical amplification of the signal beams only occurs in the forward direction, for which a perfect phase matching is satisfied (assuming a collinear configuration). Along the backward direction, the phase matching is not verified as signal and pump beams propagate in two opposite directions.

In case of a doubly resonant OPO, with mirrors reflecting both the signal and idler beams, one can show that the oscillation threshold condition satisfies:

$$\cosh(\gamma_0 L) = \frac{1 + r_1 r_1' r_2 r_2'}{r_1 r_1' + r_2 r_2'}, \tag{4.27}$$

where r_2 and r_2' are reflectance of the two cavity mirrors for the idler beam.

Although it generates coherent beams, the operation of an OPO differs from that of a laser. Optical amplification in OPOs is driven by a 2nd order nonlinear interaction, a parametric amplification, and has to be clearly distinguished from the amplification by simultaneous emission of radiation for lasers. The latter is based on the pumping of active elements or dopants (atoms, ions, molecules, electrons...) for their excitations to upper level states in order to reach the inversion of the population between the two energy states involved for the amplification transition. The parametric amplification implies no transfer of energy between the pump and the material as it is based on a non-resonant transition (we always consider lossless materials). The gain saturation observed as the pump power increases is directly monitored through the pump depletion consecutive of the transfer of energy between the pump and the two signal and idler beams. As it is based on a non-resonant interaction, an OPO can be widely tuned in frequency, where the tunability for a laser is limited by the optical transition linewidth. The tunability of an OPO is achieved by changing the phase matching condition, either through an angular position control of the crystal respectively to the cavity optical axis, or a control on the temperature of the crystal.

4.5 Quasi-Phase Matching

We have previously shown how phase matching condition can be fulfilled by exploiting birefringence properties of materials. However, birefringent phase matching can not be achieved in all materials, nor for all nonlinear interactions. More specifically, it may happen that the exploitation of a strong nonlinear susceptibility tensor component does not allow any birefringent phase matching. Indeed, some materials (for instance Lithium Niobate) are characterized by a strong $\chi^{(2)}_{ZZZ}$ coefficient implying that all the interacted waves are polarized in the same direction, which makes the phase matching impossible to realize by birefringence.

An alternative technique consists in introducing a periodicity in the nonlinear term source, more specifically by periodically inverting the sign of the effective nonlinear susceptibility. One reminds that in a non-phase matched situation, the wave intensity follows an oscillating variation. Whereas, it reaches a maximum value after a distance $z = \pi/\Delta k = L_c$, the coherence length (3.3.2), the intensity decreases down to zero at $z = 2 \times L_c$ as the nonlinear polarization being out off phase with the free running wave at ω. The solution consists in periodically inverting the sign the crystal orientation in order to introduce a π phase shift to the nonlinear polarization and to maintain a constructive interference with the free running wave.

As an illustration, let's consider the second harmonic generation case in a configuration that exploits the strong $\chi^{(2)}_{ZZZ}$ coefficient. The 2ω wave follows the wave equation (4.7)

$$\frac{dA_{2\omega}(z)}{dz} = \frac{\imath(2\omega)}{2n_{2\omega}c}\chi^{(2)}_{\text{eff}}\ A^2_\omega e^{\imath\Delta\boldsymbol{k}\cdot\boldsymbol{z}},$$

with $\chi^{(2)}_{\text{eff}} = \boldsymbol{e}_Z \cdot \chi^{(2)}_{ZZZ}\boldsymbol{e}_Z\boldsymbol{e}_Z$ the effective nonlinear susceptibility and $\Delta\boldsymbol{k} = 2\boldsymbol{k}_\omega - \boldsymbol{k}_{2\omega}$ the wave vector missmatch. By means of a technique presented below, we next introduce a periodic spatial variation for $\chi^{(2)}_{\text{eff}}(z) = \chi^{(2)}_{\text{eff},0}\cos(Kz)$ in the 2ω wave equation

$$\begin{aligned}\frac{dA_{2\omega}(z)}{dz} &= \frac{\imath(2\omega)}{2n_{2\omega}c}\chi^{(2)}_{\text{eff},0}\ A^2_\omega\ \cos(Kz)e^{\imath\Delta\boldsymbol{k}\cdot\boldsymbol{z}},\\ &= \frac{\imath(2\omega)}{2n_{2\omega}c}\chi^{(2)}_{\text{eff},0}\ A^2_\omega\ \frac{e^{\imath Kz}+e^{-\imath Kz}}{2}e^{\imath\Delta\boldsymbol{k}\cdot\boldsymbol{z}},\end{aligned} \tag{4.28}$$

which shows that a quasi-phase matched (QPM) situation is achieved since $K = \Delta\boldsymbol{k} = 2\boldsymbol{k}_\omega - \boldsymbol{k}_{2\omega}$. One concludes that a periodic inversion of the $\chi^{(2)}_{\text{eff}}$ sign, with a period $\Lambda = 2 \times L_c$, leads to a growth in the intensity at 2ω. Compare to the case of a perfect phase-matching condition with an effective susceptibility $\chi^{(2)}_{\text{eff}}$, the efficiency of SHG under the quasi-phase matching condition is reduced by a factor 4 as the effective nonlinear susceptibility is $\chi^{(2)}_{\text{eff}}/2$. Nevertheless, a phase matching condition is reached in a configuration for which no birefringent phase matching can be set !

The generalization to a 3-wave mixing configuration is straightforward. The quasi-phase matched condition for the interaction between 3 waves at ω_1, ω_2 and $\omega_3 = \omega_1 + \omega_2$ implies to satisfy the equality $\boldsymbol{k}(\omega_3) = \boldsymbol{k}(\omega_1) + \boldsymbol{k}(\omega_2) + \mathbf{K}_{\text{QPM}}$, as illustrated in figure 4.13(b) for a collinear configuration.

Material poling is achieved by applying a static field between electrodes, which leads to a permanent domain reversal of the material. A patterning of the electrodes is performed to realize a periodically poled crystal shown in figure 4.13(a) and to obtain a succession of piles with inverted domains. Considering the propagation of Z polarized waves, the effective nonlinear susceptibility for the even piles is $\chi^{(2)}_{\text{effEV}} = \boldsymbol{e}_Z \cdot \chi^{(2)}_{ZZZ}\boldsymbol{e}_Z\boldsymbol{e}_Z$, whereas it is opposite for odd piles as $\chi^{(2)}_{\text{effOD}} = (-\boldsymbol{e}_Z)\cdot\chi^{(2)}_{ZZZ}(-\boldsymbol{e}_Z)(-\boldsymbol{e}_Z) = -\chi^{(2)}_{\text{effEV}}$. A more accurate description of QPM efficiency consists in developing the effective nonlinear susceptibility with a square wave function $S(z)$

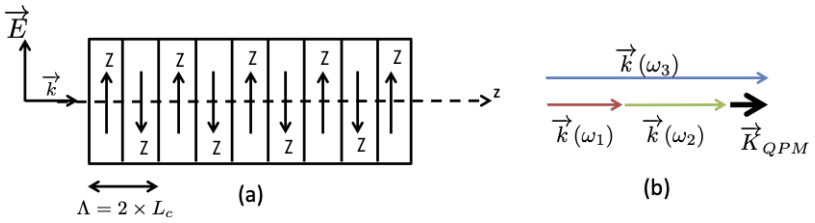

Fig. 4.13. (a) Periodically poled nonlinear crystal with a period set to $\Lambda = 2 \times L_c$ to satisfy the phase matching for the 3 wave interaction depicted in (b).

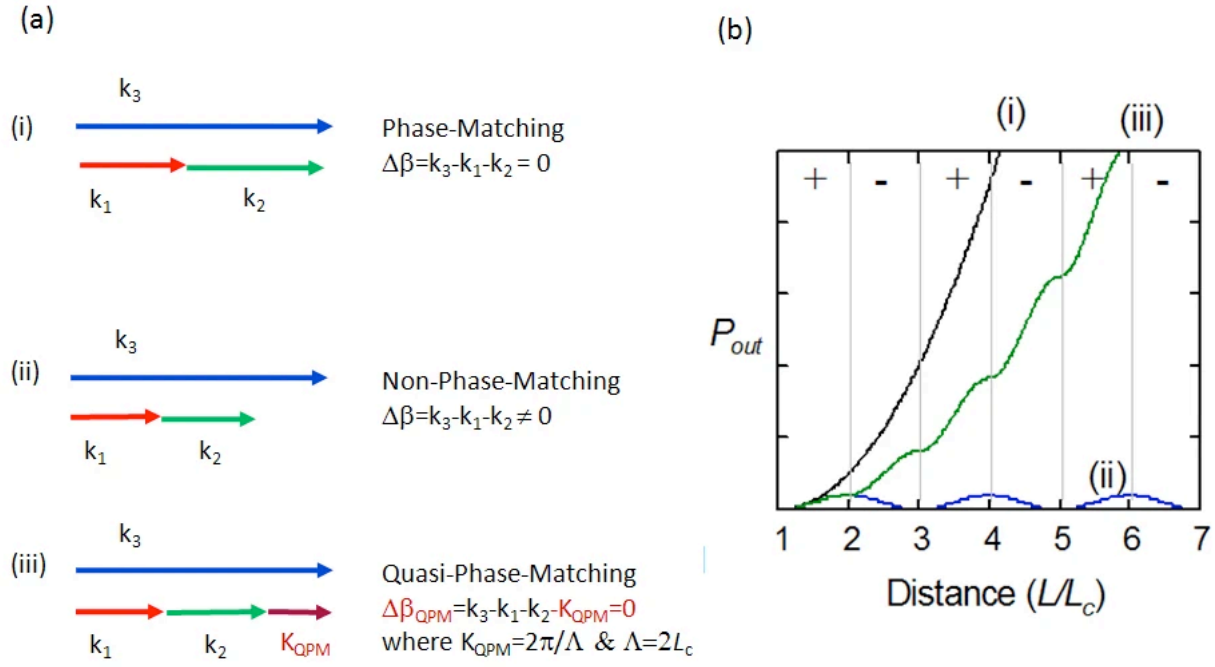

Fig. 4.14. Comparison in the power evolution under perfect phase matching (i), non-phase matching (ii) and quasi-phase matching (iii) situations. The signs represent the sign of the effective nonlinear susceptibility $\chi^{(2)}_{\text{eff}}$ along the material thickness. Figure from HCP Photonics https://www.hcphotonics.com/ppln-guide-overview

of period $\Lambda = 2 \times L_c$. Using the Fourier expansion $S(z) = \frac{4}{\pi} \sum_p \frac{1}{2p+1} \sin((2p+1)2\pi z/\Lambda)$, the effective nonlinear susceptibility is then equal to $i\frac{\chi^{(2)}_{\text{eff}}}{\pi/2}$.

Finally, a comparison of power evolutions through a $\chi^{(2)}$ nonlinear material for different phase matching situations is shown in figure 4.14 (figure from HCP Photonics web site). Under QPM, power evolution can be approximated by a parabolic curve, as for the perfect phase matched situation, with a reduced efficiency due to a lower effective nonlinear susceptibility as predicted below.

Chapter 5

3rd Order Nonlinear Optical Interactions

Contents

5.1 Introduction

This chapter is dedicated to the study of 3rd order nonlinear optical effects, through which 4 waves at ω_1, ω_2, ω_3 and $\omega_4 = \omega_1 + \omega_2 + \omega_3$ could interact in a material with a non-zero third order susceptibility $\chi^{(3)}$. In a first part, we will describe the so-called *Four-Wave Mixing (FWM)* (5.3) interactions occurring in lossless materials. Generally, these interactions refer to *parametric interactions*. Similarly to parametric interactions in $\chi^{(2)}$ materials, third order optical parametric amplification process can be exploited to amplify a signal beam by means of its interaction with a pump beam. This amplification is also accompanied by the simultaneous generation of an idler beam. An other application of FWM is the realization of *Phase-Conjugate Mirrors*, enabling the generation of a beam which is the phase-conjugated of an incoming signal.

Section (5.4) will present the *Optical Kerr Effect* related to the capability of an intense beam to modify the refractive index of the material. The consequence on the propagation of optical wave-packets (either temporal or spatial) will be analyzed in details, showing the interdependence between optical Kerr effect and dispersion (in time domain) or diffraction (in spatial domain).

The last section will focus on resonant nonlinear interactions involving a two-photon transition on the material, like two-photon absorption or emission effects, Raman or Brillouin scattering.

5.2 Transfer of energy between an electromagnetic field and a medium

We consider the propagation of an electromagnetic wave at ω through a third order nonlinear material. We suppose that it contains a nonlinear polarization $\boldsymbol{P}^{(3)}(\omega)$ radiating at the frequency ω. This term source could have been generated by the wave ω itself through

$$\boldsymbol{P}^{(3)}(\omega = \omega - \omega + \omega) = 3\epsilon_0 \underline{\underline{\underline{\chi}}}^{(3)} \boldsymbol{E}(\omega)\boldsymbol{E}(-\omega)\boldsymbol{E}(\omega),$$

or by means of a pump beam at ω_p. It that case the nonlinear polarization expression is [1] :

$$\boldsymbol{P}^{(3)}(\omega = \omega_p - \omega_p + \omega) = 6\epsilon_0 \underline{\underline{\underline{\chi}}}^{(3)} \boldsymbol{E}(\omega_p)\boldsymbol{E}(-\omega_p)\boldsymbol{E}(\omega).$$

The quantity of energy that is exchanged between the wave at ω and the material, per unit of time and volume is given by the relation (3.14) p. 21. Substituting $\boldsymbol{P}(\omega) = \boldsymbol{P}^{(1)}(\omega) + \boldsymbol{P}^{(3)}(\omega)$ into (3.14) leads to the relation :

$$-\frac{\partial W}{\partial t} = 2\omega\epsilon_0 \left(\boldsymbol{e} \cdot \underline{\underline{\chi}}^{(1)''}(\omega)\boldsymbol{e}\right) |E(\omega)|^2 + 2\omega\epsilon_0 \left(\boldsymbol{e} \cdot \underline{\underline{\underline{\chi}}}^{(3)''} \boldsymbol{e}_p \boldsymbol{e}_p \boldsymbol{e}\right) |E(\omega_p)|^2 |E(\omega)|^2. \tag{5.1}$$

A nonlinear interaction implying a transfer of energy between the interacted waves and the material requires a non-zero imaginary part $\underline{\underline{\underline{\chi}}}^{(3)''}$ of the susceptibility (as for the linear case).

[1] Beside the difference in the frequency arguments between those two relations, note the difference in the degeneracy factor. For a given effective material susceptibility, an interaction governed by $\omega = \omega_p - \omega_p + \omega$ is twice more efficient that an interaction $\omega = \omega - \omega + \omega$.

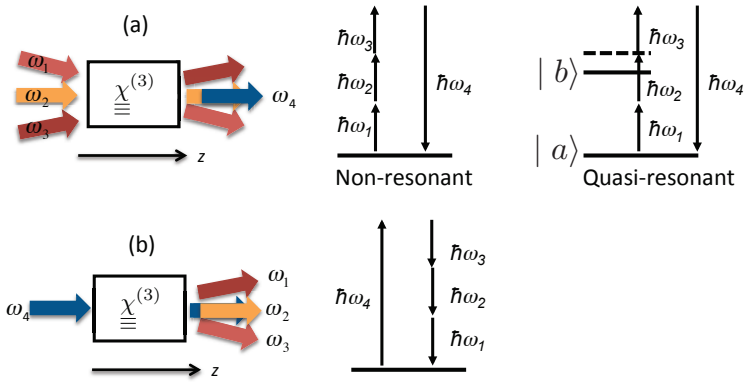

Fig. 5.1. Four Wave Mixing schemes. (a) The interaction between three waves at ω_1, ω_2 and ω_3 generate a fourth wave at $\omega_4 = \omega_1 + \omega_2 + \omega_3$. (b) One single intense pump beam at ω_4 can generate 3 waves at ω_1, ω_2 and ω_3.

5.3 Four-Wave Mixing

Third order nonlinear interactions involve interaction between 4 waves at ω_1, ω_2, ω_3 and $\omega_4 = \omega_1 + \omega_2 + \omega_3$. Hereafter, we study different Four-Wave Mixing (FWM) configurations, non-degenerate and degenerate in frequencies, through lossless nonlinear materials with a purely real $\chi^{(3)}$ nonlinear susceptibility (and a purely real linear susceptibility). As a consequence, interactions will not be accompanied by any transfer of energy between the interacted waves and the nonlinear material. As for the 2nd order nonlinear effects, one could easily show that FWM interactions in lossless material follow the energy conservation relation:

$$\hbar\omega_1 + \hbar\omega_2 + \hbar\omega_3 = \hbar\omega_4.$$

Similarly, the derivation of nonlinear wave equations would give the following phase matching condition:

$$\boldsymbol{k}_1 + \boldsymbol{k}_2 + \boldsymbol{k}_3 = \boldsymbol{k}_4,$$

which is equivalent to a law of momentum conservation.

5.3.1 Generation of UV and IR beams

Figure 5.1 schematically illustrates (a) the capability for three incident waves at ω_1, ω_2 and ω_3 to generate a fourth wave at $\omega_4 = \omega_1 + \omega_2 + \omega_3$, and (b) for one single intense pump beam at ω_4 to generate 3 waves at ω_1, ω_2 and ω_3. These interactions are governed by the phase matching condition $\boldsymbol{k}_1 + \boldsymbol{k}_2 + \boldsymbol{k}_3 = \boldsymbol{k}_4$, which determines the directions of propagation for the 4 waves (in relation with the dispersion property of the nonlinear material). Whereas the interaction described in Fig. 5.1(a), which could serve to generate a UV beam from IR pump beams, can be theoretically described solving nonlinear wave equations, the Fig. 5.1(b) interaction requires a quantum description. Following the quantization of the optical electromagnetic waves, one could show that, through the interaction, one photon at ω_4 is annihilated to generate simultaneously 3 photons respectively at ω_1, ω_2 and ω_3.

These third order interactions find some interests in centro-symetric material since their $\chi^{(2)}$ vanishes. Now, one has to underline the inherently weak efficiency of these nonlinear effects, since $\chi^{(3)}EEE \ll \chi^{(2)}EE$ for nonresonant interactions. A way to enhance the $\chi^{(3)}$ nonlinear susceptibility consists in using a quasi-resonant interaction as depicted in Figure 5.1(a) for which $\hbar\omega_1 + \hbar\omega_2 \simeq \hbar\omega_{ab}$, the energy transition between energy states $|a\rangle$ and $|b\rangle$.

5.3.2 Optical parametric amplification through FWM in an optical fiber

In the following, we illustrate the optical amplification of a signal ω_s using either two pump beams ω_{p1} and ω_{p2}, or one pump beam ω_p, through the interaction depicted in Figure 5.2 where

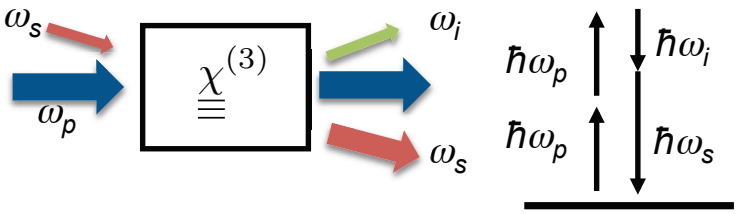

Fig. 5.2. 3rd Order optical parametric amplification : a signal beam ω_s is amplified through the interaction in a $\chi^{(3)}$ material with one single intense pump beam at ω_p. The interaction follows the energy conservation relation $\hbar\omega_p + \hbar\omega_p = \hbar\omega_s + \hbar\omega_i$, with ω_i the frequency of the idler beam that accompanies the amplification of the signal beam.

the beam frequencies follow the relation $\hbar\omega_p + \hbar\omega_p = \hbar\omega_s + \hbar\omega_i$. It is anticipated that the amplification of the signal beam ω_s is accompanied by the generation of a third beam at ω_i, referred to as the idler beam.

Optical fiber parametric amplifier: We next take the example of a parametric amplifier realized in a length of optical fiber. Typically the fiber is made in silica. Although the value of $\chi^{(3)}$ in silica remains rather small, significant amplification can be achieved in practice by using a long interaction length easily achievable in optical fibers. In addition, it would give the opportunity to play with nonlinear wave equations that has been derived in case of waveguides (see section 3.5).

The complex amplitude related to the three waves is written:

$$\boldsymbol{E}_m(\boldsymbol{r}, z) = \boldsymbol{e}_m \phi_m^q(\boldsymbol{r}) A_m(z) e^{\imath\beta_q(\omega_m)z}, \tag{5.2}$$

with $m = p, s$ or i. The three waves propagate inside a waveguide along the z direction, along which the waveguide is invariant. The mode field distribution related to each wave is characterized by the wavevector $\beta_p(\omega_m)$, the polarization state $\boldsymbol{e}_m$ and the spatial distribution $\phi_m^p(\boldsymbol{r})$. Assuming that the set of transverse modes form a complete base of normalized and orthogonal modes, we have the relation (orthogonality between the transverse modes):

$$\int\int \phi_m^q(\boldsymbol{r})\phi_m^{q'}(\boldsymbol{r})^\star d^2\boldsymbol{r} = \delta_{qq'}.$$

Using the nonlinear wave equation (3.32), one can write three coupled wave equation at ω_p, ω_s and ω_i:

$$\begin{aligned}
\frac{dA_p}{dz} &= \frac{i\omega_p}{2n_p c} 3\xi_{p-pp-p}\chi^{(3)}_{eff}|A_p|^2 A_p \\
\frac{dA_s}{dz} &= \frac{i\omega_s}{2n_s c} 3\chi^{(3)}_{eff}\left[2\xi_{p-ps-s}|A_p|^2 A_s + \xi_{ppi-s}A_p^2 A_i^* e^{i\Delta\beta z}\right] \\
\frac{dA_i}{dz} &= \frac{i\omega_i}{2n_i c} 3\chi^{(3)}_{eff}\left[2\xi_{p-pi-i}|A_p|^2 A_i + \xi_{p-ps-i}A_p^2 A_s^* e^{i\Delta\beta z}\right]
\end{aligned} \tag{5.3}$$

As underlined by the right hand side term of wave equation (3.32), the modification of the envelope field is governed by the spatial overlapping between the spatial dependent nonlinear polarization term $\boldsymbol{P}^{(NL)}(\boldsymbol{r}, \omega)$ and the spatial distribution of the mode $\phi_m^p(\boldsymbol{r})$. As a consequence, the three wave equations are expressed with overlapping coefficients, which are given by:

$$\xi_{ijk-l} = \frac{\int \phi_i\phi_j\phi_k\phi_l^\star d^2\boldsymbol{r}}{\int \phi_l\phi_l^\star d^2\boldsymbol{r}} \quad \text{and} \quad \xi_{i-jk-l} = \frac{\int \phi_i\phi_j{}^\star\phi_k\phi_l{}^\star d^2\boldsymbol{r}}{\int \phi_l\phi_l{}^\star d^2\boldsymbol{r}}, \tag{5.4}$$

where the indices i, j, k, and l refer to any of the interacted waves indices, p, s or i. Subsequently, we consider the propagation in a single mode fiber. The variation in the confinement for the

three waves is neglected and the overlapping coefficients are taken equal. Finally, the interaction efficiency is governed by the phase matching term:

$$\Delta\beta = 2\beta_p - \beta_s - \beta_i. \tag{5.5}$$

Note that nonlinear wave equations (5.3) assume that signal and idler wave intensities are much weaker than the pump intensity.

We start by deriving the wave equation for the pump:

$$\frac{dA_p}{dz} = i\gamma P_p A_p,$$

which has been expressed in terms of the pump power $P_p = 2nc\epsilon_0|A_p|^2 \int\int \phi_l\phi_l{}^\star d^2\boldsymbol{r}$ and the parametric gain coefficient γ:

$$\gamma = \frac{3\omega_p}{4\epsilon_0 n_p^2 c} \frac{\int |\phi_p|^4 d^2\boldsymbol{r}}{\left(\int |\phi_p|^2 d^2\boldsymbol{r}\right)^2} \chi^{(3)}_{eff} \tag{5.6}$$

Under a parametric regime, i.e. neglecting the pump depletion, the pump wave evolution follows

$$\begin{aligned} A_p(z) &= A_p(0)e^{i\gamma P_p z} \\ &= |A_p(0)|e^{i\theta}e^{i\gamma P_p z}, \end{aligned}$$

where θ is the linear phase related to the pump wave $A_p(z=0)$. The solution shows that, under parametric interaction, the undepleted pump wave experiences a nonlinear phase shift $\Phi_{NL}(z) = \gamma P_p z$. This nonlinear effect refers to *Optical Kerr Effect* that is studied in more details in section 5.4.

Substituting the pump wave evolution in wave equations (5.3), one can re-write wave equations for signal idler waves:

$$\frac{dA_s}{dz} = i\gamma P_p \frac{n_p}{\omega_p}\frac{\omega_s}{n_s}\left[2A_s + A_i^* e^{2i\theta}e^{i(\Delta\beta+2\gamma P_p)z}\right] \tag{5.7}$$

$$\frac{dA_i^*}{dz} = -i\gamma P_p \frac{n_p}{\omega_p}\frac{\omega_i}{n_i}\left[2A_i^* + A_s e^{-2i\theta}e^{-i(\Delta\beta+2\gamma P_p)z}\right]. \tag{5.8}$$

In order to simplify those coupled equations one can introduce new variables:

$$B_s(z) = A_s(z)\exp\left(-2i\gamma P_p \frac{n_p}{\omega_p}\frac{\omega_s}{n_s}z\right) \quad \text{and} \quad B_i^*(z) = A_i^*(z)\exp\left(+2i\gamma P_p \frac{n_p}{\omega_p}\frac{\omega_i}{n_i}z\right),$$

leading to the set of coupled equations:

$$\frac{dB_s}{dz} = i\gamma P_p \frac{n_p}{\omega_p}\frac{\omega_s}{n_s}e^{2i\theta}B_i^*(z)e^{+iK'z} \tag{5.9}$$

$$\frac{dB_i^*}{dz} = -i\gamma P_p \frac{n_p}{\omega_p}\frac{\omega_i}{n_i}e^{-2i\theta}B_s(z)e^{-iK'z}. \tag{5.10}$$

with $K' = \Delta\beta + 2\gamma P_p\left[1 - \frac{n_p}{\omega_p}\left(\frac{\omega_s}{n_s} + \frac{\omega_i}{n_i}\right)\right]$. Actually, the previous coupled equations take a form similar to those derived for the parametric amplification in a $\chi^{(2)}$ material (section 4.4.1), helping in deriving the solutions in case of parametric amplification in a $\chi^{(3)}$ material.

Assuming the boundary conditions $A_i(z=0)=0$ and $A_s(z=0)=A_{s0}$, the solutions for signal and idler optical power evolutions are:

$$P_s(z) = P_s(0)\left[1+(1+\frac{K'^2}{4g'^2})\sinh^2(g'z)\right] \tag{5.11}$$

$$P_i(z) = \frac{\omega_i n_s}{n_i \omega_s} P_s(0)(1+\frac{K'^2}{4g'^2})\sinh^2(g'z), \tag{5.12}$$

with $g'^2 = \Gamma'^2 - \frac{K'^2}{4}$ the parametric gain, and $\Gamma' = \gamma P_p \frac{n_p}{\omega_p}\sqrt{\frac{\omega_i\omega_s}{n_i n_s}}$. The amplification factor for the signal can be directly derived from (5.11):

$$G(z) = 1+\frac{K'^2}{g'^2}\sinh^2(g'z) \tag{5.13}$$

$$\simeq 1+\left(\frac{\gamma P_p}{g'}\right)^2\sinh^2(g'z). \tag{5.14}$$

As a conclusion, an incident signal wave at ω_s is subject to amplification through its interaction with a pump beam at ω_p in a $\chi^{(3)}$ nonlinear material. Assuming a lossless material, this amplification is accompanied by the generation of an idler beam at $\omega_i = 2\omega_p - \omega_s$. The amplification factor is directly proportional to the pump intensity[2] and depends on the phase matching condition given by $K' = \Delta\beta + 2\gamma P_p\left[1-\frac{n_p}{\omega_p}\left(\frac{\omega_s}{n_s}+\frac{\omega_i}{n_i}\right)\right]$. As it will be underlined below, this phase matching condition is influenced by the Optical Kerr Effect, through the term proportional to γP_p. Considering that $\frac{n_p}{\omega_p} \simeq \frac{n_s}{\omega_s} \simeq \frac{n_i}{\omega_i}$, the phase matching condition can be simplified in:

$$\begin{aligned} K' &= \Delta\beta + 2\gamma P_p\left[1-\frac{n_p}{\omega_p}\left(\frac{\omega_s}{n_s}+\frac{\omega_i}{n_i}\right)\right] \\ &\simeq \Delta\beta - 2\gamma P_p. \end{aligned} \tag{5.15}$$

In the case of a perfect phase matching condition $K'=0$, the amplification factor reaches its maximum value for $K'=0$:

$$\begin{aligned} G_{max}(z) &\simeq 1+\sinh^2(\gamma P_p z) \\ &\simeq 1+\sinh^2(\Phi_{NL}(z)) \end{aligned} \tag{5.16}$$

since $g' = \Gamma'$. We have assumed that $\frac{n_p}{\omega_p} \simeq \frac{n_s}{\omega_s} \simeq \frac{n_i}{\omega_i}$.

Comments:

- The phase matching condition is described by a linear term, $\Delta\beta$ the phase mismatch between the interacted waves, and a nonlinear effect related to the nonlinear phase $\Phi_{NL}(z) = \gamma P_p z$ experienced by the pump wave. As it will be explained in the next section, the pump intensity modifies the refractive index of the material, which directly influenced the phase matching condition.

- Concerning the phase mismatch $\Delta\beta = 2\beta_p - \beta_s - \beta_i$ between the interacted waves, we show its relation with the dispersion coefficient β_2 of the material (or the waveguide). Indeed, one can write $\omega_s = \omega_p - \Omega$, meaning that $\omega_i = \omega_p + \Omega$. if we consider a narrow spectral

[2]The amplification factor depends on the quantity γP_p and, one could note that the expression (5.6) for γ depends on the mode field distribution of the waves.

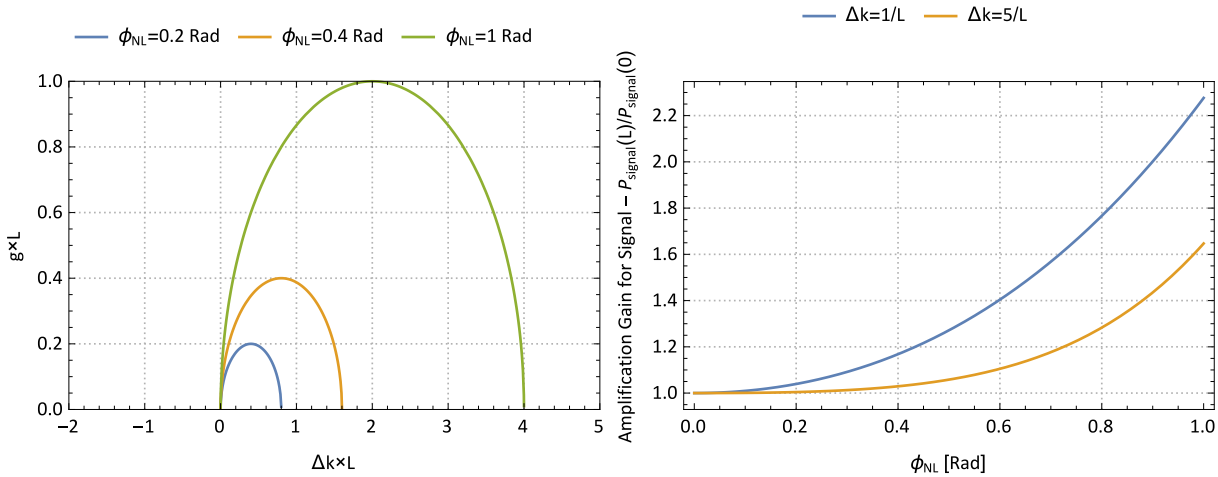

Fig. 5.3. Left: Parametric gain g' accumulated over a length L with the phase mismatch $\Delta\beta L$ for two nonlinear phase values. Right: Amplification gain for the signal $P_s(L)/P_s(0)$ for nonlinear phase varying between 0 to 1, for two phase mismatch values.

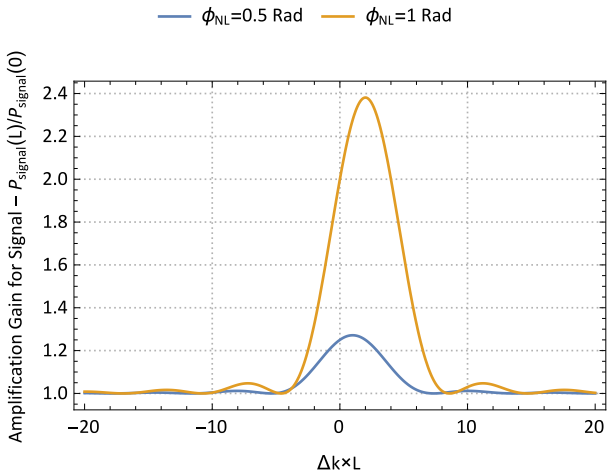

Fig. 5.4. Amplification gain bandwidth for the signal for two nonlinear phase shift values.

interval Ω between the interacted waves, i.e. $\Omega \ll \omega_p$, the Taylor's expansions for β_s and β_i show that $\Delta\beta \simeq -\beta_2\Omega^2$.

Neglecting the Optical Kerr Effect, parametric amplification would require the propagation through a waveguide with a zero dispersion, $\beta_2 = 0$. However, the phase matching is fulfilled since $K' = 0$, implying $\Delta\beta = 2\gamma P_p(z = 0)$. Now, depending on the sign of the nonlinear coefficient $\chi^{(3)}_{eff}$ (equivalently of γ), phase matching can only be fulfilled with dispersion coefficient β_2 which takes an opposite sign. Considering for instance, parametric amplification in a silica fiber, for which $\gamma > 0$, amplification implies the propagation in anomalous dispersion regime with $\beta_2 < 0$ [3].

- Parametric amplification occurs only if $g'^2 > 0$, or $\Gamma'^2 > K'^2/4$, which implies the following condition for the linear phase missmatch: $0 < \Delta\beta < 4\gamma P_p$. The maximum value for amplification is reached for $\Delta\beta = 2\gamma P_p$, coinciding with $K'^2 = 0$.

[3] $\beta_2 < 0$ coincides with a positive dispersion coefficient D.

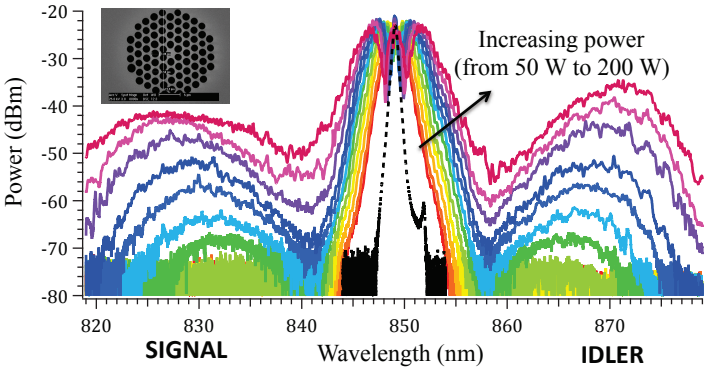

Fig. 5.5. Measured spectra at the output of the photonics crystal fiber (inset) injected with 1 ps pulse duration at 850 nm. As the injected pulse power increases, signal and idler side lobes are generated through an amplified parametric fluorescence effect. The spectrum of the injected pulse is shown in black line. From Margaux Barbier, PhD manuscript (2014).

5.3.3 Optical Parametric Fluorescence Effect

We next consider the FWM depicted in Figure 5.2, but where we suppose that only one pump beam is incident on the $\chi^{(3)}$ material. The solutions (5.11) for the FWM wave equations show that, with the boundary conditions $A_s(z=0)=0$ and $A_i(z=0)=0$, the signal and idler power remains null: $P_s(z)=0$ and $P_i(z)=0$. However, and similarly to the parametric fluorescence effect observed in a $\chi^{(2)}$ material, signal and idler photons are generated at frequencies which minimize the phase matching condition for the material (or the waveguide) used in the experiment. A complete description of such an effect requires the optical field quantization at ω_s and ω_i, with an approach similar to that of a $\chi^{(2)}$ fluorescence effect.

Figure 5.5 illustrates the generation of signal and idlers photons in a photonics crystal fiber (inset) subject to the injection of 1 ps pulse duration at 850 nm. As the pulse power increases, the signal and idler side-bands are amplified, corresponding to the amplification by FWM of photons being initially generated through a parametric fluorescence effect.

5.4 Optical Kerr Effect

5.4.1 Nonlinear refractive index

We consider the propagation of a monochromatic wave at ω in a $\chi^{(3)}$ nonlinear material and study the consequence of the nonlinear polarization at ω:

$$\boldsymbol{P}^{(3)}(\omega = \omega - \omega + \omega) = \epsilon_0 \underset{\equiv\equiv\equiv}{\chi}^{(3)}(\omega; \omega, -\omega, \omega)\boldsymbol{E}(\omega)\boldsymbol{E}(-\omega)\boldsymbol{E}(\omega). \tag{5.17}$$

The total polarization that is generated inside the material is:

$$\begin{aligned}\boldsymbol{P}(\omega) &= \boldsymbol{P}^{(1)}(\omega) + \boldsymbol{P}^{(3)}(\omega) \\ &= \epsilon_0 \left[\underset{\equiv}{\chi}^{(1)}(\omega)\boldsymbol{E}(\omega) + \underset{\equiv\equiv\equiv}{\chi}^{(3)}(\omega; \omega, -\omega, \omega)\boldsymbol{E}(\omega)\boldsymbol{E}(-\omega)\boldsymbol{E}(\omega)\right].\end{aligned} \tag{5.18}$$

During its propagation the wave ω will be modified through the effective polarization

$$\boldsymbol{e} \cdot \boldsymbol{P}(\omega) = \epsilon_0 \left[\chi_{\text{eff}} + \underbrace{\chi^{(3)}_{\text{eff}}|A(\omega)|^2}\right] A(\omega)e^{\imath kz}, \tag{5.19}$$

which shows a modification of the linear susceptibility proportionally to the wave intensity. The contribution from the imaginary part χ''_{eff} of the third order nonlinear susceptibility induces a modification of either the absorption or the amplification coefficient of the material (depending on its sign). One can refer to the situation of the two-photon absorption (or emission) that will be studied later.

Subsequently in this section, we will consider the contribution from the real part χ'_{eff} of the third order nonlinear susceptibility, which modifies the refractive index of the material proportionally to the wave intensity. Such an effect refers to as optical Kerr effect. Next, we assume a lossless material in order to neglect the contribution from the the imaginary part χ''_{eff}. One reminds the relation between the linear refractive index and the linear susceptibility for an isotropic material: $n_0(\omega) = \sqrt{1 + \chi_{\text{eff}}(\omega)}$. The modification of the refractive index from optical Kerr effect follows the relation :

$$\begin{aligned}n^2(\omega) &= 1 + \chi_{\text{eff}}(\omega) + \chi^{(3)}_{\text{eff}}|A(\omega)|^2 \\ &= n_0^2(\omega)\left[1 + \frac{\chi^{(3)}_{\text{eff}}}{2n_0^3(\omega)\epsilon_0 c}I(\omega)\right].\end{aligned}$$

The nonlinear interactions lead to very weak refractive index variation, enabling to write

$$\boxed{n(\omega) = n_0(\omega) + n_2 I(\omega),} \tag{5.20}$$

with

$$n_2 = \frac{\chi^{(3)}_{\text{eff}}}{4n_0^2(\omega)\epsilon_0 c} = \frac{3\left(\boldsymbol{e} \cdot \underset{\equiv\equiv\equiv}{\chi}^{(3)}\boldsymbol{eee}\right)}{4n_0^2(\omega)\epsilon_0 c}, \tag{5.21}$$

the nonlinear refractive index. As underlined by the relation (5.20), the nonlinear refractive index unity is m^2/W.

To conclude, we have shown the capability for a wave to modify the refractive index of a material, proportionally to the wave intensity and a nonlinear refractive index (a characteristic of the material)[4]. As an example, the nonlinear refractive index for silica is $n_2 \simeq 3\ 10^{-20}\ \text{m}^2/\text{W}$.

[4] A modification of the absorption (or the gain) originates from the $\chi^{(3)}$ imaginary part.

Interestingly, optical Kerr effect can also be induced on a wave ω through its interaction with a second intense beam at ω_p. As the refractive index change is governed by a distinct wave, the nonlinear polarization at ω is:

$$\begin{aligned}\boldsymbol{P}^{(3)}(\omega) &= \epsilon_0 \underset{\equiv\equiv}{\chi}^{(3)}(\omega;\omega,-\omega,\omega)\boldsymbol{E}(\omega)\boldsymbol{E}(-\omega)\boldsymbol{E}(\omega) + \epsilon_0 \underset{\equiv\equiv}{\chi}^{(3)}(\omega;\omega_p,-\omega_p,\omega)\boldsymbol{E}(\omega_p)\boldsymbol{E}(-\omega_p)\boldsymbol{E}(\omega) \\ &\simeq \epsilon_0 \underset{\equiv\equiv}{\chi}^{(3)}(\omega;\omega_p,-\omega_p,\omega)\boldsymbol{E}(\omega_p)\boldsymbol{E}(-\omega_p)\boldsymbol{E}(\omega),\end{aligned}$$

assuming that $|E(\omega_p)|^2 \gg |E(\omega)|^2$. In such a cross-effect, the nonlinear refractive index differs by a factor 2 (because of the difference in the degeneracy factor) and we get:

$$n(\omega) = n_0(\omega) + 2n_2 I(\omega_p).$$

5.4.2 Physical origin of n_2

We briefly mention various physical origins that generate a nonlinear refractive index in materials.

Nonresonant electronic nonlinearities: This contribution arises from the bound electrons of polarized entities. It coincides with a very fast response time, typically of the order of 10^{-15} s. As a non resonant effect, it gives rise to a very weak efficiency with n_2 of the order of 10^{-20} to 10^{-18} m^2/W.

Kerr effect induced by molecular orientation: The interaction between coherent electric fields from intense laser beams and anisotropic molecules induces an orientation of the molecules, which exhibits a refractive index variation proportional to $|E|^2$. Despite a lower response time, 10^{-11} to 10^{-12} s, the n_2 values are higher ($10^{-18} - 10^{-17}$ m^2/W).

Electrostriction effect: The modification of the material density under an inhomogeneous illumination contributes to higher value for n_2 (10^{-18} m^2/W), but with a low response time (about $\neg\mu$s).

Thermal effect: In materials with absorption, the absorbed energy contributes to increase the temperature of the illuminating portion of the material, and leads to a variation of the refractive index. It may be very efficient but very slow.

5.4.3 Self-phase modulation

The modification of the refractive index necessarily induces a phase shift of the wave, which is proportional to its intensity. In a case of the wave packet, either a temporal or spatial wave packet, the respective intensity varies with time or space leading to a spectral broadening. This time- or space- dependent phase shift induced by an intensity-dependent refractive index change is called *self-phase modulation effect* (SPM).

As a first analysis, the linear effects such as dispersion or diffraction, which govern the propagation of temporal or spatial wave packets in linear regime, will be neglected. The nonlinear wave equation for a lonely wave packet propagating through an optical Kerr medium is given by

$$\frac{\partial A(\rho,z)}{\partial z} = \imath k_0 n_2 I(\rho,z) A(\rho,z), \tag{5.22}$$

where the envelope distribution $A(\rho,z)$ is either described in time ($\rho = t$) or space ($\rho = \boldsymbol{r}$) domain. Prior to further analysis, one can notice that the phase matching condition is automatically fulfilled with SPM effect.

Considering the propagation in a lossless material, the nonlinear refractive index n_2 is a purely real quantity, and equation (5.22) shows that the wave intensity is invariant with z. The wave equation (5.22) can be easily integrated and the solution is:

$$\begin{aligned} A(\rho, z) &= A(\rho, 0)e^{\imath k_0 n_2 I(\rho) z} \\ &= A(\rho, 0)e^{\imath \Phi_{\mathrm{NL}}(\rho, z)}, \end{aligned} \tag{5.23}$$

where $\Phi_{\mathrm{NL}}(\rho, z) = k_0 n_2 I(\rho) z$ describes the accumulated nonlinear phase shift along the propagation distance z. Whereas, the envelope (or the intensity) distribution of the wave-packet remains unchanged[5], optical Kerr effect induces a self-phase modulation effect. The time, or space, dependent nonlinear phase $\Phi_{\mathrm{NL}}(\rho, z)$ exhibits a spectral broadening of the pulse.

Taking the example of a temporal pulse, an order of magnitude of the spectral broadening can be calculated by expanding the phase term related to the wave-packet electric field:

$$\begin{aligned} \boldsymbol{\mathcal{E}}(t) &= \boldsymbol{e} A(t) e^{\imath(\omega_0 t - \Phi_{\mathrm{NL}}(t))} + C.C. \\ &\simeq \boldsymbol{e} A(t) e^{\imath\left(\omega_0 - \frac{d\Phi_{\mathrm{NL}}(t)}{dt}\right)t} + C.C. \end{aligned}$$

The self-phase modulation induced spectral broadening can be approximated by:

$$\Delta\omega_{\mathrm{NL}} \simeq -\frac{d\Phi_{\mathrm{NL}}(t)}{dt} = -k_0 n_2 \frac{dI(t)}{dt} z. \tag{5.24}$$

For a symmetric temporal evolution of the pulse, one expects a symmetric spectral broadening since the intensity time variations follow the same variation for the front and tailing edge of the pulse. However, they differ with their sign. Indeed, dI/dt is positive at the front edge of the pulse, leading to a negative (resp. positive) frequency shift $\Delta\omega_{\mathrm{NL}}$ for a positive (resp. negative) nonlinear refractive index n_2. During the tailing edge of the pulse, a positive (resp. negative) frequency shift $\Delta\omega_{\mathrm{NL}}$ is expected for a negative (resp. positive) nonlinear refractive index n_2.

Self-phase modulation of a temporal pulse through a positive Kerr material ($n_2 > 0$) is illustrated in Figure 5.6. Whereas the envelop pulse shape remains unchanged along the propagation, the optical carrier frequencies vary with time with red spectral components coinciding with the front edge of the pulse, and blue spectral components with the tailing edge. The output optical spectrum exhibits a broadening respect to the input spectral linewidth.

The evolution of self-phase modulation induced spectral broadening with the accumulated nonlinear phase is plotted in Figure 5.7 for a gaussian shape pulse and experiencing nonlinear phase from 0 to 3.5π. The amount of nonlinear phase is evaluated through $\Phi_{\mathrm{NL}} = k_0 n_2 I_0 z$, with I_0 the intensity peak power of the pulse. As the nonlinear phase Φ_{NL} increases, the optical spectrum for the outgoing pulse undertakes a larger symmetric broadening, which is a characteristic of a self-phase modulation induced spectral broadening.

5.4.4 Nonlinear Schrödinger equation

From the previous section, we have learned that the propagation of a wave packet through a pure Kerr medium leads to a phase modification proportionally to the wave intensity. A pure Kerr and lossless medium is then equivalent to a spatial or/and a temporal phase modulator, for which the phase level is linearly coded with the wave intensity (and the propagation length), and can be referred to as *Kerr lens effect*. Since the optical Kerr effect can be equivalently described by a lens effect, one can easily understand the importance (and the richness) in describing the propagation of a wave packet in a medium that includes both a nonlinear Kerr term combined with linear effects, such as diffraction and/or dispersion.

[5] as $|A(\rho, z)| = |A(\rho, 0)|$ in Eq. (5.23)

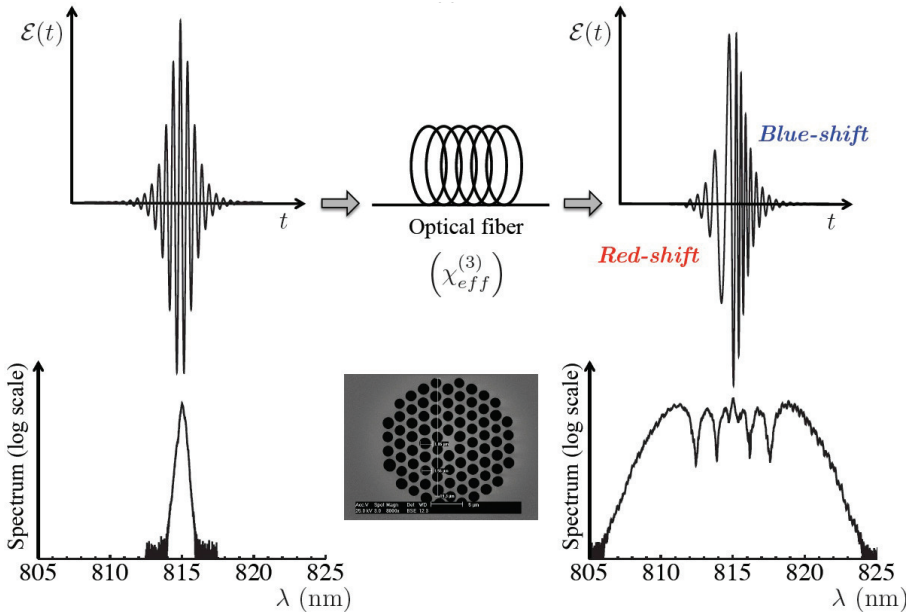

Fig. 5.6. Self-phase modulation effect induced spectral broadening for a pulse propagating through a length of optical fiber, characterized by positive n_2. Whereas the pulse experiences a spectral broadening, the pulse shape and duration are not altered. [Picture courtesy of Margaux Barbier]

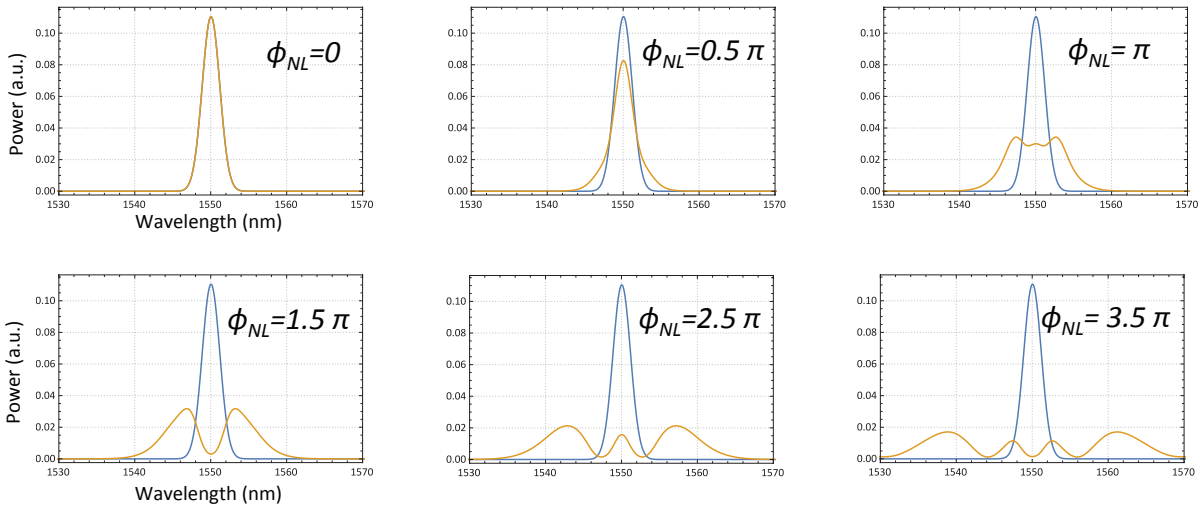

Fig. 5.7. Spectral broadening of a gaussian pulse through self-phase modulation effect and for nonlinear phase varying from 0 to 3.5π.

At this stage, and without any formalism, one can easily anticipate three basic features that will arise by considering the propagation through a Kerr material taking into account the diffraction or the dispersion effects:

Self-focusing effect: Whereas the beam would expand along the propagation due to the linear term (diffraction in space, dispersion in time domains), as the intensity increases and considering a positive $n_2 > 0$, the accumulated Kerr lens along the propagation will tend to counter-balance the linear effect and to focus the beam. As it will be shown below, self-focusing effect for a temporal wave packet requires an anomalous dispersion regime ($\beta_2 < 0$).

De-focusing effect: For a spatial beam, a defocusing effect appears once the Kerr lens acts as a divergent lens for $n_2 < 0$. In the time domain, defocusing arises when the nonlinear refractive index n_2 and the second order dispersion coefficient β_2 are similar in signs.

Soliton effect: Finally, one can easily anticipate a situation where the beam expansion, governed by a linear term, is perfectly counter-balanced by the nonlinear Kerr lens effect, which leads to an invariance in the beam size along the propagation. Such a specific situation refers to as a *soliton effect*, and can be observed either in time or space domain. While the beam propagates, it records its own Kerr lens that strictly compensates for the expansion driven by either the diffraction of the dispersion effects. Such a nonlinear propagation regime founds similitudes with the propagation in optical waveguides[6]. Whereas a spatial soliton is similar to a two-dimension waveguide, with an index profile self-recorded by the spatial beam, a temporal soliton is temporal analogue waveguide !

A more accurate description requires to derive a nonlinear equation that includes both a linear and Kerr terms. Subsequently, the linear effects coincide either to diffraction, which operates in the spatial domain, or to the second-order dispersion effect, which operates in time. Using the nonlinear equations (3.26) and (3.28), and substituting the expression for the nonlinear polarization envelop in case of a pure Kerr effect:

$$\mathbf{\Pi}_{NL}(\rho, z) = \epsilon_0 \chi^{(3)}_{\text{eff}} |A(\rho, z)|^2 A(\rho, z) \boldsymbol{e},$$

yields the derivation of two wave equations in time and space:

$$\frac{\partial A(\tau, z)}{\partial z} + \frac{\imath \beta_2}{2} \frac{\partial^2 A(\tau, z)}{\partial \tau^2} - \imath \gamma |A(\tau, z)|^2 A(\tau, z) = 0, \tag{5.25}$$

$$\frac{\partial A(\boldsymbol{r}, z)}{\partial z} + \frac{1}{2\imath k} \Delta_T A(\boldsymbol{r}, z) - \imath \gamma |A(\boldsymbol{r}, z)|^2 A(\boldsymbol{r}, z) = 0, \tag{5.26}$$

with $\gamma = \frac{\omega_0}{2nc} \chi^{(3)}_{\text{eff}}$. Note that the wave equation in time (5.25) implies to neglect the nonlinear susceptibility dispersion of the material, such as the effective susceptibility $\chi^{(3)}_{\text{eff}}$ is kept constant with negligible frequency variation. In an other way, one considers the time response of the materials much faster than the pulse duration, which is an assumption easily verified for sub picosecond pulse in dielectric materials.

Normalized Equation - Dispersion and Nonlinear lengths

In order to give physics insight into the derived nonlinear equations and to handle their numerical simulation, the following unitary variables are introduced:

[6] A guided mode is a solution of a linear wave equation in an inhomogeneous linear material for which, diffraction effect is strictly counterbalanced by the refractive index inhomogeneity of the wave guide.

- Unitary time $T = \frac{\tau}{\tau_0}$, with τ_0 the pulse duration,
- Unitary transverse coordinate $\boldsymbol{R} = \frac{\sqrt{2}\boldsymbol{r}}{w_0}$, with w_0 the beam waist,
- Unitary field envelope u with $A(\rho, z) = \sqrt{\frac{I_0}{2nc\epsilon_0}}u(\rho, z)$, where I_0 the peak intensity of the pulse or beam.

After substitution in (5.25) and (5.26), one gets:

$$\boxed{\frac{\partial u}{\partial z} + \frac{\imath sign(\beta_2)}{2L_D}\frac{\partial^2 u}{\partial T^2} - \imath\frac{|u|^2 u}{L_{NL}} = 0} \tag{5.27}$$

and

$$\boxed{\frac{\partial u}{\partial z} - \frac{\imath}{2L_R}\frac{\partial^2 u}{\partial \boldsymbol{R}^2} - \imath\frac{|u|^2 u}{L_{NL}} = 0} \tag{5.28}$$

where the quantities:

- $L_D = \frac{\tau_0^2}{|\beta_2|}$ refers to the *dispersion length*,
- $L_R = \frac{\pi w_0^2}{\lambda}$ refers to the *Rayleigh length*,
- and $L_{NL} = \frac{1}{k_0 n_2 I_0}$ refers to the *nonlinear length* or *Kerr length*.

The similitude between the two wave equations (5.27) and (5.28) is straightforward as they both describe the envelop distribution $u(T, z)$ or $u(\boldsymbol{R}, z)$ evolution along the propagation distance z. The propagation is governed by a linear term, the second order dispersion effect for (5.27) and the diffraction for (5.28), and a nonlinear Kerr term proportional to wave packet intensity distribution $|u(T, z)|^2$ or $|u(\boldsymbol{R}, z)|^2$.

By priorly calculating an order of magnitude of the linear and nonlinear lengths, one can easily anticipate the regime of propagation involved in any specific application. Setting the total propagation distance to L and if $L \ll L_R$ or L_D, the diffraction or dispersion effects can be neglected. Similarly, $L \ll L_{NL}$ implies a propagation in a linear regime for which the Kerr effect can be neglected.

Non-Linear Schrödinger Equation (NLSE)

Actually, the wave equations (5.27), (5.28) can be rewritten under unitary parameters by introducing a normalized distance $\xi = z/L_D$:

$$\boxed{\imath\frac{\partial u}{\partial \xi} \pm \frac{1}{2}\frac{\partial^2 u}{\partial \rho^2} + N^2|u|^2 u = 0,} \tag{5.29}$$

with the parameter $N^2 = L_D/L_{NL}$ that sets the strength between the linear and nonlinear effects. This equation corresponds to the well known *Non-Linear Schrödinger Equation* (NLSE). Except for some specific cases, solutions for the NLSE can not be derived analytically and their derivations require a numerical method. The choice for the $\pm$ sign in front of the second term of the NLSE is equal to $-sign(\beta_2)$ for pulses, and $+$ for beam propagation subject to optical diffraction.

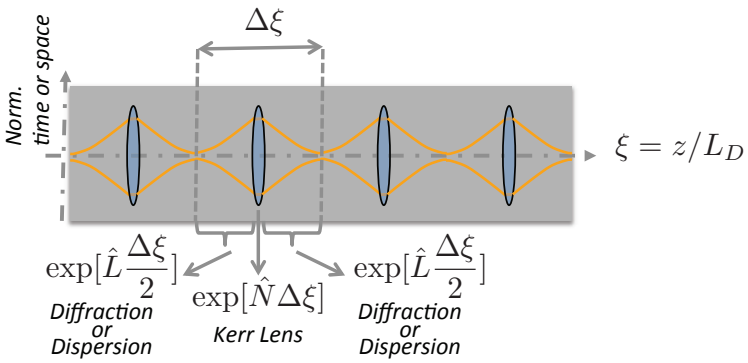

Fig. 5.8. Split-Step Fourier algorithm for a numerical simulation of the NLSE that described the nonlinear propagation a wave packet (pulse or beam) through a nonlinear medium along the direction ξ. The medium is divided in cells of thickness $\Delta\xi \ll 1$. Within each cell, one successively apply the linear and nonlinear operators.

Numerical simulation: the Split Step Fourier method

In order to illustrate some of the behaviors undergone by a wave packet, one first introduces a standard numerical recipe for the NLSE. The wave equation (5.29) can be written in a following symbolic form:

$$\frac{\partial u}{\partial \xi} + \hat{L}u + \hat{N}u = 0, \tag{5.30}$$

with $\hat{L} = +\imath\frac{sign(\beta_2)}{2}\frac{\partial^2}{\partial T^2}$ or $\hat{L} = -\imath\frac{\partial^2}{\partial \boldsymbol{R}^2}$, a linear operator that accounts for either the second-order dispersion (in case of a pulse propagation) or the diffraction (in case of a beam propagation), and $\hat{N} = -\imath N^2|u|^2$ a nonlinear operator. A general solution takes the form:

$$u(\rho, \xi + \Delta\xi) = \exp\big((\hat{L} + \hat{N})\Delta\xi\big)u(\rho, \xi).$$

The operator $\exp\big((\hat{L}+\hat{N})\Delta\xi\big)$ takes into account simultaneously the linear and nonlinear effects. However, one can simplify this operator using the Baker-Hausdorff formula [7]:

$$\exp\big((\hat{L} + \hat{N})\Delta\xi\big) \simeq \exp\big(\hat{N}\Delta\xi\big)\exp\big(\hat{L}\Delta\xi\big)\exp\big(-[\hat{L}, \hat{N}](\Delta\xi)^2\big) \tag{5.31}$$

The exponential term $[\hat{L}, \hat{N}] = \hat{L}\hat{N} - \hat{N}\hat{L}$ can be neglected as it contains a second order term in $(\Delta\xi)^2$. The wave equation (5.30) can then be approximated by the relation:

$$u(\rho, \xi + \Delta\xi) \simeq \exp[\hat{L}\frac{\Delta\xi}{2}]\exp[\hat{N}\Delta\xi]\exp[\hat{L}\frac{\Delta\xi}{2}]u(\rho, \xi). \tag{5.32}$$

Whereas the propagation is governed by two simultaneous effects, the linear and optical Kerr effects, equation (5.32) approximates the propagation by separating these two contributions. Such an approximation is valid since the propagation distance $\Delta\xi$ is kept small. The medium is then split along ξ in slices with an equal thickness $\Delta\xi$. The numerical resolution follows the iterative algorithm describes in Fig. (5.8). Within each slice of medium, one first apply the linear term (diffraction or dispersion) under which the wave packet undergoes an expansion (in space or time). In general, this calculation step is achieved in the Fourier domain as the linear operator in the Fourier domain takes the form of a phasor. Following this first step, the nonlinear operator is applied, symbolically described by a thin lens effect in Fig. (5.8). One reminds that the Kerr lens effect can be either a convergent or divergent lens depending on the sign of the nonlinear refractive index n_2.

[7] Approximation used in quantum physics to simplify quantum operators. For instance, refer to chapter 4 of the book "Contemporary optical image processing with MathLab" from Poon and Banerjee, Elsevier (2001).

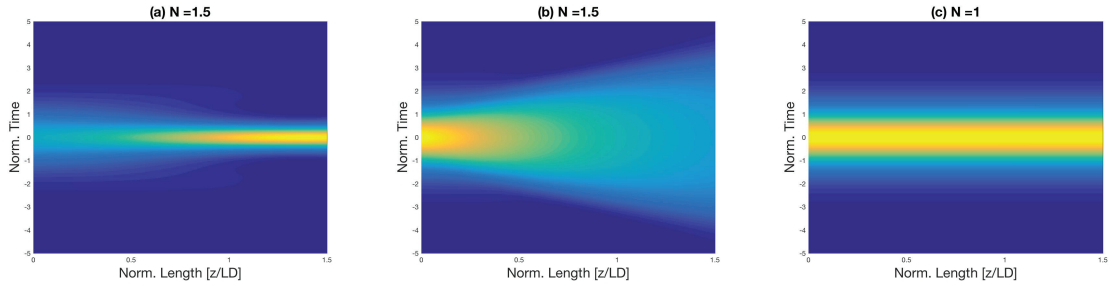

Fig. 5.9. Nonlinear propagation of a wave packet for various nonlinear strength set by the parameter N. (a) Self-focusing effect with $N = 1.5$, (b) De-focusing effect with $N = 1.5$, (c) Fundamental Soliton solution with $N = 1$.

Self-focusing and De-focusing effects

Considering a nonlinear propagation, with $N > 1$, one can easily understand that the Kerr lens effect may produce a self-focusing or de-focusing of the wave-packet, which depends on the signs of the linear and nonlinear coefficients in the NLSE. Figures (5.9)(a) and (b) show the temporal shape of a pulse along the propagation in a nonlinear regime that is simulated with the parameters : $N = 1.5$, anomalous dispersion regime ($\beta_2 < 0$), and $n_2 > 0$ for (a) and $n_2 < 0$ for (b). In such a nonlinear regime (as $L_{NL} < L_D$) the Kerr lens effect is dominant and the lens property (converging or diverging) is set by the sign of the nonlinear refractive index n_2.

A similar result could have been achieved with the propagation of spatial wave packets (transverse beams). As the diffraction in standard materials implies a fixed sign for the linear operator, self-focusing and de-focusing effects respectively requires positive and negative n_2 materials.

Soliton effect

A very interesting situation happens once the Kerr nonlinear operator strictly counter-balances the diffusing like linear operator in the NLSE. Actually, it can be shown with standard gaussian shape beam (pulse) that a strict compensation of diffraction (2nd order dispersion) by a positive Kerr lens effect arises since $N = 1$. Using the graphical representation of the NLSE depicted in Fig. (5.8), the nonlinear regime $N = 1$ coincides with a situation where the Kerr Lens in each elementary slice $\Delta\xi$ of material perfectly conjugates the incoming and out-coming wave packet shapes. In an other word, for every slice the linear expansion of the wave-packet (driven either by the diffraction or the 2nd order dispersion effects) is strictly compensated by the Kerr lens ! Under such a condition, and as illustrated in Fig. 5.9(c), the wave-packet shape can be conserved along the propagation and coincides to a *soliton*, either a *temporal or spatial soliton*.

Now, this solution requires to perfectly control the incoming pulse or beam shape, as it will directly impact on the Kerr lens profile. Actually one type of solution of the NLSE equation (5.29) for solitons are given by :

$$u(\rho) = N\mathrm{sech}(\rho),$$

for which $N = 1$ coincides to the fundamental soliton shown in Fig. 5.9(c). For further information about optical soliton, one can refer to *Nonlinear Fiber Optics*, Ch.5 by Govind P. Agrawal.

5.4.5 Modulation instability

!!!! WORK AREA !!!

Part to be completed in the next version, sorry !

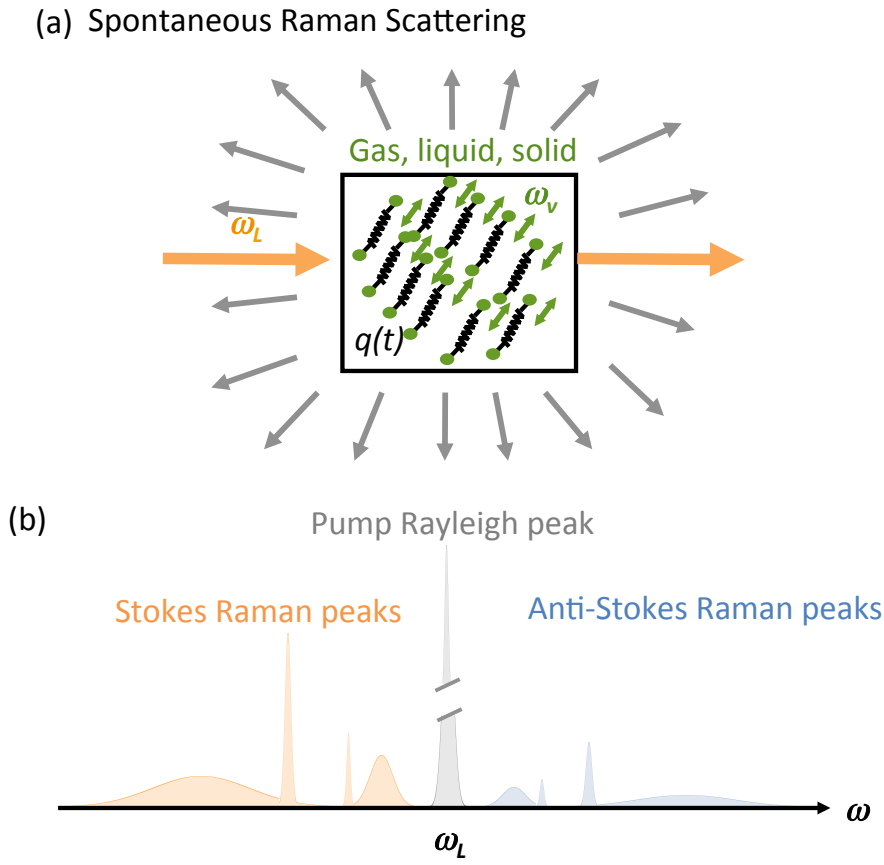

Fig. 5.10. Scattered light from a molecular material (gas, liquid) or a solid (amorphous or crystal) with an incident wave at ω_L. The spectrum analysis of the isotropic scattered light shows (b) Stokes and Anti-Stokes spectral peaks symmetrically located to a strong Rayleigh peak at ω_L.

5.4.6 Nonlinear Kerr optical cavity: optical bistability

!!!! WORK AREA !!!

Part to be completed in the next version, sorry !

5.5 Raman Scattering

The so-called Spontaneous Raman Scattering has been first observed experimentally by Sir C.V. Raman in 1928[8]. As illustrated in Fig. 5.10(a), an incident wave at ω_L is focused inside a material composed of molecules (gas, liquid) or bounded atoms (amorphous or crystal solids) and the experiment consists in analyzing the spectrum of the scattered light. In addition to a strong peak at ω_L, due to Rayleigh scattering, additional peaks can be observed (see Fig. 5.10(b)) with a much weaker intensity (several orders of magnitude weaker) than the Rayleigh peak. Moreover, those additional peaks are symmetrically located respectively to the Rayleigh peak: the spectral lines with a lower frequency (lower energy) referred to as *Stokes* Raman lines, whereas the spectral lines with a higher frequency (higher energy) referred to as *Anti-Stokes* Raman lines.

Experimental observations show that, for any Stokes peak located at a frequency ω_S, one can observe an Anti-Stokes peak at $\omega_{AS} = \omega_L + (\omega_L - \omega_S)$. The equal quantity $\omega_L - \omega_S = \omega_{AS} - \omega_L$ is called the Raman shift and coincides with a vibrational mode of the molecules or bounded atoms

[8]See, C.V. Raman and K.S. Krishnan, *A new type of secondary radiation*, Nature **121**, 501-502 (1928).

that compose the materials. Despite a modification of the incident light frequency ω_L, the Stokes and Anti-Stokes peaks move, keeping symmetric respectively to ω_L and conserving their related Raman shifts. As illustrated in Fig. 5.10(b), the spontaneous Raman spectrum is composed of different Raman shifts, which characterize the material under study. Raman spectroscopy consists in identifying Stokes peaks, in terms of positions and relative magnitudes, enabling to identify the compounds of a material. An other important observation concern the relative magnitude between the Stokes and Anti-Stokes peaks, the latter being always much weaker than the former. Moreover, the magnitude of the Anti-Stokes peaks varies with temperature and can be used to realize optical sensing.

In the following, we first introduce a classical description of spontaneous Raman scattering which originates from the polarizibility fluctuations of molecules due to vibrating modes. We will show that Raman scattering can be stimulated by through a double excitation at ω_L and ω_S, providing that $\omega_L - \omega_S$ match with the Raman shift ω_v of the molecular material. Under a stimulated regime, the Stokes beam at ω_S is amplified at the expense of the pump beam at at ω_L, leading to a cascading regime with the generation of successive Stokes peaks at $\omega_{S1} = \omega_L - \omega_v$, $\omega_{S2} = \omega_{S1} - \omega_v$, $\omega_{S3} = \omega_{S2} - \omega_v$, *etc.* Such a Raman cascading effect is used in Raman fiber lasers.

5.5.1 Spontaneous Raman Scattering

Microscopic origin

A classical interpretation of the Raman scattering consists in analyzing the polarizability of a molecule, for instance a bi-atomic molecule, shown in Fig. 5.10, subjects to a monochromatic field at ω. The Raman scattering arises from the fact that we consider the vibrating motion of molecules, characterized by a vibrating mode (elongation, rotation) with an eigen (or resonant) frequency ω_v.

Under this vibrating mode, the distance between the two atoms varies in time and modifies the polarizability of the molecule following the relation:

$$\alpha(q) = \alpha_0 + \frac{\partial \alpha}{\partial q}(q - q_0) + \cdots , \tag{5.33}$$

where q_0 and α_0 denote respectively the distance between the two atoms, and the linear polarizability for the non-vibrating molecule. Considering a vibrating motion at the frequency ω_v, the distance between the two atoms is given by:

$$\delta q = q - q_0 = q_1 \cos(\omega_v t). \tag{5.34}$$

A monochromatic wave $\mathcal{E}(t) = E_0 \cos \omega t$ is now interacting with the molecule and the induced dipole $p = \alpha E$ yields:

$$p = \alpha_0 \cos \omega t + \frac{1}{2}\frac{\partial \alpha}{\partial q} q_1 \left[\cos(\omega + \omega_v)t + \cos(\omega - \omega_v)t\right] + \cdots \tag{5.35}$$

This relation shows that the interaction between a wave at ω with molecules vibrating at ω_v, which is responsible for a modification of the polarizability of the molecules, leads to an induced dipole with frequency components at ω (linear regime, related to Rayleigh scattering), and two components at $\omega - \omega_v$ and $\omega + \omega_v$, referred respectively to as *Stokes* and *anti-Stokes* Raman scattering spectral components. This classical model gives a simple insight in the origin of the Stokes and Anti-Stokes Raman lines that are observed, for instance, in Raman spectroscopy experiments. It justifies that the two lines are symmetrically located respectively to the frequency of the excited field, or pump wave, at ω, the spectral interval being related to the eigen

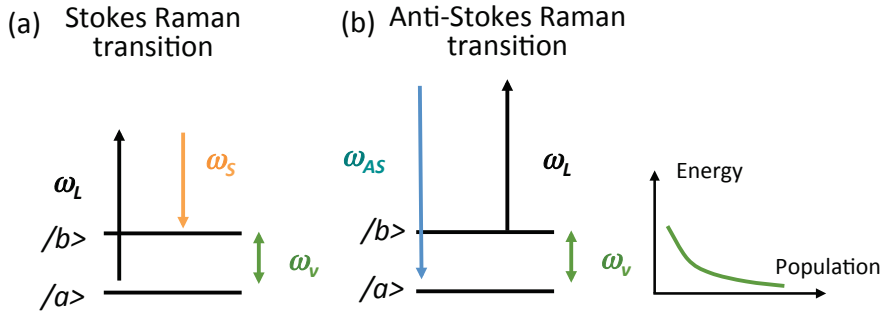

Fig. 5.11. Raman scattering energy diagram related to the generation of (a) Stokes and (b) Anti-Stokes spectral compounds.

frequency of the vibrating mode of the molecule. By conducting such a Raman spectroscopy and using tabular values for the vibrational mode of molecules, one can identify the compounds of a material.

However, this model does not account for a systematic asymmetry in the magnitude of the two lines. The Anti-Stokes Raman components are always weaker than the Stokes Raman components. Actually, such a Raman type interaction can be described using energy diagrams shown in Fig. 5.11, where an incident wave at ω_L interacts with a vibrational mode at ω_v. The latter coincides with a transition between two molecular states $|a\rangle$ and $|b\rangle$. As the various interactions involve the energy conservation relation, the Stokes Raman scattering (Fig. 5.11(a)) coincides with the excitation of a molecule from states $|a\rangle$ to $|b\rangle$, assisted by two photons at ω_L and ω_S. Such a two-photon transition is conducted through the annihilation of one photon ω_L, leading to the creation of one Stokes photon ω_S and one optical phonon at ω_v. The Anti-Stokes Raman scattering (Fig. 5.11(b)) originates from the interaction between a wave at ω_L with an excited molecule (on state $|b\rangle$) : the simultaneous annihilations of one photon ω_L and one optical phonon at ω_v, lead to the generation of one Anti-Stokes photon ω_{AS}. If we consider the population distribution of molecules respectively on states $|a\rangle$ and $|b\rangle$, which can be described through a Boltzmann distribution shown in Fig. 5.11, one can easily understand why the Anti-Stokes Raman peaks are weaker than the Stokes Raman peaks. Since $\hbar\omega_v \gg k_B T$, the Anti-Stokes Raman transition rate is smaller as the density population on the excited state $|b\rangle$ is lower than that on state $|a\rangle$.

5.5.2 Stimulated Raman Scattering

Hereafter we consider the interaction of an intense pump beam at ω_L with a weaker signal beam at ω_S through a molecular material (gas, liquid) or a solid (amorphous or crystal) characterized by at least one vibrational mode at ω_v. We will show that a resonant interaction for which $\omega_S = \omega_L - \omega_v$ leads to a transfer of energy from the pump to the signal beam as illustrated in Fig. 5.12.

A classical description of a vibrating mode consists in deriving an equation of motion for a harmonic oscillator characterized by a resonance frequency ω_v, equal to that of the vibrational mode of the molecular material to be considered, and a damping constant γ. From the relation (5.34), the modification of the distance $q(t)$ between two-bounded atoms of the molecule follows the equation:

$$\frac{d^2q}{dt^2} + 2\gamma\frac{dq}{dt} + \omega_v^2 q = \frac{F(t)}{m} \tag{5.36}$$

with $F(t)$ the force that drives the molecular vibration and m the reduced nuclear mass. Similarly to the spontaneous Raman scattering effect, the interaction of an external field $\mathcal{E}(t)$ will polarized each molecule for which the induced dipole is $p(t) = \alpha\mathcal{E}(t)$. By expressing the energy

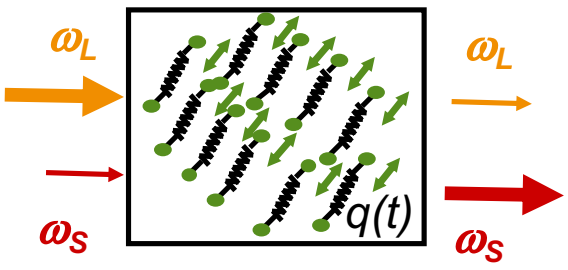

Fig. 5.12. Stimulated Raman Scattering configuration that involves the interaction between two waves at ω_L and ω_S through a material characterized by a Raman transition at ω_v. A resonant interaction for which $\omega_S = \omega_L - \omega_v$ leads to an amplification of the Stokes wave at the expense of the pump wave at ω_L.

required to drive the induced dipole as

$$W = \frac{1}{2}\alpha\langle\mathcal{E}^2(z,t)\rangle,$$

where $\langle\ldots\rangle$ stands for an average in time, one can derive a relation for the force applied onto the dipole:

$$F(t) = \frac{dW}{dq} = \frac{1}{2}\frac{d\alpha}{dq}\langle\mathcal{E}^2(z,t)\rangle.$$

In the case of stimulated Raman scattering depicted in Fig. 5.12, the applied field comprised two frequencies at ω_L and ω_S and

$$\mathcal{E}(z,t) = A_L e^{i(k_L z-\omega_L t)} + A_S e^{i(k_S z-\omega_S t)} + CC.$$

As the driven force applied on the dipole is proportional to $\langle\mathcal{E}^2(z,t)\rangle$, a beating term at $\omega_L-\omega_S$ appears on the right hand side term of the equation of motion (5.36) and may match with the frequency vibration of the molecule at ω_v. For a resonant interaction, i.e. for $\omega_L - \omega_S = \omega_v$, the molecular vibration is expected to be strengthened inducing a dipole moment related to each molecule. The collective and coherent excitation of the vibrating molecules generate a macroscopic polarization term that may modify the optical wave properties as it will be shown below.

Following the substitution of the expression for the applied electric field, the equation of motion yields

$$\frac{d^2q}{dt^2} + 2\gamma\frac{dq}{dt} + \omega_v^2 q = \frac{1}{m}\frac{d\alpha}{dq}[A_L A_S^* e^{i(Kz-\Omega t)} + CC],$$

with $K = k_L - k_S$ and $\Omega = \omega_L - \omega_S$, and were we have only retained the beating terms at frequencies Ω closed to the resonance frequency ω_v [9]. The driven solution takes the following form:

$$q(t) = q(\Omega)e^{i(Kz-\Omega t)} + CC$$

where the amplitude $q(\Omega)$ is equal to:

$$q(\Omega) = \frac{\frac{1}{m}\left(\frac{d\alpha}{dq}\right)A_L A_S^*}{\omega_v^2 - \Omega^2 - 2i\Omega\gamma}.$$

By assuming that the all the molecules are aligned along the polarization direction of the applied field, the macroscopic polarization generated inside the molecular material is given by:

$$P(z,t) = N\alpha(z,t)\mathcal{E}(z,t) = N[\alpha_0 + \left(\frac{d\alpha}{dq}\right)q(z,t)]\mathcal{E}(z,t),$$

[9] The right hand side terms vibrating at $2\omega_L$, $2\omega_S$ and 0 do not efficiently contribute to the molecular vibration as these frequencies are largely detuned from the resonance frequency ω_v.

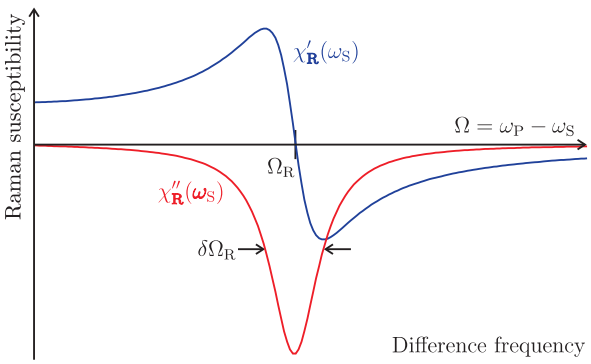

Fig. 5.13. Real part and imaginary part of the Raman susceptibility at ω_S as a function of the difference frequency $\Omega = \omega_P - \omega_S$. The imaginary part of the susceptibility exhibits a Lorentzian shape nearby the vibrational resonance $\Omega = \Omega_R$. At resonance, the Raman susceptibility at ω_S is purely negative imaginary. (Picture courtesy of Felix Kroeger)

which can be expressed as the sum of the linear contribution $N\alpha_0\mathcal{E}(z,t)$ plus a perturbative polarization term:

$$P_{NL}(z,t) = N\left(\frac{d\alpha}{dq}\right)[q(\Omega)e^{i(Kz-\Omega t)} + CC].[A_L e^{i(k_L z-\omega_L t} + A_S e^{i(k_S z-\omega_S t} + CC].$$

The latter contribution contains vibrating terms at ω_L and ω_S and, conversely to the linear contribution, their expressions exhibit a nonlinear dependence with the field amplitudes characteristic of a 3rd order nonlinear interaction. Actually, the complexe amplitude of the perturbative term at ω_S is provided by:

$$P_{NL}(\omega_S) = N\left(\frac{d\alpha}{dq}\right)q^*(\Omega)A_L e^{ik_S z},$$

as $\Omega = \omega_L - \omega_S$, and it can be re-written in the following closed form:

$$P_{NL}(\omega_S) = 3\epsilon_0\chi_R^{(3)}(\omega_S;\omega_L,-\omega_L,\omega_S)|A_L|^2 A_S e^{ik_S z},$$

where $\chi_R^{(3)}(\omega_S;\omega_L,-\omega_L,\omega_S)$ stands for the Raman susceptibility at ω_S that is equal to:

$$\chi_R^{(3)}(\omega_S) = \frac{\frac{N}{3\epsilon_0 m}\left(\frac{d\alpha}{dq}\right)^2}{\omega_v^2 - (\omega_L-\omega_S)^2 + 2i(\omega_L-\omega_S)\gamma}.$$

The evolution of the real and imaginary parts of the Raman susceptibility at ω_S with the difference frequency $\Omega = \omega_P - \omega_S$ is plotted in Fig. 5.13. As expected above, the Raman susceptibility exhibits a resonance nearby Ω equal to the vibrational frequency ω_v (denoted Ω_R on the plot), with a purely imaginary contribution exactly at resonance that will consequently explain the transfer of energy between the pump to the signal throughout the vibrational molecules.

Appendix A

Model for light-metals interaction

In the following, it is assumed that the electrical and optical properties of a metal can be represented in a similar manner by those of a free electron gas with a density N. The density of negative charges is compensated by a positive charge density, which is assumed to be fixed. In the case of a plasma-gas, the motion of the positive charges, which are heavier, should also be taken into account. The free electron gas is assumed diluted enough such as the charges interact with the electromagnetic field separately and independently of each others.

We consider the following electromagnetic wave propagating along the direction z:

$$\begin{aligned} \boldsymbol{\mathcal{E}} &= E_0 \cos(\omega t - kz)\boldsymbol{x} \\ \boldsymbol{B} &= B_0 \cos(\omega t - kz)\boldsymbol{y}, \end{aligned} \tag{A.1}$$

Assuming the case of a dilute gas, the relation between the magnetic and electric field amplitude is $B_0 = E_0/c$, with c the speed of light in vacuum (dilute gas). In order to determine an expression for the induced polarization $\boldsymbol{\mathcal{P}} = N\boldsymbol{p}$, with $\boldsymbol{p} = -e\boldsymbol{r}$ the induced dipole, one can solve the equation of motion for an electron, with a mass m, which is subject to the Lorentz force:

$$m\frac{d^2\boldsymbol{r}}{dt^2} = -e(\boldsymbol{\mathcal{E}} + \boldsymbol{v} \times \boldsymbol{B}), \tag{A.2}$$

where $\boldsymbol{v} = \frac{d\boldsymbol{r}}{dt}$ defines the electron velocity. The previous equation neglects the friction forces. Substituting the field expressions (A.1), the equation of motion becomes:

$$\begin{cases} m\dfrac{d^2x}{dt^2} = -eE_0 \cos(\omega t - kz) + \dfrac{e}{c}E_0 \cos(\omega t - kz)\dfrac{dz}{dt} \\ m\dfrac{d^2y}{dt^2} = 0 \\ m\dfrac{d^2z}{dt^2} = -\dfrac{e}{c}E_0 \cos(\omega t - kz)\dfrac{dx}{dt} \end{cases} \tag{A.3}$$

Taking into account that the magnetic part of the Lorentz force can be neglected with respect to the electrical contribution, the equation of motion (A.3) is solved by means of a perturbative method, the seeked solution being expressed as:

$$\boldsymbol{r}(t) = \boldsymbol{r}^{(0)}(t) + \boldsymbol{r}^{(1)}(t) + \boldsymbol{r}^{(2)}(t) + \cdots,$$

with $\boldsymbol{r}^{(0)}$ the initial position of the electron, without any applied field, and $\boldsymbol{r}^{(1)}$, $\boldsymbol{r}^{(2)}$ the first and second order perturbative solutions resulting from the application of an external field. The

first order solution is obtained by neglecting the magnetic contribution of the Lorentz force:

$$\boldsymbol{r}^{(1)}(t) = \frac{e}{m\omega^2} E_0 \cos(\omega t - kz)\boldsymbol{x} + O\boldsymbol{y} + O\boldsymbol{z}. \tag{A.4}$$

The first order solution exhibits a linear relation between the motion of the electron and the electric field strength, along the direction of the electric field polarization state $\boldsymbol{x}$. The first order solution is then substituted in the right hand side of (A.3), enabling the derivation of the second order solution:

$$\boldsymbol{r}^{(2)}(t) = 0\boldsymbol{x} + 0\boldsymbol{y} - \frac{e^2}{8m^2c\omega^3} E_0^2 \sin(2(\omega t - kz))\boldsymbol{z}. \tag{A.5}$$

This procedure can be reiterated to calculate the third order solution for the position of the electron.

Following the motion of the charges, a current density $\boldsymbol{j} = -Ne\frac{d\boldsymbol{r}}{dt}$ and a polarization $\boldsymbol{\mathcal{P}} = -Ne\boldsymbol{r}$ are generated within the free electron gas. The expression for the polarization will take the following form:

$$\boldsymbol{\mathcal{P}} = \boldsymbol{\mathcal{P}}^{(1)}(t) + \boldsymbol{\mathcal{P}}^{(2)}(t) + \boldsymbol{\mathcal{P}}^{(3)}(t) + \cdots .$$

The first order polarization term $\boldsymbol{\mathcal{P}}^{(1)}(t)$ is proportional to the strength of the applied field and corresponds to the linear polarization. Whereas, the second order polarization $\boldsymbol{\mathcal{P}}^{(2)}(t)$, related to (A.5), vibrates at the frequency 2ω with a direction of polarization aligned along $\boldsymbol{z}$. This direction being orthogonal to the polarization states of $\boldsymbol{\mathcal{E}}$ and $\boldsymbol{B}$, the second order polarization can not radiate in the medium, except in the vicinity of an interface or defects.

Finally, the expression of the third order polarization $\boldsymbol{\mathcal{P}}^{(3)}(t)$ is:

$$\boldsymbol{\mathcal{P}}^{(3)}(t) = -\frac{Ne^4}{8m^3c^2\omega^4} E_0^3 \left[\cos(\omega t - kz) + \frac{1}{9}\cos 3(\omega t - kz)\right]\boldsymbol{x}.$$

It shows that the medium can radiate a source term at the frequencies 3ω, and ω. The latter, whose amplitude depends on the square of the field is responsible for a nonlinear self-action of light in the medium.

In conclusion, we have shown that the origin of nonlinearities in metals and plasma-gas comes from the **magnetic** contribution of the Lorentz force. The ratio between the strength of the first, second and third order polarizations is given by $eE_0/mc\omega$.

Note that this model does not account for interactions between the charges that could be described introducing additional terms in the equation of motion. It does not either account for variations of the charge density in the electron gas.